Fundamental Modes and Abrupt Changes in North Atlantic Circulation and Climate over the last 60 ky – Concepts, Reconstruction and Numerical Modeling

Michael Sarnthein[1], Karl Stattegger[1], Derek Dreger[1,2], Helmut Erlenkeuser[3], Pieter Grootes[3], Bernd J. Haupt[1,2], Simon Jung[2,4], Thorsten Kiefer[1], Wolfgang Kuhnt[1], Uwe Pflaumann[1], Christian Schäfer-Neth[2], Hartmut Schulz[1,5], Michael Schulz[1,2], Dan Seidov[1,6], Johannes Simstich[1,2], Shirley van Kreveld[1], Elke Vogelsang[1,2], Antje Völker[1,2] and Mara Weinelt[1,2]

[1] Institute for Geosciences, Kiel University, Olshausenstrasse 40, 24118 Kiel, Germany
[2] SFB 313, Kiel University, Heinrich-Hecht-Platz 10, 24118 Kiel, Germany
[3] Leibniz Laboratory, Kiel University, Max-Eyth-Strasse 11–13, 24118 Kiel, Germany
[4] Research School of Sedimentary Geology, Center for Marine Earth Sciences, Free University, De Boelelaan 1085, 1081 HV Amsterdam, The Netherlands
[5] Baltic Sea Research Institute, Rostock University, Seestrasse 15, 18119 Warnemünde, Germany
[6] ESSC, Pennsylvania State University, University Park, PA 16802, USA

Abstract: Centennial- to millennial-scale changes in global climate over the last 60 ky were first documented in ice cores from Greenland, with ice sheets around the North Atlantic and its thermohaline circulation (THC) as prime candidates for a potential trigger mechanism. To reach a new quality in understanding the origin and causal links behind these changes, two strategies were intimately tied together in this synthesis, high-resolution 3-D ocean modeling and paleoceanographic reconstructions. Here, five time series with a time resolution of several decades and various time slices of surface and deep-water paleoceanography were established from hundreds of deep-sea cores for the purpose of monitoring rapid changes across the North Atlantic and testing or initiating model results. Three fundamental modes were found to operate Atlantic THC. Today, mode I shows intensive formation of North Atlantic Deep Water (NADW) and strong heat and moisture fluxes to the continents adjacent to the North Atlantic. Peak glacial mode II leads to a reduction in NADW formation by 30–50 %, in line with a clear drop in heat flux to Europe. The glacial Nordic Seas, however, remain ice-free during summer and little influenced by meltwater, in contrast to the sea west of Ireland, where iceberg meltwater blocks an eastbound flow into the Norwegian Sea and induces a cold longshore current from Faeroe to the Pyrenees. The subsequent Heinrich 1 (H1) meltwater mode III leads to an entire stop in NADW and intermediate-water production as well as a reversed pattern of THC, stopping any heat advection from the central and South Atlantic to the north. In contrast to earlier views, the Younger Dryas, possibly induced by Siberian meltwater, began with mode I and ended with mode III, continuing into the Preboreal. Modeling the impact of modes I to III on the global carbon budget, we find that the atmosphere has lost 34–54 ppmv CO_2 from interglacial to glacial times, but has gained 23–62 ppmv CO_2 at the end of H1 within a few decades, equivalent to 33–90 % of modern, man-made CO_2 release. The robust 1500-y Dansgaard-Oeschger (D-O) cycles and their multiples of as much as 7200 years, the Heinrich event cycles, are tied to periodical changes between THC modes I/II and II/III. In the Irminger Sea rapid D-O coolings are in phase with initial meltwater injections from glaciers on East Greenland, here suggesting an internal trigger process in accordance with binge-purge models. Ice rafting from East Greenland and Iceland occurs only 240–280 y later, probably inducing a slight sea-level rise and,

From *The Northern North Atlantic: A Changing Environment*, edited by P. Schäfer, W. Ritzrau, M. Schlüter, and J. Thiede, pp. 365–410, Springer, Berlin, 2000

in turn, Heinrich ice rafting from the Laurentian ice sheet during H1, H2, H4, H5. At H1 a major surge from the Barents shelf has lagged initial cooling by 1500 y and entails the most prominent and extended reversal in Atlantic THC over the last 60 ky (probably also at the end of glacial stage 4, at H6). Meltwater stratification in the Irminger Sea reaches its maximum only 640 y after initial meltwater injection and induces, via seasonal sea-ice formation, brine-water injections down to 4 km water depth, signals leading the classic D-O jump to maximum warmth by only 125 y. It may be inferred from this short-phase lag that brine water-controlled deep-water formation probably entrains warm water from further south, thereby forming the key trigger mechanism for the final turn-on of the Atlantic THC mode II roughly within a decade (or mode I, in case of favorable Milankovitch forcing).

Introduction

The Northern North Atlantic: Amplifier and Potential Trigger of Climate Variability

In contrast to the North Pacific, both the extension into very high latitudes and the funnel-style narrow geometry of the northern North Atlantic result in a bundle of unique effects on the climate system. Here, warm surface water originates from the Caribbean Sea via the Gulf Stream and North Atlantic Drift. This inflow water, which is more saline than anywhere else in the high-latitude oceans, is finally advected to sites with extreme cooling and deep-water formation, sites which mark the onset and terminus of the Atlantic and global thermohaline circulation system (Fig. 1; Schmitz 1995). Deep-water convection results in a huge release of heat and moisture to the atmosphere, the Nordic "heat pump" of Europe (Berger et al. 1987), which is partly based on "heat piracy" (Berger and Wefer 1996) in the central and South Atlantic. The Arctic connection across the Barents shelf and the Fram Strait further enhances this potential of high-latitude climatic forcing via Arctic sea-ice export, freshwater advection from Siberian rivers, differential states of albedo linked to variable sea-ice cover, and finally, by deep-water formation, currently an important factor, on the Barents shelf. The features and variability of modern oceanography in the northern North Atlantic have recently been reviewed by Hopkins (1991), Lozier et al. (1995), Dickson et al. (1996), Sy et al. (1997) and Schäfer-Neth and Paul (this volume). Some major structures relevant to this study are summarized in Figure 1.

Different from the Southern Ocean, North Atlantic deep-water formation follows a long-lasting exposure of Atlantic surface water to the atmosphere and hence leads to oxygen enrichment in the deep Atlantic, which finally provides the principal oxygen source of the global deep ocean (Bainbridge 1981). In addition, the modern North Atlantic also forms an important sink for CO_2 transfer in deep water from the northern to the southern hemisphere (Tans et al. 1990; Broecker and Peng 1992).

The strong cooling induced by the Greenland ice sheet results in a zonal temperature contrast unique to the Nordic Seas. It has lasted, at least, over the last three million years (Thiede et al. 1998; Jansen et al. 1996; Henrich 1990). Over this time, the high latitudes of the Greenland-Iceland-Norwegian (GIN) Seas and the adjacent Eurasian landmass were particularly sensitive to changes in summer insolation, that is, to Milankovitch orbital forcing, as has been established for the numerous major and minor glacial-to-interglacial cycles in many studies (Thiede et al. 1998; Raymo et al. 1989; Ruddiman et al. 1989; Ruddiman and McIntyre 1981; Imbrie et al. 1992, 1993; Robinson and McCave 1994). Variations in both atmospheric CO_2 concentration and the size of continental ice sheets via their crustal isostasy are important in modifying the orbital periodicities of climate. Many authors link the origin of quasi-100-ky glacial cycles to these two variables, particularly since there is little insolation forcing in this frequency band (e.g. Imbrie et al. 1993; Saltzman and Verbitsky 1993).

What Makes the Last 60 ky Special?

The results presented here focus on climate variability over the last 60 ky, that is, nearly half a 100-ky glacial cycle, for a number of reasons:

(1) During this time, chronostratigraphic resolution has reached a precision of decades to centuries in both ^{14}C datings of marine sediments and annual layer counts in polar ice records, back to more than 50 ky ago (ka).

(2) Based on ice-core records, the climate showed an extreme natural variability over the time span 60–10 ka (Dansgaard et al. 1993; Grootes and Stuiver 1997). Similar variations, but of smaller amplitude, were recently discovered in marine and ice-core records from the Holocene (Sirocko et al. 1996; Bond et al. 1997;

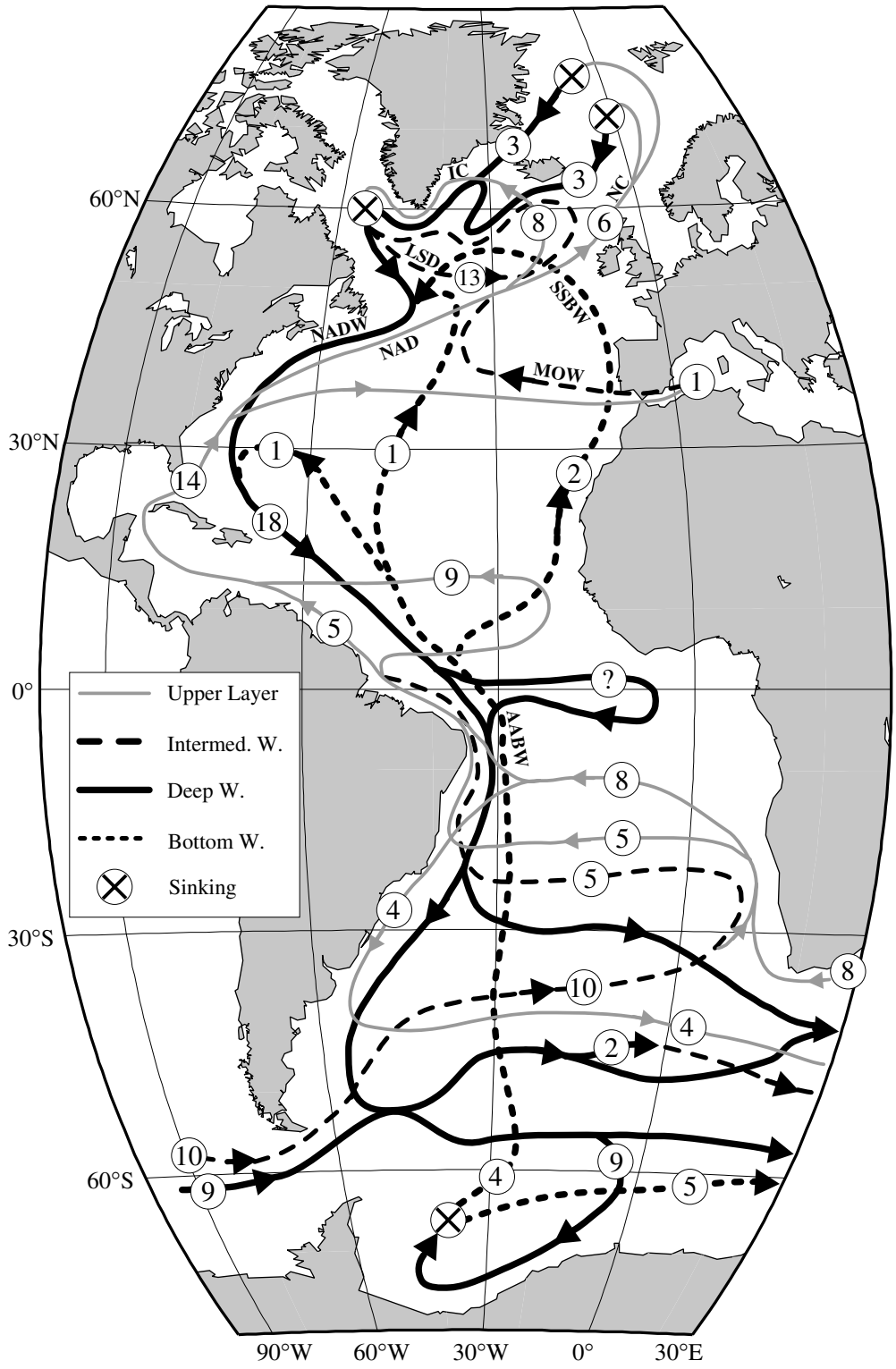

Fig. 1: Modern Atlantic thermohaline circulation, presented as a four-layer system (modified after Schmitz 1995; Dickson and Brown 1994; Schmitz and McCartney 1993). Numbers denote water transport in Sverdrups (1 million m^3 per second). AABW = Antarctic Bottom Water; IC = Irminger Current; LSD = Labrador Sea Water; MOW = Mediterranean Outflow Water; NAD = North Atlantic Drift; NADW = North Atlantic Deep Water; NC = Norwegian Current; SSBW = Southern Source Bottom Water, a dilute derivative of AABW

Wang et al. 1999). Great hemispheric temperature changes probably took less than ten years (Dansgaard et al. 1989; Alley et al. 1993). These short-term changes imply various alternative "pacemakers", such as processes in the ocean and atmosphere, which remain poorly understood. In Table 1 an overview of current prime objectives and alternative concepts in North Atlantic paleoceanography is given. While three major modes of Atlantic thermohaline circulation now appear as basically established (Sarnthein et al. 1994; Alley and Clark 1999), the processes responsible for abrupt, that is, on a scale of decades, changes in climate and on a scale of centuries to millennia in climate periodicities, remain generally unknown. This particularly applies to questions of high vs. low latitude and external vs. internal forcing of changes in the ocean. The vast quantity of new findings, arguments and controversial conceptual models is partly listed in Table 1. It urgently requires an up-to-date review and synthesis, the goal of this paper.

(3) Finally, some technical constraints enforce a focusing of our high-resolution studies in the Nordic Seas to the last 60 ky. Because of high concentrations of ice-rafted debris (IRD) the length of sediment sections obtained in conventional marine kasten and piston cores rarely exceeds 7–9 m. These cores, retrieved from a total of nearly 120 sites, provide a sound spatial and temporal (spanning several decades) sampling density for paleoceanographic proxy data in the Greenland-Iceland-Norwegian Seas, required as input for our numerical modeling experiments. Only recently have a number of ODP and IMAGES-CALYPSO cores overcome this "magic" boundary in core length (Dreger 1999; Jansen et al. 1998; Jansen et al. 1996; Thiede et al. 1996).

To improve our understanding of the complex climatic modes and the external and internal forcing mechanisms listed in Table 1, a "new quality" in the reconstruction of North Atlantic paleoceanographic time series and time slices, which each represent extreme climatic states, has been attempted. In particular, two different strategies were inherently interrelated, (1) the generation of space filling (Fig. 2) and ultrahigh-resolution, quantitative proxy data which serve for either model boundary conditions or an appropriate validation of the model output, and (2) high-resolution (0.5–1.0°) three-dimensional (3-D) ocean modeling (Fig. 3/Table 3).

Both the initialization of these numerical models and the calibration of paleoceanographic proxy data are based on the modern ocean temperature and salinity data set of Levitus et al. (1994) and Levitus and Boyer (1994). These data were modified by Seidov et al. (1996) to cope with the loss of important fine structures in the Levitus data such as the Polar Front, a loss largely due to gridding long-term data series. For recent and more precise calibrations of the $\delta^{18}O$ signal of planktonic foraminifera, the new superior "Hydro-Base" data set (Curry 1996; Lozier et al. 1994; Simstich 1998) was employed. The data base for the proxy data used in this paper is outlined in Figure 4. More details on the transfer functions, quality and error ranges of the proxy data are given by Weinelt et al. (this volume). All proxy data are stored in the PANGAEA data bank <http://www.pangaea.de>.

Records and Mechanisms of Climatic Change on a Scale of Millennia to Centuries

The Ice-Core Record

The Milankovitch orbital cycles (Berger and Loutre 1991; Koç and Jansen 1994; Stoner et al. 1998) set the stage for the pronounced and global climate variability observed on time scales of decades to millennia. Such variability reaching back to 110,000 y B.P. was first demonstrated convincingly in the twin ice cores from the Greenland summit (Dansgaard et al. 1993; Grootes et al. 1993; Taylor et al. 1993). Counting of annual layers in the GISP2 ice core provided age control back to 50,000 years B.P. (Meese et al. 1994; Bender et al. 1994). Brief but large climate fluctuations, with warm phases lasting from approximately one hundred to several thousand years, are most prominent in marine isotope stage (MIS) 3, 58–30 ka (Fig. 5). The most striking features of these climate oscillations are rapid jumps from episodes of peak cold to phases of moderately warm climate, the Dansgaard-Oeschger (D-O) events. The jumps occur within less than 10–20 years (Dansgaard et al. 1989; Alley et al. 1993) and correspond to a warming of 7–15 °C / 20 °C (Johnsen et al. 1995; Cuffey et al. 1995). The D-O events terminate with a gradual deterioration of climate over time, ending with a jump back to peak cold.

The major sub-Milankovitch period in the GISP2 ice-core record is approximately 1470 years between 60 and 10 ka (Fig. 5; Grootes and Stuiver 1997). This periodicity weakens or disappears from the ice $\delta^{18}O$ record under extremely cold (MIS 2) and warm (MIS 1 and 5.1–5.3) conditions, but persists in chemical signals of atmospheric change in both high and low latitudes (O'Brien et al. 1995; Sirocko et al. 1996) in the GISP2 record dominated by a strong 2300-y cyclicity (Mayewski et al. 1997).

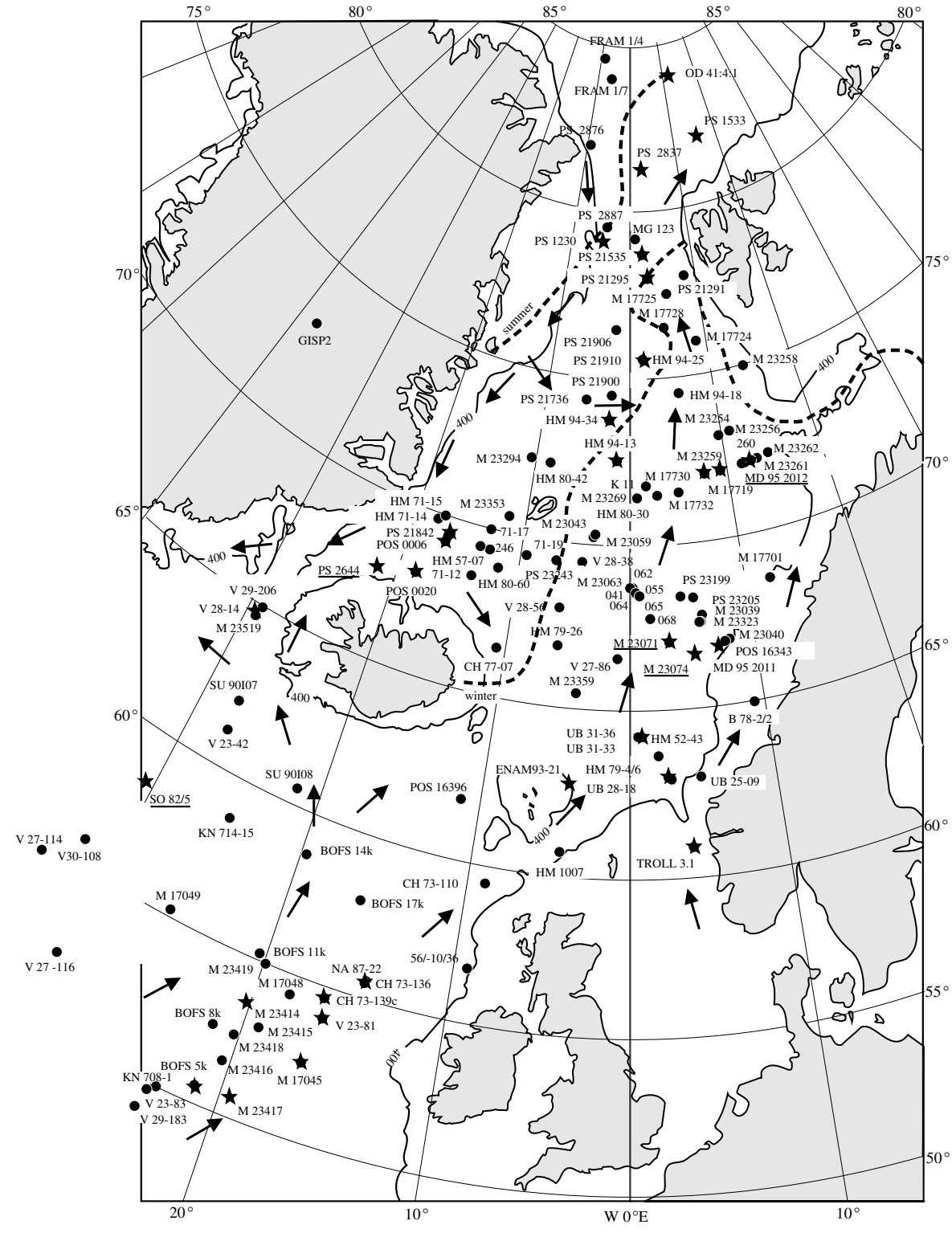

Fig. 2: Location of sediment cores (Sarnthein et al. 1995, supplemented by positions from Jung 1996; Rasmussen et al. 1996; Kroon et al. 1997; Völker et al. 1998; Dreger 1999; Spielhagen et al. 1997). Arrows mark main surface-water currents, broken lines modern sea-ice boundaries in the Nordic Seas during winter and summer. Asterisks mark cores with AMS ^{14}C age control. Underlined sites have time series with a resolution of several decades. See Table 2 for cores discussed in text

Table 1: Prime objectives in paleoceanography to be tested by proxydata and ocean modeling in the Northern North Atlantic

Objectives	References
1. Fundamental Modes of the Atlantic Ocean:	
• Assessing the principal modes of North Atlantic thermohaline circulation.	*(Bryan 1986; Ganopolski et al. 1998; Hopkins 1991; Manabe and Stouffer 1988; Marotzke and Willebrand 1991; Rahmstorf et al. 1996; Stommel 1961; Tziperman 1997)*
• Disclosing the LGM ice cover on the GIN Sea (and its sediment response):	
– as perennial?	*(Kellogg 1980; CLIMAP 1981; Duplessy, et al. 1991; Koç et al. 1993)*
– as seasonal?	*(Hebbeln et al. 1994; Sarnthein et al. 1995; Weinelt et al. 1996; Henrich 1998; Elliot et al. 1998)*
• Monitoring the LGM pathways of Atlantic surface water into the GIN Sea:	
– via the Denmark Strait	*(Sarnthein et al. 1995; Eiriksson et al. 1998)*
– via the Faeroe Channel	*(Kellogg 1980; Hebbeln et al. 1994; Rasmussen et al. 1996)*
– off southeast Iceland	*(Seidov et al. 1996; Schäfer-Neth 1998)*
• Quantifying	
(1) the absence or	*(Boyle and Keigwin 1987; Broecker et al. 1985; Hillaire-Marcel et al. 1994)*
(2) presence of LGM deepwater formation at North Atlantic sites in the	
– GIN Sea? (including the role of brine water formation)	*(Veum et al. 1992; Sarnthein et al. 1995; Seidov et al. 1996; Schäfer-Neth 1994)*
– Labrador and Irminger Seas?	*(Boyle 1992, 1995; Duplessy et al. 1988; Sarnthein et al. 1994; Labeyrie et al. 1995; Fichefet et al. 1994; Yu et al. 1996)*
(3) the role of the Mediterranean outflow in this process,	*(Zahn et al. 1997; Rahmstorf 1998)*
(4) and the sediment and benthic response in the deep sea.	*(Altenbach 1992; Struck 1995; McCave et al. 1995; Costello and Bauch 1997)*
• Quantifying North Atlantic deep-water formation along with Heinrich-type meltwater events.	*(Elliot et al. 1998; Labeyrie et al. 1995; Alley and Clark 1998; Rasmussen et al. 1996)*
• Investigating the transient storage of salt and heat in subtropical Atlantic surfacewaters during Heinrich meltwater events and its impact on the North Atlantic circulation.	*(Curry and Oppo 1997; Zahn et al. 1997; Seidov and Maslin 1996)*
2. Impact on the Marine Carbon Cycle:	
• Linking past changes in North Atlantic high-latitude plankton productivity	
– to the principal modes of thermohaline circulation?	*(Hass et al. this volume; Maslin et al. 1997)*
– to differential high-latitude insolation only?	*(Imbrie et al. 1992)*
– to nutrient supply along with Heinrich iceberg drifts?	*(Kiefer 1998)*
• Estimating the differential impact of North Atlantic circulation modes on	
– the global atmospheric CO_2 budget?	*(Broecker and Peng 1986, 1987, 1989; Broecker and Henderson 1998; Heinze et al. 1990)*
– the atmospheric ^{14}C content?	*(Stocker and Wright 1996; Schulz 1998; Hughen et al. 1998; Broecker 1998)*

Table 1 (continued):

3. Millennial-Scale Variability:	
• Establishing a joint centennial-scale chronostratigraphy of	
– marine and	*(Broecker et al. 1988; Bard 1998; Bard et al. 1993; Bond et al. 1993; Bond and Lotti 1995; Bokken and Hald 1996; Fronval et al. 1995; Fronval and Jansen 1997; Hughen et al. 1998; McManus et al. 1998; van Kreveld et al. 1996; Voelker et al. 1998)*
– ice-core records.	*(Grootes and Stuiver 1997; Johnsen et al. 1997)*
• Determining the sources and duration of Heinrich IRD supply to identify	*(Heinrich 1988)*
– the major Atlantic iceberg routes and "scrap yards",	*(Bond et al. 1992, 1993; Broecker et al. 1989; Cortijo et al. 1997; Dowdeswell et al. 1995; Grousset et al. 1993; Gwiazda et al. 1996a, b; Robinson et al. 1995)*
– potential leads and lags of surges from either North America, Iceland, Greenland, the British Islands, or Scandinavia as prime pacemaker of Heinrich events,	*(Alley and Clark 1998; McCabe and Clark 1998)*
– differential rates of meltwater production, and	*(Peltier 1994; Schäfer-Neth in prep.)*
– their differential regional impact on NADW formation.	*(Schäfer-Neth and Stattegger 1997)*
• Distinguishing	
– true periodicities in Dansgaard-Oeschger, Heinrich events, and "Bond cycles" from	(*Grootes and Stuiver 1997; McIntyre and Molfino 1996; Berger and Loutre 1997; Mayewski et al. 1997)*
– aperiodic events and "bands of variability".	*(Bond et al. 1997; Alley and Clark 1998)*
• Estimating the phase relationships of ocean and climate signals linked to Dansgaard-Oeschger events to uncover	
– the leads and lags between surface and deep-water signals,	*(Voelker 1999)*
– the origin and response of the antiphase relationship between northern and southern latitude climates.	*(Bard et al. 1997; Bender et al. 1994; Blunier et al. 1998; Charles et al. 1996; Stocker 1998)*
• Tracing the "origin" of Heinrich and "1500-y" climatic cycles as induced by	
– an internal ice oscillator as proposed for Heinrich events	*(MacAyeal 1993a, b; Hunt and Malin 1998)*
– an internal ocean/atmosphere oscillator?	*(Alley and Clark 1998; Broecker et al. 1990; Sakai and Peltier 1995; Winton 1993)*
– high or low latitude forcings?	*(Clement and Cane 1998; McIntyre and Molfino 1996)*
– northern and/or southern high-latitude forcing?	*(Bond et al. 1992; Broecker 1998; Charles et al. 1996; Little et al. 1997; Stocker et al. 1992)*
– and as leading to abrupt changes within less than 10 y.	*(Dansgaard et al. 1989; Alley et al. 1993)*
• Understanding the Younger Dryas cold spell as:	
– another Heinrich event with turned-off NADW production?	*(Boyle 1992; Boyle and Keigwin 1987; Broecker 1991; Keigwin and Jones 1995; Marchal et al. 1998)*
– just another D-O oscillation with little THC turnoff?	*(Charles and Fairbanks 1990; de Vernal et al. 1996; Jansen and Veum 1990; Sarnthein et al. 1994; Stocker and Wright 1996; Marchitto et al. 1998; Renssen 1997; Isarin et al. 1997)*
– a result of sudden Arctic meltwater supply?	*(Spielhagen et al. 1998)*
– an ongoing conundrum?	*(Sarnthein and Tiedemann 1990; Berger and Jansen 1995)*

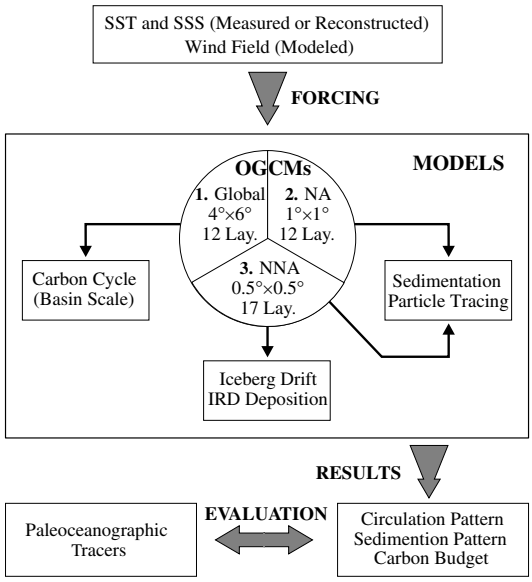

Fig. 3: Scheme of Ocean General Circulation Models (OGCMs) employed in this paper (modeling constraints in Table 3). NNA = Northern North Atlantic; NA = North Atlantic; Lay. = Layers; SST = sea surface temperature; SSS = sea surface salinity; IRD = Ice rafted debris

Potential Mechanisms of Rapid Change

To explain the severe and rapid temperature variations on top of Greenland many models have been put forward (Broecker et al. 1985; Broecker et al. 1990; Broecker 1991; Broecker and Denton 1991). Some models use internal ocean oscillators akin to El Niño events (e.g. Clement and Cane 1998, in prep.). Others employ ice- and/or meltwater-caused disturbances of ocean thermohaline circulation as external forcing in the presence of continental ice sheets in one way or another (MacAyeal 1993a, b; Paillard and Labeyrie 1994). The bifurcation process in the Rahmstorf model (1995), which uses an iceberg surge-derived low-salinity meltwater lid offshore Labrador to throttle Atlantic thermohaline circulation (THC), may come closest to reproducing the climate features observed. It shows that meltwater produces a prolonged initial phase of strong climatic instability, but little deterioration, lasting up to 700 years, followed by an abrupt cooling over approximately a decade. The cooling leads to a cold phase of undefined length, terminated by a nearly instantaneous transition back to stable warm conditions. This THC mechanism may also help to explain, by turning North Atlantic "heat piracy" off or on (Berger and Wefer 1996; Stocker 1998), the interhemispheric anti-phase relationship of short-term climate variability recently found in ice cores from parts of Antarctica (Blunier et al. 1998) and in South Atlantic sediment cores (Little et al. 1997).

Over the past ten years some of the postulated events of giant glacial surges during MIS 1–3 and the resulting tracks of iceberg armadas across the North Atlantic have been in fact identified as "Heinrich" layers of ice-rafted debris in many marine sediment cores (Heinrich 1988; Bond et al. 1992, 1993; Grousset et al. 1993; Cortijo et al. 1997). Moreover, Maslin et al. (1995), Rasmussen et al. (1996), Jung (1996), Vidal et al. (1997) and Elliot et al. (1998) have documented linkages between past

Table 2: Core locations mentioned in the text

Core	Latitude	Longitude	Water Depth
ENAM 93-21	62°44.0' N	03°59.9' W	1020 m
M 15612	44°21.6' N	26°32.6' W	3050 m
M 23071	67°05.1' N	02°54.5' E	1308 m
M 23259	72°02.0' N	09°16.0' E	2518 m
M 23414	53°32.2' N	20°17.3' W	2196 m
M 23415	53°10.7' N	19°08.7' W	2472 m
M 23416	51°34.1' N	20°00.0' W	3616 m
M 23417	50°40.1' N	19°25.9' W	3850 m
M 23418	52°33.0' N	20°20.0' W	2841 m
M 23419	54°57.7' N	19°45.3' W	1491 m
MD 95-2011	66°58.2' N	07°38.4' E	1048 m
MD 95-2012	72°09.1' N	11°26.1' E	2094 m
ODP 609	50°00.0' N	24°00.0' W	3900 m
PS 2644	67°52.0' N	21°45.9' W	778 m
SO 82-5	59°11.2' N	30°54.3' W	1416 m
V 23-81	54°15.0' N	16°50.0' W	2393 m

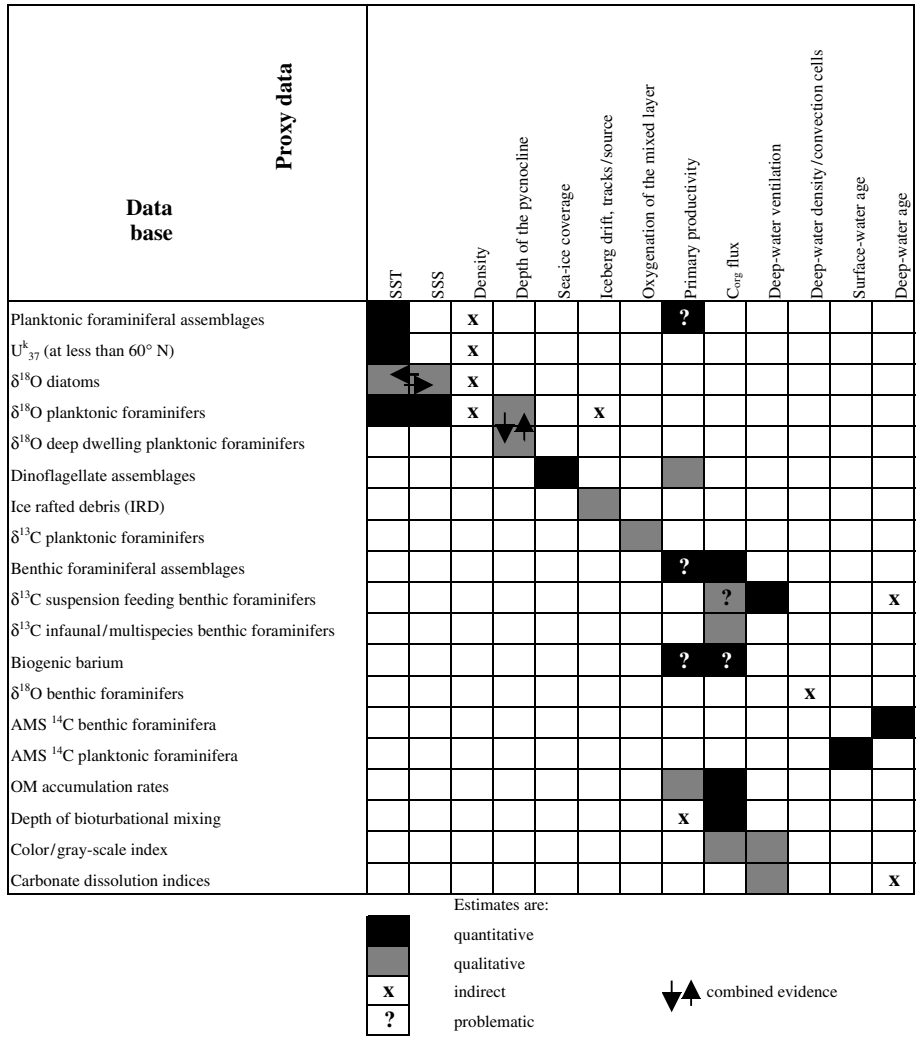

Fig. 4: Derivation and quality of paleoceanographic proxy data (Weinelt et al. this volume) used in this paper

changes in Atlantic THC and both the high-frequency D-O cycles and the low-frequency Heinrich events superimposed.

Variations in Surface-Water Oceanography

A number of new paleoceanographic records with an ultrahigh resolution of 20–80 years over MIS 2–3 (Fig. 5) define the various processes linked to D-O cycles on a more precise time scale (Table 4) and thus help to better constrain the origin of Heinrich (H) and D-O events. The records stem from a four-core transect extending from the Irminger Sea across the Icelandic Sea to the northeastern Norwegian Sea, from 59°–72° N (Fig. 2). Age control is based both on tuning characteristic features of SST, planktonic $\delta^{18}O$ minima, or IRD records to the GISP2 ice record and on a total of more than 320 accelerator mass spectrometry (AMS) ^{14}C ages (Voelker et al. 1998; Dreger 1999; van Kreveld et al. subm.). In this manner the age uncertainty of the (narrowly spaced) age control points may reach one-third of a D-O cycle (500 y), in most cases 50–100 y (equal to one sample spacing) relative to the GISP2 record, which is sufficient for high-resolution phase analyses within the 1460- (or 1470-)y frequency band (Fig. 6).

Based on this transect summer sea-surface temperatures (SST) in the Nordic Seas have only varied at the low level of 1–5 °C from 60–11.6 cal. ka (Fig. 5). Hence, the short-term but marked planktonic $\delta^{18}O$ minima in cores PS2644, M23071 and MD952012,

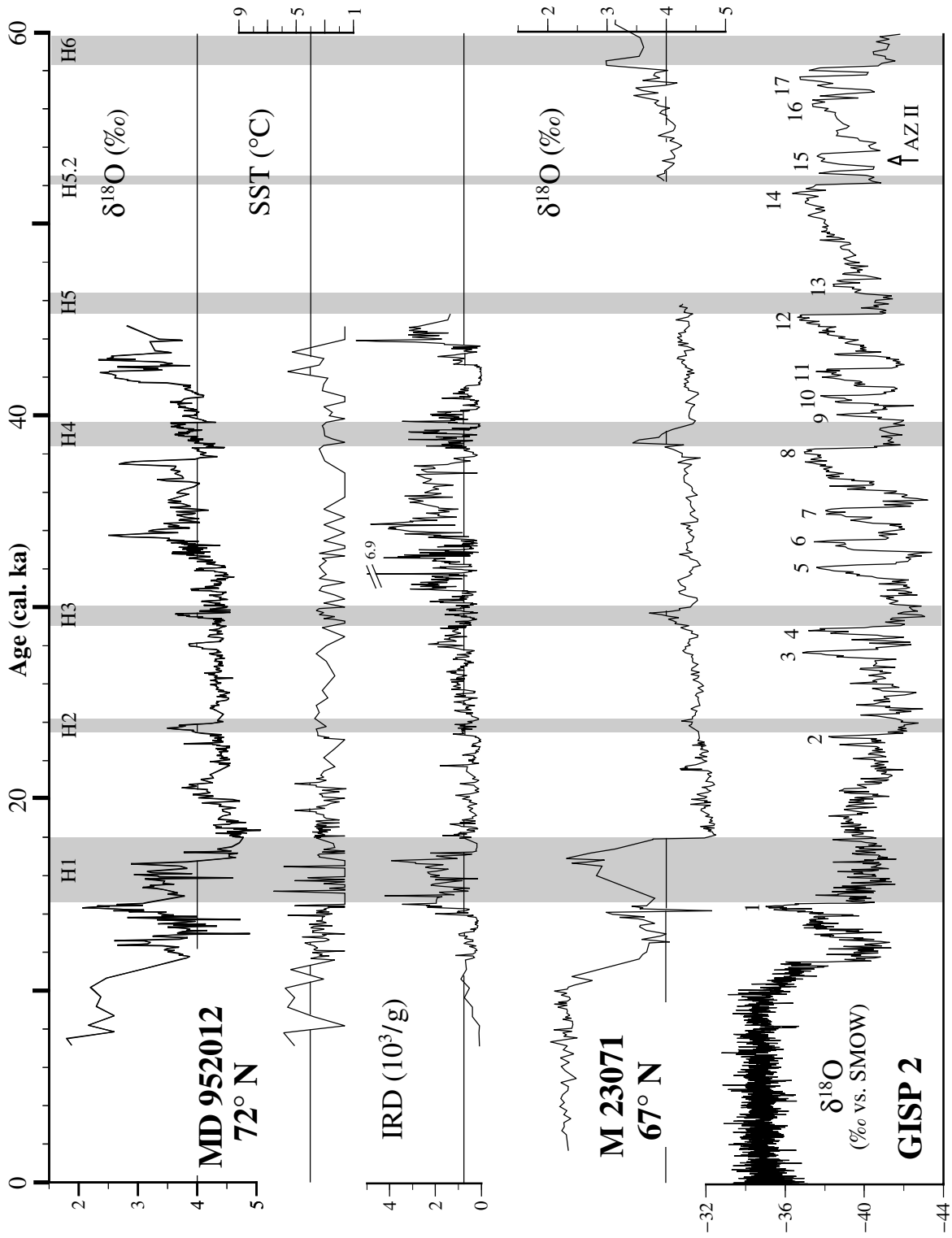

Fig. 5: Southwest-northeast running transect (see Fig. 2 and Table 2) of marine sediment records sampled in cm increments (MD952012: 20–500 cm/ky; 23071: 7–16 cm/ky; PS2644: 20 cm/ky; SO82-5: 12 cm/ky) of climatic change in the northern North Atlantic and GISP2 $\delta^{18}O$ record of temperature changes on Greenland summit (numbers are Dansgaard-Oeschger events; Grootes and Stuiver 1997). $\delta^{18}O$ minima of planktonic *N. pachyderma* (sin) reflect low-salinity meltwater spikes, where SST values (based on planktonic foraminifera census counts) are low

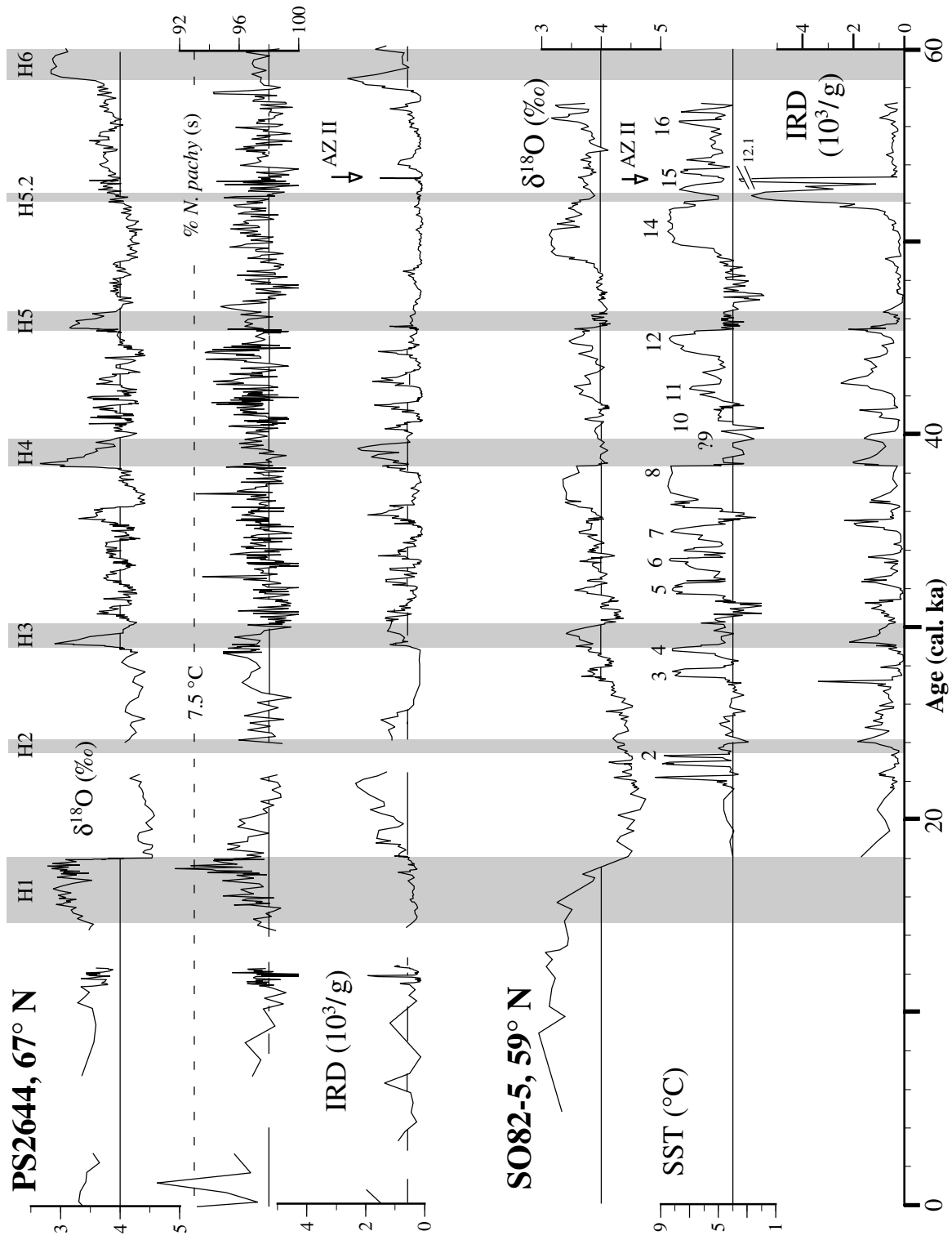

Fig. 5 (continued): Gray bars mark Heinrich events H1–H6. AZ 2 = Ash Zone II. IRD = Ice rafted debris. N. pachy (s) = *N. pachyderma* (sin). Time scale based on total of > 320 AMS ^{14}C ages and on fine tuning to annual layer counted GISP2 time scale (Meese et al. 1994), with relative age uncertainties of 50–100 y, rarely up to 500 y (Voelker et al. 1998; Dreger 1999; van Kreveld et al. subm.). Horizontal lines serve intercore comparison of data

Table 3a: Ocean circulation models employed and modeling constraints

Ocean Circulation	**1. Global**	**2. North Atlantic (NA)**	**3. Northern North Atlantic (NNA)**
Model Type	MOM (Pacanowski et al. 1993)	IM (Seidov 1996)	MOM (Pacanowski et al. 1993)
Setup Description	Seidov and Haupt (1999)	Seidov et al. (1996)	Schäfer-Neth (1998)
Parameters			
Resolution (lon. × lat.) / Vertical Layers	6° × 4° / 12	1° × 1° / 12	0.5° × 0.5° / 17
Horizontal Diffusivity / Viscosity [$cm^2\ s^{-1}$]	2×10^7 / 2.5×10^9	1×10^7 / nonexistent	5×10^6 / 5×10^8
Vertical Diffusivity / Viscosity [$cm^2\ s^{-1}$]	1.0 / 10.0	1.0 / 2.5	1.0 / 1.0
Surface Relaxation Time [d]	50	50	30
Surface Layer Thickness [m]	100	100	50
Tracer Time Step [d]	1	2	0.5
Modern Forcing	* = Summer ** = Winter	*** = Annual Mean	
SST	Levitus and Boyer (1994)***	Idem***	Idem**
SSS	Levitus et al. (1994)***	Idem***	Idem**
Wind	Lorenz et al. (1996)***	Lautenschlager (unpubl.)***	Hellermann and Rosenstein (1983)**
Integration Time [a]	10000	1200	500
LGM Forcing			
SST from planktonic foraminifera census counts	Sarnthein et al. (1995); Schulz (1995); Weinelt et al. (1996); CLIMAP (1981)***	Idem***	Weinelt et al. (1996); CLIMAP (1981); supplemented by new Kiel data*
SSS from foraminifera $\delta^{18}O$ and SST	Duplessy (1982); Duplessy et al. (1991, 1996)***	Sarnthein et al. (1995); Weinelt et al. (1996)***	Sarnthein et al. (1995); Weinelt et al. (1996); supplemented by new Kiel data*
Wind	Lorenz et al. (1996)***	Lautenschlager (unpubl.)***	Hoffmann (unpubl.)*
Integration Time [a]	8500	950	500
Meltwater Forcing			
SST from planktonic foraminifera census counts / Heat Flux	Sarnthein et al. (1995); Schulz (1995); Weinelt et al. (1996)***	Idem***	Diagnosed LGM fluxes*
SSS from foraminifera $\delta^{18}O$ and SST / Freshwater Flux	Sarnthein et al. (1995); Weinelt et al. (1996) plus LGM data***	Idem***	Freshwater input (from new Kiel data) added to diagnosed LGM fluxes*
Wind	as for LGM***	Idem***	Idem*
Integration Time [a]	1200	1050	50–100
Sea Ice	No air-sea heat and momentum fluxes if SST drops below −1.88 °C.		

Table 3b: Models of iceberg drift, sediment dispersal and the oceanic carbon cycle

Icebergs, IRD Deposition (Schäfer-Neth and Stattegger 1998)
- Free drifting cylindrical icebergs (diameter = 10 km; height = 300 m)
- IRD deposition proportional to iceberg melt rate (IRD concentration = 1‰ per volume)
- Techniques:
  - ocean-iceberg feedbacks including:
    - currents (passive drift transport)
    - temperature (using an empirical temperature vs. melt-rate relationship)
    - heat transfer from ocean to icebergs (proportional to amount of melting ice)
    - meltwater runoff from the icebergs into the ocean
  - iceberg drift velocity enhanced by wind; proportional to wind speed (based on observations)

Sedimentation, Particle Tracing (Haupt et al. 1998)
- Sediment volume transport and pelagic sediment dynamics
- Sediment distribution pattern on the sea floor
- Pathways of particle transport
- Routes of the major ocean currents and/or transports of settling particles
- Techniques:
  - semi-Lagrangian formulation
  - particles with uniform settling velocity (0.05 cm s^{-1})
  - sedimentation and erosion rates based on observations (flocculation ignored)
  - benthic boundary layer with smooth topography (thickness = 1 cm)
  - fluvial and aeolian sediment sources
  - particle transport velocity affected by bottom slope

Carbon Cycle (Schulz et al. in press)
- Ocean-atmosphere distribution of inorganic carbon and carbon isotopes ($\delta^{13}C$, $\Delta^{14}C$)
- Techniques:
  - formation/remineralization of particulate organic matter and $CaCO_3$-skeletons
  - export production as function of nutrients available in surface water
  - temperature-dependent isotope fractionation during gas exchange
  - isotopic composition of particulate organic matter as function of the ambient CO_2-concentration
- Resolution: 5 major oceanic basins (12 layers) plus homogeneous atmosphere
- Forcing: Water fluxes derived from global OGCM velocity fields (annual average)

Table 4: Timing of Heinrich Events and the LGM on ^{14}C and calendar time scales, primarily based on newly ^{14}C dated IRD and $\delta^{18}O$ meltwater records in cores 23071 and PS2644, choosing dates with a minimum ^{14}C reservoir effect. Details of the location of Heinrich events in the marine sediment record and their definition in GISP2 as in Figure 5 (Voelker et al. 1998; Voelker 1999)

Heinrich-Event	Marine ^{14}C Ages (corr. for −400 y)	Calendar Age (GISP2)	Interval (ky) (between age means of H.E.)
H1	> 12.8–14.8 ka	14.67–18.1 ka (!)	
			Δ 7.4
(LGM)	(15.0–18.0 ka)	(18.0–21.5 ka)	
H2	20.4–21.0 ka	23.4–24.2 ka	
			Δ 5.8
H3	25.6–26.4 ka	29.0–30.2 ka	
			Δ 9.6
H4	32.4–34.2 ka	38.4 – < 40.0 ka	
			Δ 6.7
H5	43.5–44.4 ka	45.4–46.4 ka	
			Δ 13.6 = 2 · 6.8
H6	> 57 ka	58.3 – about 60 ka	
			Average: 7.2 ± 2.4

(for spatial variations of ^{14}C ages at base of H4 compare Fig. 10)

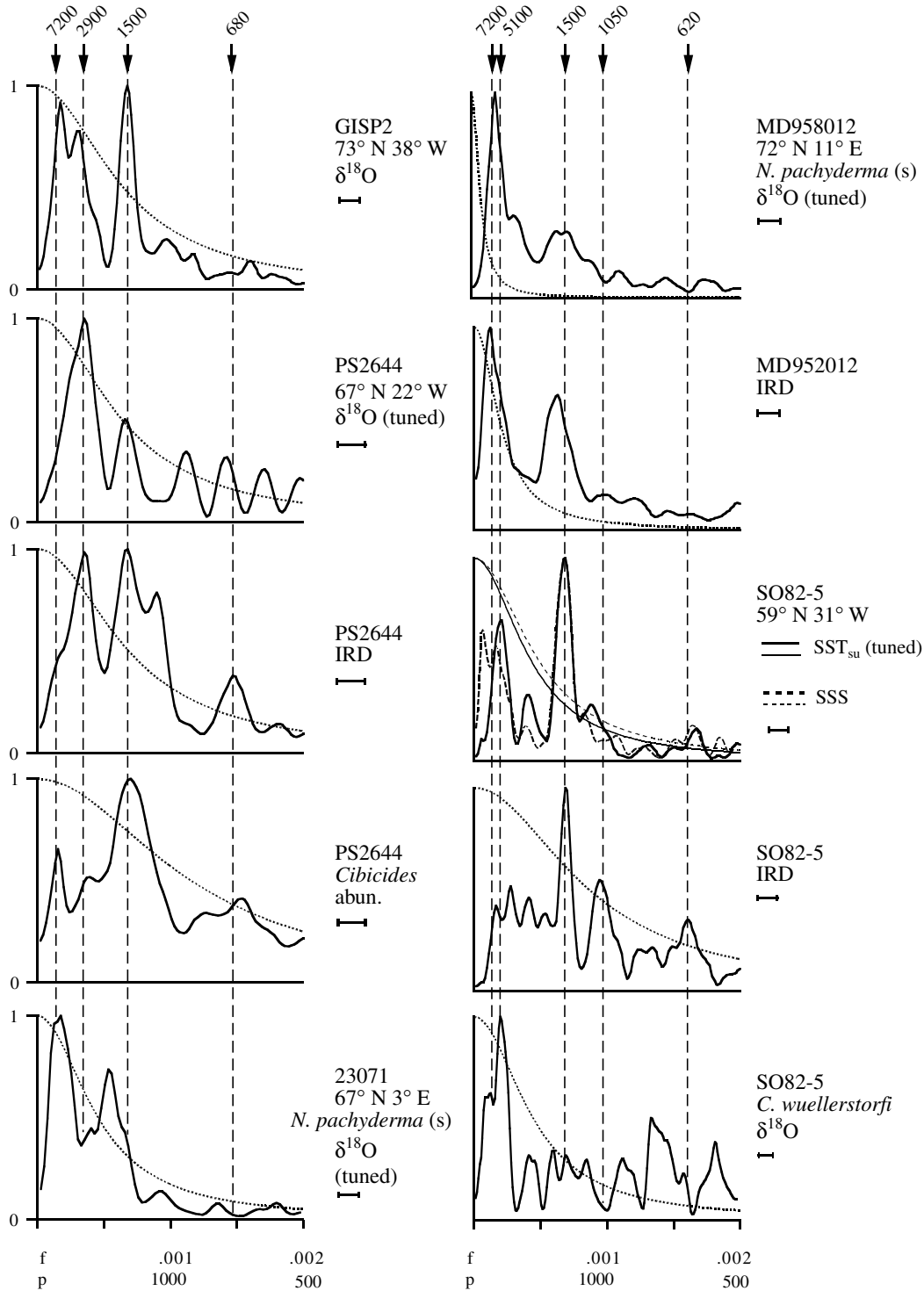

Fig. 6: Centennial-to-millennial-scale periodicities (with spectral power normalized to 1) in the GISP2 δ^{18}O-record and in marine sediment records of climatic change (f = frequency; p = periods; horizontal bars = bandwidth; further abbreviations see Figure 5, where most records are shown in the time domain). Core locations in Table 2. Abundance (abun.) of *Cibicides* at site PS2644 reflects intensity of overflow, δ^{18}O of *C. wuellerstorfi* brine-water signals in the deep water. Dominant Dansgaard-Oeschger cycles are marked at 1500 y, other cyclicities at 620–680 y, 1050 y, 2900 y, 5100 y and 7200 y. Power spectra calculated with Spectrum program (Schulz and Stattegger 1997), dotted 80 % confidence line with AnalySerie program (Paillard et al. 1996)

which comprise shifts of up to 1.5‰, in many cases opposed to the SST trend, are largely ascribed to short-term meltwater pulses. The larger $\delta^{18}O$ spikes correspond to Heinrich events H1–H6, as confirmed by coeval IRD spikes and planktonic foraminiferal $\delta^{13}C$ minima (lit. cit.). Following the ice-surge model, meltwater pulses have been connected to the cold episodes in the age-calibrated isotopic temperature record of GISP2 to create a common time scale (lit. cit.). In contrast to the Nordic Seas, summer SST in the warm Irminger Current southwest of Iceland (core SO82-5) vary over a broad range of < 2–9 °C and depict in great detail the rapid warmings and coolings of each D-O cycle in the ice record. However, the $\delta^{18}O$ record in this part of the Irminger Sea remains largely unaffected by meltwater, except for a distinct meltwater signal at H3 (Fig. 5; van Kreveld et al. subm.).

The surface-water records of MIS 2–3 also reveal striking zonal difference (Fig. 5): In the west, the IRD and $\delta^{18}O$ records of cores SO82-5 and PS2644 were able to depict every single D-O cycle with distinct amplitudes. In the east, in cores M23071 and MD952012 from the Norwegian Sea, most $\delta^{18}O$ oscillations rarely exceed the noise level and can only be recognized by comparison with parallel, stronger variations in planktonic $\delta^{13}C$ (Völker 1999). In addition to these, several wide-spaced, modest $\delta^{18}O$ excursions reflect Heinrich meltwater events H3 and H4 and, more pronouncedly, H1 and H6. H1 spikes are most prominent near the Faeroe Islands (ENAM 93–21) and to the west of the Barents shelf (23259, MD952012; compare Fig. 12c). Here, however, the onset of the event was possibly delayed by 1500 ^{14}C years (Fig. 7; Dreger 1999).

In conclusion, the origin of frequent, possibly meltwater-induced, climate disturbances during MIS 2–3 may be more closely constrained, in part, similar to Elliot et al. (1998): Surging ice sheets on Greenland and Iceland, easily traced by hematite-stained quartz (Bond et al. 1997) and volcanic glass produced flows of meltwater and icebergs along with *each* D-O stadial, whereas surges from Canada, traced by dolomite debris, and from Europe only accentuated some major stadials, the Heinrich events. Surges from the Barents Shelf contributed particularly to H6 and late H1. Moreover, since basaltic glass from Iceland always increased prior to the increase of any other IRD in the Heinrich layers (Bond and Lotti 1995), it is evident that the Nordic iceberg discharge clearly preceded, thus in some way triggered ice surges and IRD input from North America and elsewhere at any stadial event.

Variations in North Atlantic Deep Water Oceanography

The variations in surface-water oceanography outlined above correspond to major changes in the origin and ventilation of North Atlantic Deep and Intermediate Water (Rasmussen et al. 1996). Jung (1996) traces their spatial variability along the southern slope of the Rockall Plateau in the (epi-) benthic stable-isotope records of six cores (Figs. 2 and 8). The records form a 1-D time transect from 1500–3800 m depth over the last 60 ky, with a mean time resolution of 350 – > 1000 y, rising to 160–250 y across the H events.

Beyond some ongoing problems in precisely matching the "wiggle-waggles" of the six stable-isotope records on centennial time scales, major long-term change can be identified between (1) the warm and fairly stable THC regime over the last 11.6 ky, i.e., since the end of the Younger Dryas, and (2) the highly instable regime of MIS 2–3, 11.6–60 ka, with abundant bottom water momentarily advected from sources in the Southern Ocean (SSBW; $\delta^{13}C$ values of < 0.4 – < 0.8‰), which ascended up to < 2.6–2.0 km depth, in contrast to depths of > 3.6 km today. Nevertheless, the glacial regime of MIS 2–3 also finally reached some stability between H1 and H2 (Fig. 8a).

(3) Superimposed upon these long-term trends in deep-water chemistry, flickering extreme ventilation minima (< 0.2 – < 0.4‰ $\delta^{13}C$) record the incursion of SSBW along with the Heinrich events (including a Heinrich-style event H5.2 prior to D-O event 14) and many other stadials. On the other hand, the short-term $\delta^{13}C$-ventilation maxima reaching down to > 3 km (blue spikes > 0.8‰ in Fig. 8a) are characteristic of North Atlantic Deep Water (NADW) and match most warm D-O events, such as D-O 5–8 and 11–14 between H3 and H5.2.

(4) In parallel, the $\delta^{18}O$ transect in Figure 8b reveals some short-term but extreme $\delta^{18}O$ minima (Δ 0.5–1.0‰), extending across all water depths during H1, H3–H6 and once more, during the early LGM (confined to less than 2300 m w.d.). Jansen and Veum (1990) first suggested that these synglacial $\delta^{18}O$ minima may record cold brine-water spikes. They bear an excellent, barely fractionated $\delta^{18}O$ signal of extensive seasonal sea-ice formation which was tied to the highly ^{18}O depleted meltwater lids of iceberg flotillas during Heinrich and, less importantly, during other D-O stadials. The deep-water records of Figure 8 thus closely match the various surface-water records of frequent meltwater incursions into the North Atlantic during MIS 2–3.

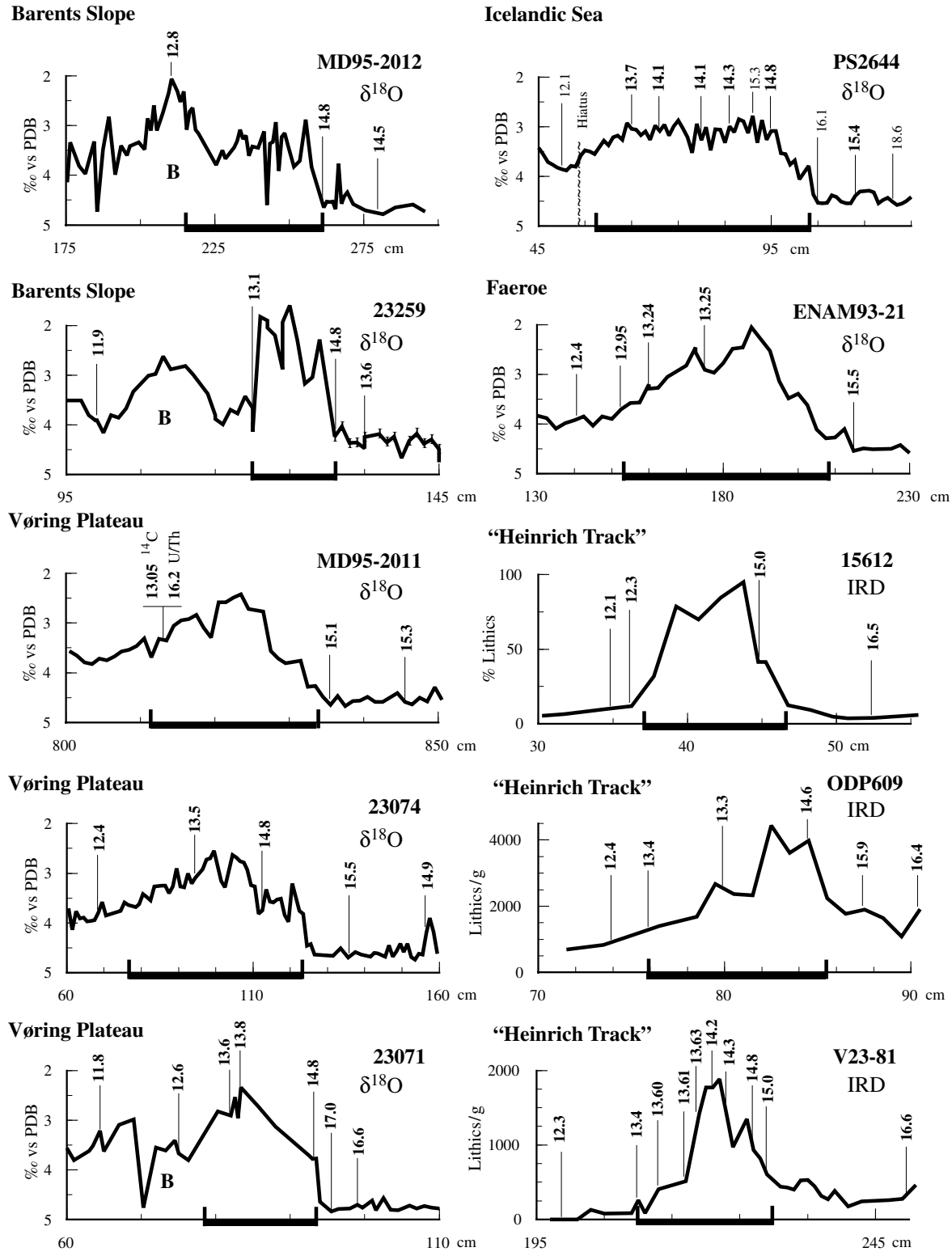

Fig. 7: ^{14}C ages (ka; corrected for a ^{14}C reservoir age of 400 y) and a U/Th age constraining the age window of Heinrich meltwater event H1 as defined by IRD layers and $\delta^{18}O$ meltwater signals. Bold numbers in core PS2644 are benthic ages, non-bold numbers are higher planktonic ages, biased by an extreme ^{14}C reservoir effect. Core locations in Table 2

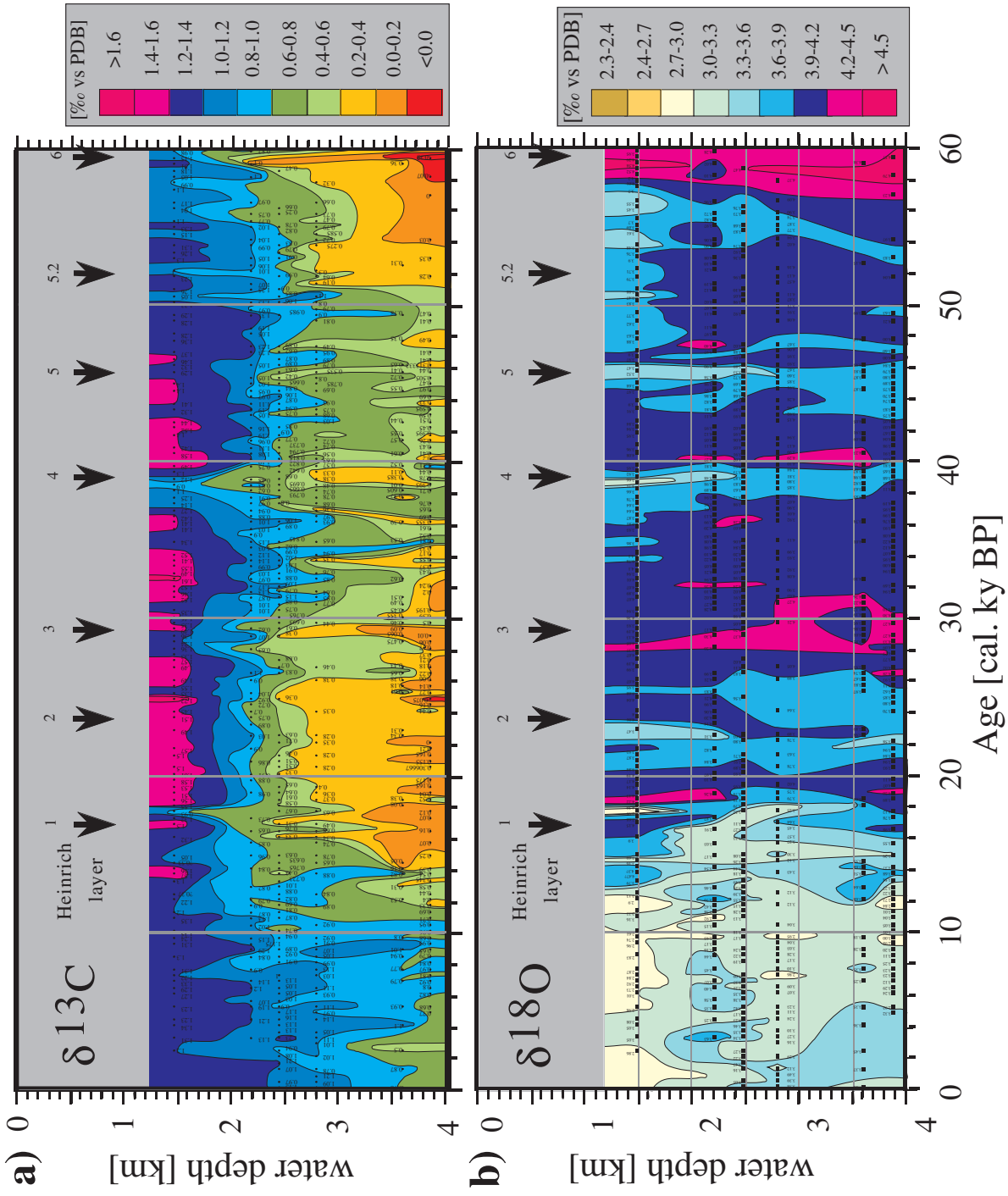

Fig. 8: Vertical 1-D paleoceanographic time transect of the last 60 ka, showing **a)** a $\delta^{13}C$ record of changes in deep-water ventilation and **b)** a $\delta^{18}O$ record of changes in temperature and brine-water content. Records are based on *C. wuellerstorfi* in sediment cores 23214–23419 from the southern flank of the Rockall Plateau (core locations in Table 2 and Fig. 2). Stable isotope data correspond to 400-y averages and were linearly interpolated. $\delta^{18}O$ values were corrected to the ambient sea-water equilibrium by +0.64‰ (Ganssen 1983) and for global ice effect (Fairbanks 1989; Labeyrie et al. 1987). Arrows mark Heinrich events H1–H6. Joint stratigraphy based on AMS-^{14}C ages and IRD layers (Jung 1996; Weinelt et al. unpubl. data)

D-O and Heinrich Events in the Spectral Domain

Detailed records of THC variability provide a new age basis for calibrating Heinrich events on the calendar time scale (Table 4; Voelker et al. 1998). In part, the new ages differ considerably from previous estimates (Bond et al. 1993; Cortijo 1995; Elliot et al. 1998). From H1 to H5 the average time span between two successive Heinrich events in the records presented here amounts to 7.4 ka, but increases to 13.6 ky between H5 and H6. If the probable Heinrich event 5.2 between H5 and H6 is included, prior to D-O event 14 near 52 ka (Fig. 8), the average spacing between Heinrich events 1 and 6 drops to a relatively uniform time span of 7.2 ± 2.4 ky, equal to several D-O cycles. The postulated "5.2" event is indeed supported by major IRD layers found at the respective depths in various cores from the Rockall Bank (Jung 1996) and in core SO82-5 (Fig. 5).

In the spectral domain, however, dominant power is centered on 1.5 ky (1460–1510 years) for most of the marine proxy records in the four cores, such as for GISP2 (Fig. 6; Grootes and Stuiver 1997; van Kreveld et al. subm.; Völker 1999). Further prominent periodicities occur near 2.9 (such as with D-O cycles 8, 12 and 14) and 5.1 ky, probably multiples of the 1500-y cycle. A weak periodicity near 620–740 years may reflect a harmonic. A minor periodicity persists near 1.05 ky, possibly a harmonic of the 2.3 ky cycle found by Mayewski et al. (1997). Unexpectedly, little power is centered near 7.2 ky for the Heinrich events, except for the stable isotope records of core 23071, salinity at site SO82-5 and the IRD record of core MD952012 (Fig. 6).

The 1480-/2900-y cycles in the marine sediment record rarely show the characteristic asymmetry of D-O cycles in the Greenland ice records (Fig. 5; SO82-5). As is the case on Greenland, they also begin with an abrupt jump from peak cold to moderately warm climate, which in some cases is interrupted by a very short "Younger Dryas-style" setback (van Kreveld et al. subm.). The warm interstadials, however, have each persisted over a few hundred up to 1,500 years, prior to jumping back directly to peak cold.

In the frequency domain (Fig. 9), the maximum coolings at site SO82-5 lie in phase with SSS minima, which means with meltwater injections to the Irminger Sea (van Kreveld et al. subm.). This evidence clearly supports the models invoking glacial surges and meltwater as the ultimate source of climatic instability during MIS 3 (Broecker et al. 1990; MacAyeal 1993a, b; Paillard and Labeyrie 1994; Rahmstorf 1995). On the other hand, the 240-y lag of IRD spikes vs. sea-surface cooling at site SO82-5, similar to early findings by Bond and Lotti (1995), appears to be opposed to these models, but is of little significance. Not the icebergs but their meltwater injections to the specific sites of deep-water convection (such as the Irminger and Labrador Seas) are crucial in throttling Atlantic THC. Over the first 250 years, the melting icebergs from East Greenland were obviously jammed in the narrow Denmark Strait and advanced to the south only later, after size reduction. This view is supported by the timing of IRD spikes to the north of the Denmark Strait, at site PS2644, where they appear > 100 years earlier, nearly in phase with the SSS minima to the south and cooling (Fig. 9; Voelker 1999).

The IRD spikes, in turn, lead (1) the planktonic $\delta^{13}C$ minima by nearly 300 y, recording a maximum in surface-water stratification, (2) the related brine-water signals in the benthic $\delta^{18}O$ record by approximately 330 y, and (3) the final abrupt returns to maximum warmth by 460 y (van Kreveld et al. subm.). Accordingly, the brine-water signals lead the D-O events of abrupt warming by less than 130 y, nearly within our sampling resolution. Based on these leads and lags it is evident that intensive brine-water formation has finally triggered the enigmatic abrupt onset of THC and flushing of the deep Atlantic within approximately a decade through entraining further deep water and, in consequence, further surface water from farther south. Thereby, a long-term slow-down or even reversal of THC during the last third of the D-O cycles was suddenly ended, initiating the D-O events which remain unexplained.

Résumé on Processes Driving the 1500-Year D-O Cycles

The spatial and temporal patterns in short-term SST variability and iceberg-derived meltwater injections yield a number of features in North Atlantic paleoceanography, which in total may have controlled climatic variability between 60 and 10 ka at periodicities of centuries to millennia:

- Based on clear phase relationships (Fig. 9) it is clear that, in harmony with various models, the rapid cooling of the D-O stadials was indeed linked to meltwater injections throttling the convection of NADW. As surmised by Bond and Lotti (1995) this meltwater primarily originated from icebergs surging from Iceland, East Greenland and/or farther north, as shown by (1) the dispersal of low SSS, (2) a persistent input of hematite-stained quartz to the Irminger Sea during D-O stadials (van Kreveld et al. subm.), and (3) a decline in the accumulation rates of IRD from the Icelandic to

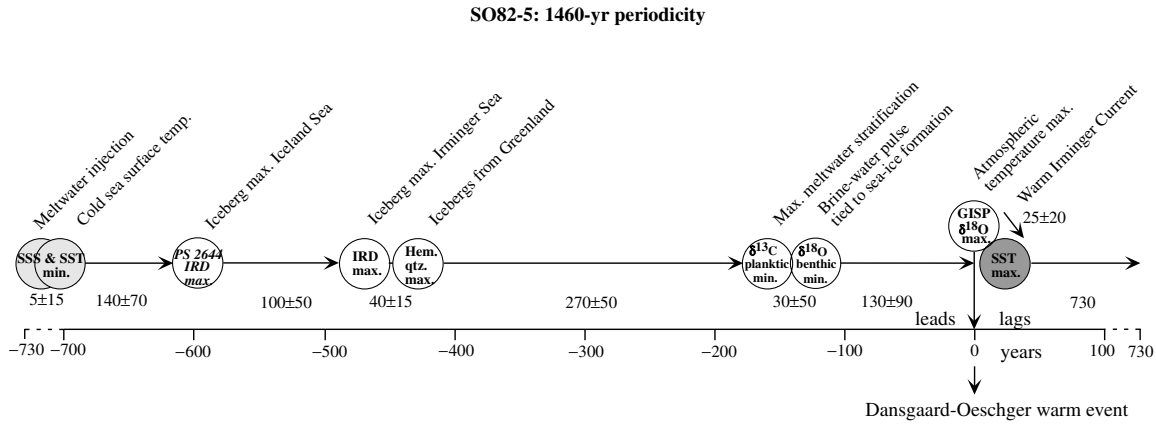

Fig. 9: Mean temporal leads of iceberg, meltwater and brine-water events at site SO82-5 in the North Atlantic (van Kreveld et al. subm.; Voelker 1999; core locations in Table 2 and Fig. 2) with respect to maximum warming in the Irminger Current and on Greenland summit (GISP2; in phase) in a 1460-y D-O cycle. Numbers indicate internal response time in years and single-phase errors (based on coherent signals only)

the Irminger Sea by a factor of ~ 2 (Fig. 5; PS2644 vs. SO82-5, when data are supplemented by differential sedimentation rates). Thus, internal binge-purge processes in parts of the East Greenland ice sheet with a time constant of 1500/3000 years may have acted as *the* pacemaker of global cooling.

- Prior to reaching the "open" North Atlantic via the Irminger Sea, most icebergs from Greenland were probably jammed in the Denmark Strait for nearly 250 years, as shown by the lead of IRD and SSS signals in the western Icelandic Sea.
- In the Irminger and Icelandic Seas prominent IRD spikes equally mark both the Heinrich events and the other cold D-O stadials. Therefore, no basic but only gradual differences in the origin of average D-O stadials and the major Heinrich events can be seen, apparently accentuating some "normal" D-O stadials.
- Based on a phase lead of Icelandic IRD, each Heinrich event was probably induced by a slight sea-level rise proceeding from initial D-O surges from Iceland and East Greenland and triggering much larger surges from major ice sheets near sea level with an internal time constant of ~ 7.2 ky. In particular, H5, H4 and H2 resulted from great iceberg and meltwater injections from eastern Canada, in addition to abundant meltwater in the North Iceland and East Greenland Currents (Grousset et al. 1993; Gwiazda et al. 1996b; Cortijo et al. 1997). Only during H3 did the flux of meltwater and icebergs from East Greenland, which passed across the Icelandic and Irminger Seas, dominate any other Heinrich meltwater discharge (in harmony Grousset et al. 1993). Relatively modest traces of European meltwater and IRD occur in the Norwegian Sea, except for H6 and H1. Here most prominent $\delta^{18}O$ meltwater signals southwest of the Barents shelf (Figs. 5, 7 and 12c; Sarnthein et al. 1995) suggest large surges from a glaciated Barents shelf (Laberg and Vorren 1995; Landvik et al. 1998), which produced the most extended and pronounced reversals in Atlantic THC together with major ice rafting from Labrador to the mid-latitudes, marking the end of glacial stages 4 and 2.
- In view of its extremely short phase lead (< 130 y in core SO82-5; Fig. 9) to the SST maximum in the D-O cycles, intensive brine-water convection in the northern North Atlantic is considered to be the crucial process which has finally entrained warm surface water from the subtropics and thereby triggered the resumption of the "conveyor belt" and rapid warming, the "jump" characteristic of D-O events which each corresponded to a general recovery of northern hemisphere climate.
- However, a major problem remains unsolved, i.e. how the mechanisms of D-O cycles during MIS 2–3 continued over the Holocene (Sirocko et al. 1996; Bond et al. 1997; Wang et al. 1999) and MIS 5 (Ninnemann et al. 1999), since no major surges are known at these times (only once, 8.2 cal. ka) and the climate proxies on Greenland exhibit much smaller variability on a scale of centuries to millennia during the Holocene than was the case during MIS 2–3 (Grootes and Stuiver 1997).

Age of the LGM and Heinrich 1 Time Slices: Problems by the ^{14}C Reservoir Effect

Finally, the high-resolution time series has permitted improvements on the age definition of two time slices

which represent the most prominent climatic extremes over the last 60 ky, the Last Glacial Maximum (LGM) and Heinrich event 1. Both time slices present intervals of short-term relative climatic stability, sufficiently long for assembling basin- and ocean-wide sets of paleoceanographic data at sedimentation rates of > 2.5 – > 5.0 cm/ky to parameterize and validate general ocean circulation models discussed in the section below. In the North Atlantic the LGM is clearly defined at the age interval between D-O interstadial 2 and Heinrich event 1, that is, at 18–15 ^{14}C ka (equal to approximately 22–18.1 cal. ka; Fig. 5; Table 3). However, the precise age boundaries of Heinrich event 1 appear to be more controversial.

In cores from the Rockall Plateau and mid-Atlantic ridge, directly below the "Heinrich IRD track" (Bond and Lotti 1995), the base of IRD layer H1 is largely coeval with the abrupt decrease in benthic and planktonic δ^{13}C and δ^{18}O values (Fig. 7; Jung 1996; Vidal et al. 1997; Kiefer 1998; Chapman and Shackleton 1998). This is different from the upper continental margin of Portugal, where Zahn et al. (1997) found an enigmatic 1000-y lag in the local IRD signal vs. the benthic and planktonic δ^{18}O and δ^{13}C signals at 1100 m water depth.

Based on rough ^{14}C dates of planktonic *N. pachyderma* (sin), H1 first began northwest of Iceland 16.1 ^{14}C ka, in the central North Atlantic approximately 15 ^{14}C ka and west of the Barents shelf only < 14.5 / < 13.6 ^{14}C ka (Fig. 7; Sarnthein et al. 1995; Völker et al. 1998; Dreger 1999). This age transgression may only partially reflect a real time lag between initial ice surges from Iceland and/or Greenland, subsequent surges from Labrador, and a final response of the ice sheet on the Barents shelf, where Laberg and Vorren (1996) dated a last glacial advance near 13.7 ^{14}C ka.

In part, age differences in Figure 7 merely reflect a variable ^{14}C reservoir effect in different marine regions, implying that the onset of Heinrich 1 may have been coeval all over the northern North Atlantic. This model is supported (1) by the benthic ^{14}C ages in core PS2644 northwest of Iceland which are systematically younger than the planktonic ^{14}C ages measured in parallel and fully confirm the general base age of approximately 15 ka. (2) Similar to Heinrich 1, extremely variable ^{14}C reservoir effects also mark the base of the Heinrich-4 IRD layers and meltwater signals, supposed to be generated synchronously across the northern North Atlantic. Here, local shifts in ^{14}C age reach as much as 2.5 ky, with maximum ages directly below the center of the Heinrich meltwater track as traced by Cortijo et al. (1997) and minimum ages along its periphery (Fig. 10). This small-scale variability in ^{14}C reservoir ages may come from long-term suppressing exchange with the atmosphere. It may also result from the wind-driven transport of Heinrich icebergs, entrenching several hundred meters deep below the sea surface (down to > 800 m according to sidescan records of plough marks; von Bodungen et al. 1988) and inducing multiple processes to vertically admix "old" intermediate water of unknown origin. In addition, the extensive release of "old" CO_2 and CH_4 from air bubbles in melting iceberg flotillas may significantly increase the local reservoir age by as much as > 5000 y (Domack et al. 1989).

However, low planktonic ^{14}C ages in front of the Barents shelf, which put the base of the most prominent local "H1" meltwater spike at much less than 14.5 and at less than 13.6 ka (Fig. 7, cores MD952012 and 23259), indeed reflect a date which is significantly younger than the base of H1 in the North Atlantic elsewhere (Dreger 1999; in accordance with Vorren and Laberg 1996). The higher ^{14}C age of 14.8 ky in core MD952012 is ascribed to the local ^{14}C reservoir effect, rising with the onset of meltwater discharge. Based on an age reversal in core 23074, the same bias can be assumed for most ^{14}C ages near the base of H1 in neighboring cores 23071 and 23074 as well as MD952011 from the Vøring Plateau. Here the low age of "14.9 ka", dating a tiny precursor meltwater spike as a distal signal of the onset of H1 further south, is specifically regarded as the only trustworthy number (Dreger 1999). Thus the main meltwater spike will be as young as that in front of the Barents Shelf, to which it is spatially connected (Sarnthein et al. 1995).

Accordingly, it can be inferred that H1 resulted from an overlap of at least two separate major surges, approximately 1500 years apart, an early surge from Labrador and a later surge from the Barents shelf, in addition to initial surging from East Greenland. Indeed, a number of high-resolution cores from the North Atlantic reveal a markedly duplicate structure of the H1 IRD maximum (Elliot et al. 1998).

The end of Heinrich 1 meltwater and IRD signals is constrained more uniformly near 13.0–13.4 ^{14}C ka (in harmony with Steinsund et al. 1991; Bond and Lotti 1995; Vidal et al. 1997; Vorren and Laberg 1996). *Below* the top, a deep-water coral is dated at < 13.1 ^{14}C ka equal to < 16.2 U/Th ka (MD952011 in Fig. 7; Dreger 1999). The ^{14}C age of 12.7 ka can be converted to 14.8 cal. ka (Bard et al. 1993; Alley et al. 1993; Hughen et al. 1998), and the basal age of 15 ^{14}C ka to ~ 18.0 cal. ka (Voelker et al. 1998). Accordingly, the Heinrich 1 cold phase formed the most extensive and

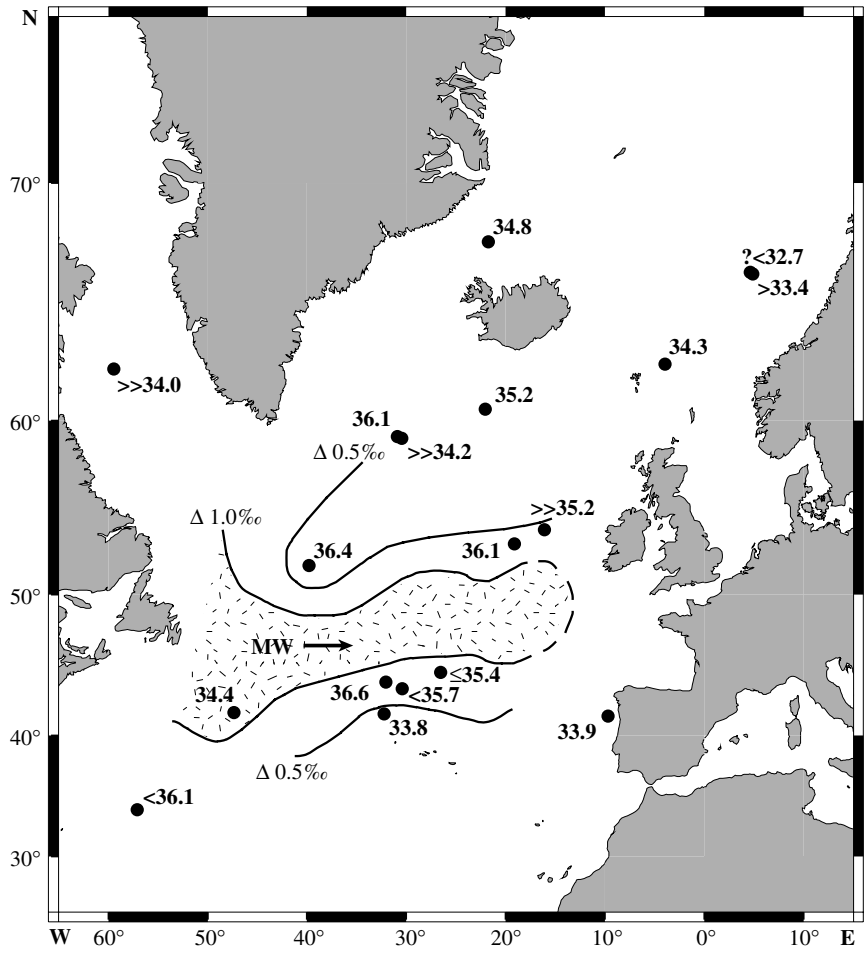

Fig. 10: Variations in ^{14}C ages at the base of Heinrich 4 IRD layers and $\delta^{18}O$ meltwater signals (Sarnthein et al. in prep.). Δ 0.5 and Δ 1.0‰ isolines indicate meltwater- (MW) induced planktonic $\delta^{18}O$ minimum belt along the Heinrich iceberg track (Cortijo et al. 1997)

extended D-O stadial of MIS 2–3, lasting approximately 3 ky, the equivalent to two average Dansgaard-Oeschger cycles.

Three Fundamental Modes of Surface and Deep-Water Circulation

Since Stommel (1961) most authors agree that the Atlantic and global thermohaline circulation system (Fig. 1) underwent fundamental changes from interglacial to glacial times (Table 1). In contrast to previous concepts (Broecker et al. 1985; Bryan 1986; Duplessy et al. 1988) this basin-wide compilation of epibenthic $\delta^{13}C$ data (Fig. 11a; Sarnthein et al. 1994), a proxy of deep-water ventilation (Duplessy et al. 1981; Broecker and Peng 1982; Zahn et al. 1986; Boyle 1992; Mackensen et al. 1993), has revealed three main states of deep-water circulation in the eastern Atlantic consistent with records from the western and southern Atlantic (e.g. Boyle and Keigwin 1986; Ninnemann et al. 1999): (I) The modern/Holocene state with vigorous NADW formation in both the Greenland-Iceland and Labrador Seas is responsible for relatively strong heat advection to the adjacent continents in high latitudes, particularly to northwestern Europe. (II) A more moderate NADW formation is characteristic of peak glacial times, the LGM. During this time, deep convection primarily took place in the Irminger and Labrador Seas and was only modest and occasionally brine-water supported in the Greenland-Iceland-Norwegian Seas, with poor warming of the adjacent northern continents. (III) During the Heinrich 1-type meltwater mode, North Atlantic deep-water formation was turned off completely except for brine-water production. Accordingly, the amount of oceanic heat ad-

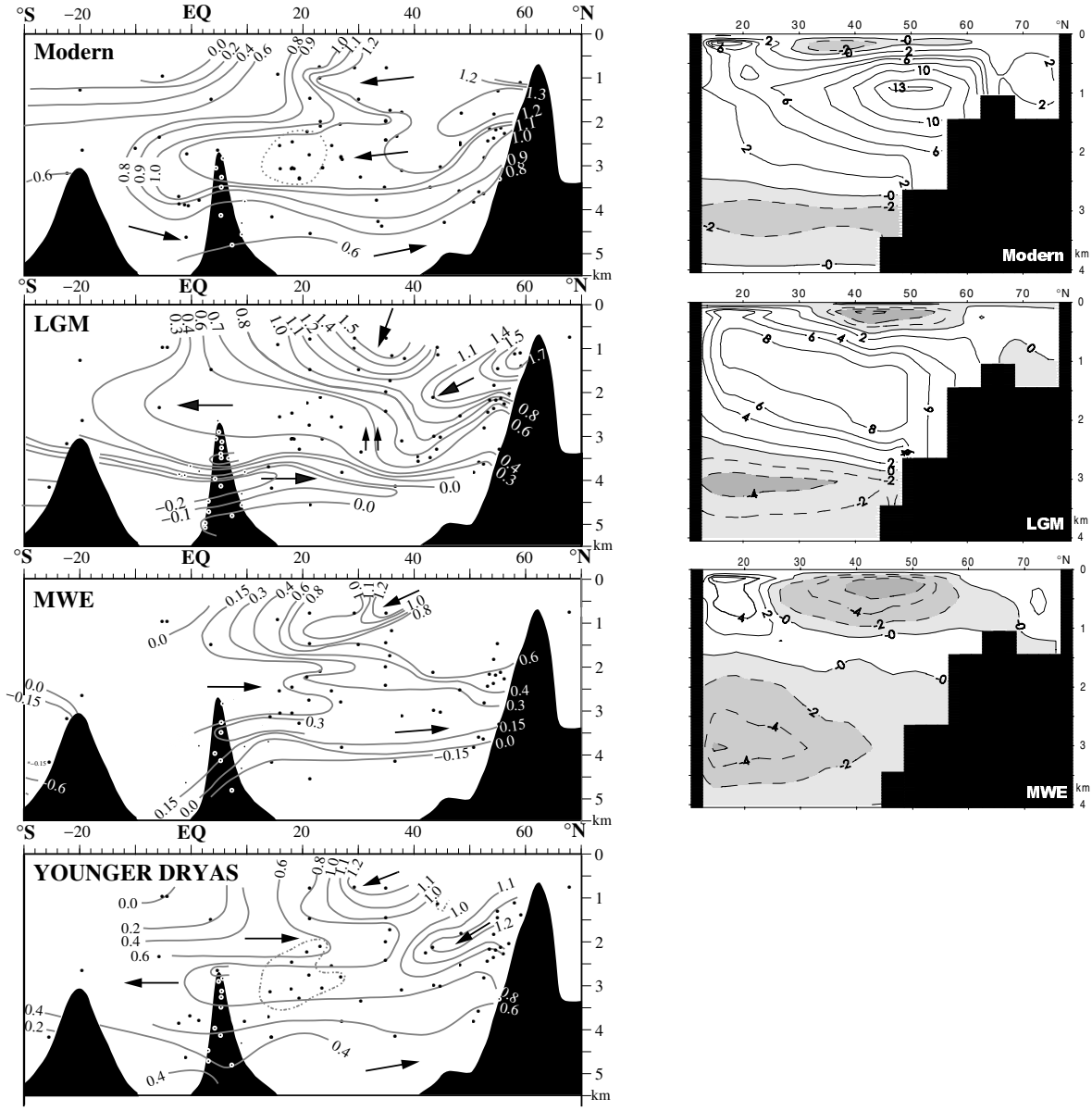

Fig. 11: Modes of (eastern) Atlantic thermohaline circulation. Vertical transects are based on both epibenthic $\delta^{13}C$ values (left column, in per mill; Sarnthein et al. 1994; supplemented) and model results (right column, with meridional overturning rates in Sverdrups; Seidov et al. 1996). LGM = Last Glacial Maximum, lumping 15–16 and 18–20 ^{14}C ka and excluding a short-lasting negative excursion along the NADW-SSBW boundary near 17–18 ^{14}C ka. MWE = Heinrich 1 meltwater event; YD = Younger Dryas. Arrows in $\delta^{13}C$ transects show main directions of meridional flow, deduced from $\delta^{13}C$-distribution patterns

vection to the northern continents approached zero. Mode III probably also applies to various other Heinrich events and further century-long cold spells immediately prior to the D-O events (Fig. 8).

In harmony with these major modes of deep- and intermediate-water circulation, we have defined three corresponding modes of surface-water hydrology which cover nearly the total bandwidth of glacial-to-interglacial variability in the North Atlantic (Fig. 12). In contrast to modern and LGM modes, which are dominated by the advection of subtropical warm surface water up to Svalbard, mode III is outstanding because of two major (Heinrich 1) meltwater plumes, a large one west of the Barents shelf, a minor one to the northwest of Iceland. In contrast, the peak glacial mode II shows little meltwater all over the North Atlantic, ex-

cept for the region to the west of Ireland. In contrast to previous expectations (Table 1) the horizontal and vertical distribution of water masses during the early half of the Younger Dryas (YD) lasting 1300 y does not resemble mode III but, rather, the modern mode I (Figs. 11a and 12d). Only the meltwater episode near the end of the Younger Dryas and the early Preboreal (Fairbanks 1989) are in keeping with mode III (discussion of stratigraphic details below).

For a better understanding of the physical mechanisms which control the three modes and their alternation, numerical equilibrium experiments with a 3-D ocean circulation model (Fig. 3; Table 3) were driven by the spatial distribution of SST and SSS in the northern North Atlantic during modern, glacial, and Heinrich 1 times (Fig. 11b; Seidov et al. 1996; Schäfer-Neth and Stattegger 1997; Schäfer-Neth 1998). The model results clearly reproduce the three fundamental modes of deep-water circulation reconstructed from our proxy data (Fig. 11a) and, likewise, the consistent patterns of associated surface-water currents.

The Glacial Mode

In contrast to the expectations based on previous surface reconstructions (CLIMAP 1981; Ruddiman and McIntyre 1981; Duplessy et al. 1991), the peak glacial North Atlantic differed little from the modern mode (Figs. 12a, b). SST values in the northeastern Atlantic and (eastern) Nordic Seas were indeed much reduced, down to approximately 3–5 °C during summer (similar to early data of Kellogg 1980). On the other hand, they were still high enough to preclude a perennial sea-ice cover, even provided the error range of foraminifera-based SST proxy data (Weinelt et al. 1996; Pflaumann et al. in prep.). A continuous CLIMAP-style (1981) sea-ice cover occurred only during glacial winter. In harmony with this interpretation, the late LGM percentages of $CaCO_3$ (10–14 %) in sediments from the central Nordic Seas (Fig. 13) directly resemble $CaCO_3$ values below the modern Arctic water mass which is largely ice-free during summer and is a major site of deep-water convection today.

Based on summer SST and planktonic $\delta^{18}O$ values, glacial SSS values reached approximately 36–36.5 per mill in large parts of the Greenland-Iceland-Norwegian Seas as compared to 36.5–38.0 per mill in the glacial subtropical Atlantic (Seidov et al. 1996). These values imply a high density, sufficient to permit (seasonal) deep-water convection in both the Irminger-Labrador and Greenland-Iceland-Norwegian Seas (Weinelt et al. 1996), which in turn entails an ongoing inflow of Atlantic surface water deep into the Greenland-Iceland-Norwegian Seas.

This inflow is indeed registered in both the distribution of proxy data and modeled current patterns at sites immediately west and northwest of Iceland and, particularly, to the southeast of Iceland (Fig. 12). LGM water masses from the Atlantic finally reached the northern slope of Svalbard (Hebbeln et al. 1994; Sarnthein et al. 1995; Hald et al. 1996; Spielhagen et al. 1997) and largely contributed to continuing northward heat transport, to high evaporation and to a positive atmospheric moisture balance over northwestern Europe, important for the continued build-up of continental ice sheets during the LGM. This holds particularly true for the ice sheet on the Barents shelf, which advanced to the shelf break only after 19 ^{14}C ka, a last time as late as 13.7 ^{14}C ka, as evidenced in marine sediment cores from the Barents shelf (Vorren and Laberg 1996) and slope (Dreger 1999) and in model experiments (Lambeck 1995).

In contrast to small glaciers surging into the LGM Nordic Seas, abundant icebergs drifting from Labrador and Greenland ended by melting in a widespread "scrap yard" around the Rockall Bank. This is documented by extensive IRD deposits (Robinson et al. 1995) and frequent deep plough marks down to > 800 m depth (von Bodungen et al. 1988) along the southern slope of the Iceland-Scotland Ridge, which at that time was less than 300 m deep and hence blocked the drift of larger icebergs farther to the north. Iceberg melt led to an extensive lid of low-salinity surface water to the west of Ireland (Fig. 12b; ~ Δ 0.4 ‰ $\delta^{18}O$). This lid, in turn, induced a clockwise gyre and a north-south flowing cold longshore current down to western France (Sarnthein et al. 1995), which strongly enhanced the LGM cooling of Western Europe. Furthermore, the meltwater lid led to a steep SSS gradient of > 1 ‰ along its northern boundary and hindered the direct flow of Atlantic surface water in the east, via the Faeroe Channel into the Nordic Seas, different from the situation today. Rather, the inflow of Atlantic water followed the west-east running salinity front near 63° N from the southeastern tip of Iceland to the north side of the Faeroe Islands (Fig. 12b). Fairly warm glacial summer SST (3.5 °C) around the southern tip of Greenland were possibly induced by the westward flowing branch of the Irminger Current.

In Atlantic intermediate and deep-water compartments, the composite evidence of epibenthic $\delta^{18}O$ and $\delta^{13}C$ values makes it possible to distinguish four different water masses during the LGM and to trace them back to their source regions (Figs. 11a and 14; Jung 1996; Sarnthein et al. 1994; Zahn et al. 1997):

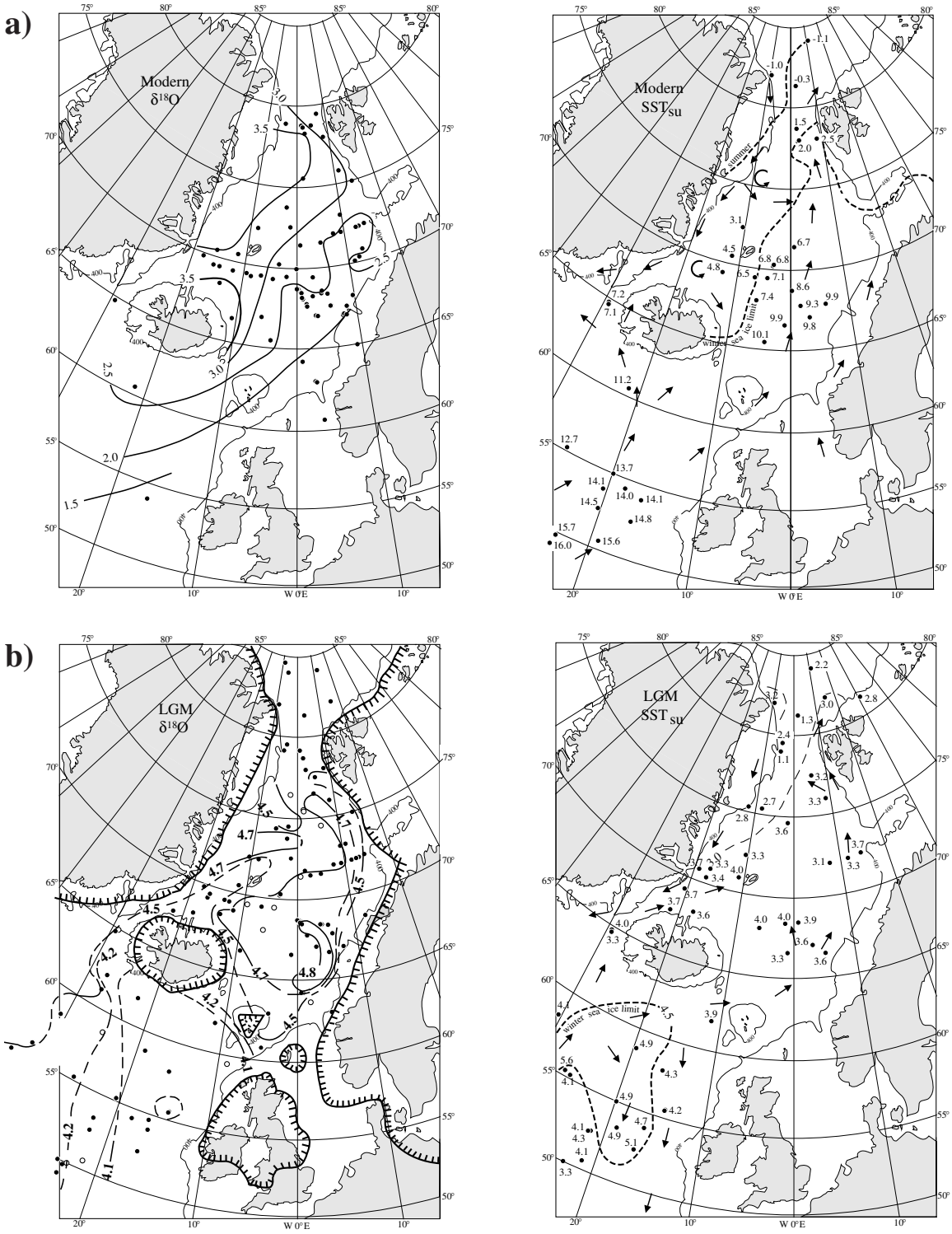

Fig. 12: Distribution of planktonic $\delta^{18}O$ (*N. pachyderma* (sin)) and SST values at 10 m water depth and modeled circulation at 25 m depth (= from left to right) **a)** for today, **b)** the LGM, **c)** Heinrich 1 MWE and **d)** the Younger Dryas (YD) (Sarnthein et al. 1995, supplemented by own unpubl. data and data from Rasmussen et al. 1996; Kroon et al. 1997; Spielhagen et al. 1997). Modern SST values are from Levitus et al. (1994), paleo-SST data are foraminifera-based (Pflaumann et al. in prep.). Limits of winter sea-ice correspond to winter SST values < 1 °C

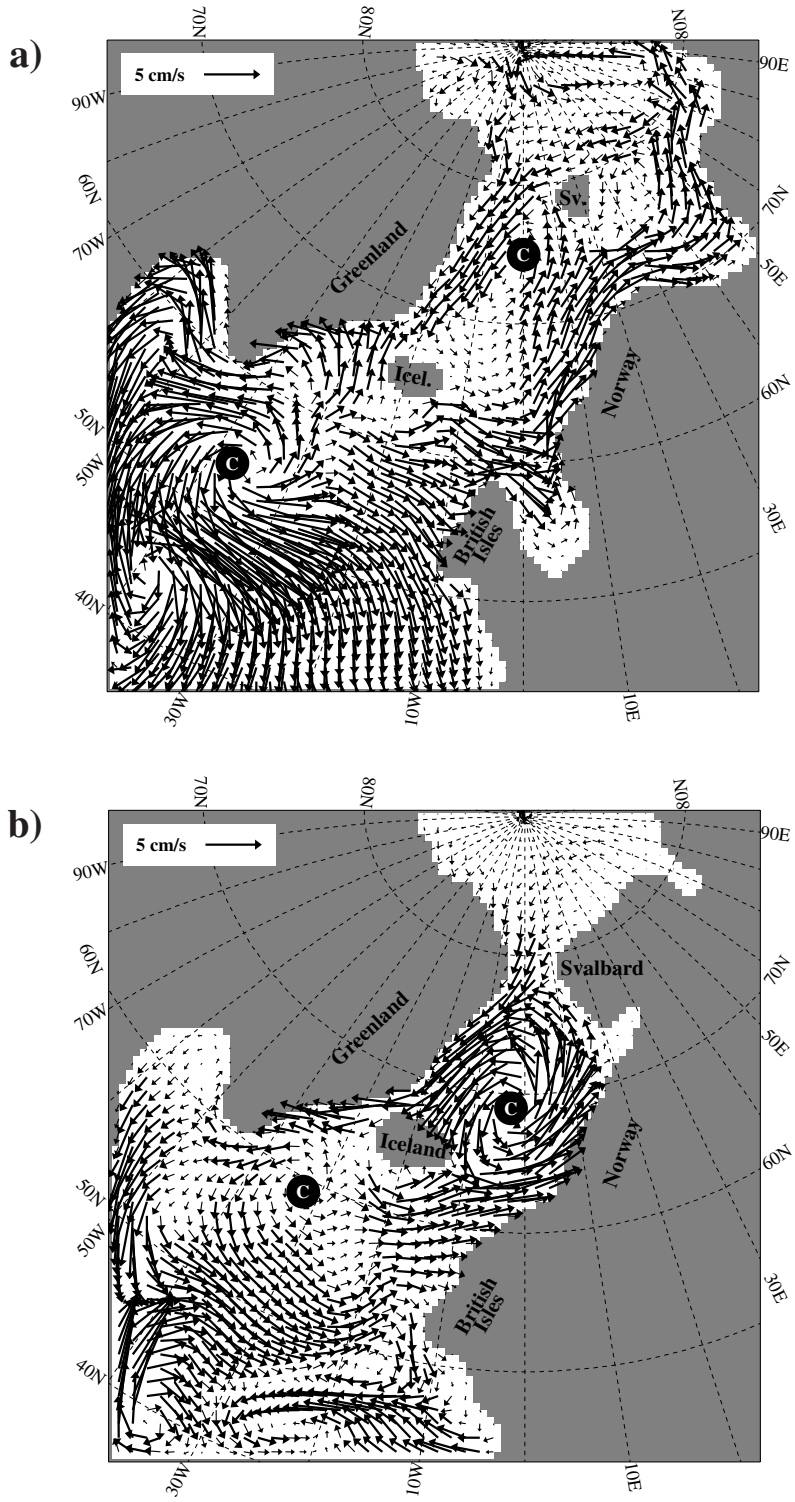

Fig. 12 (continued): Indented lines mark extent of continental ice sheets. $\delta^{18}O$ values during LGM and H1 largely reflect SSS variations. Horizontal hatching at MWE marks salient meltwater lids. Current arrows on paleo-SST maps are deduced from main SSS gradients and Coriolis forcing. Paleocirculation model is driven by SST and SSS values, deduced from planktonic $\delta^{18}O$ data and paleo-SST (Figs. 3 and 4). "C" denotes convection areas (Schäfer-Neth and Paul this volume)

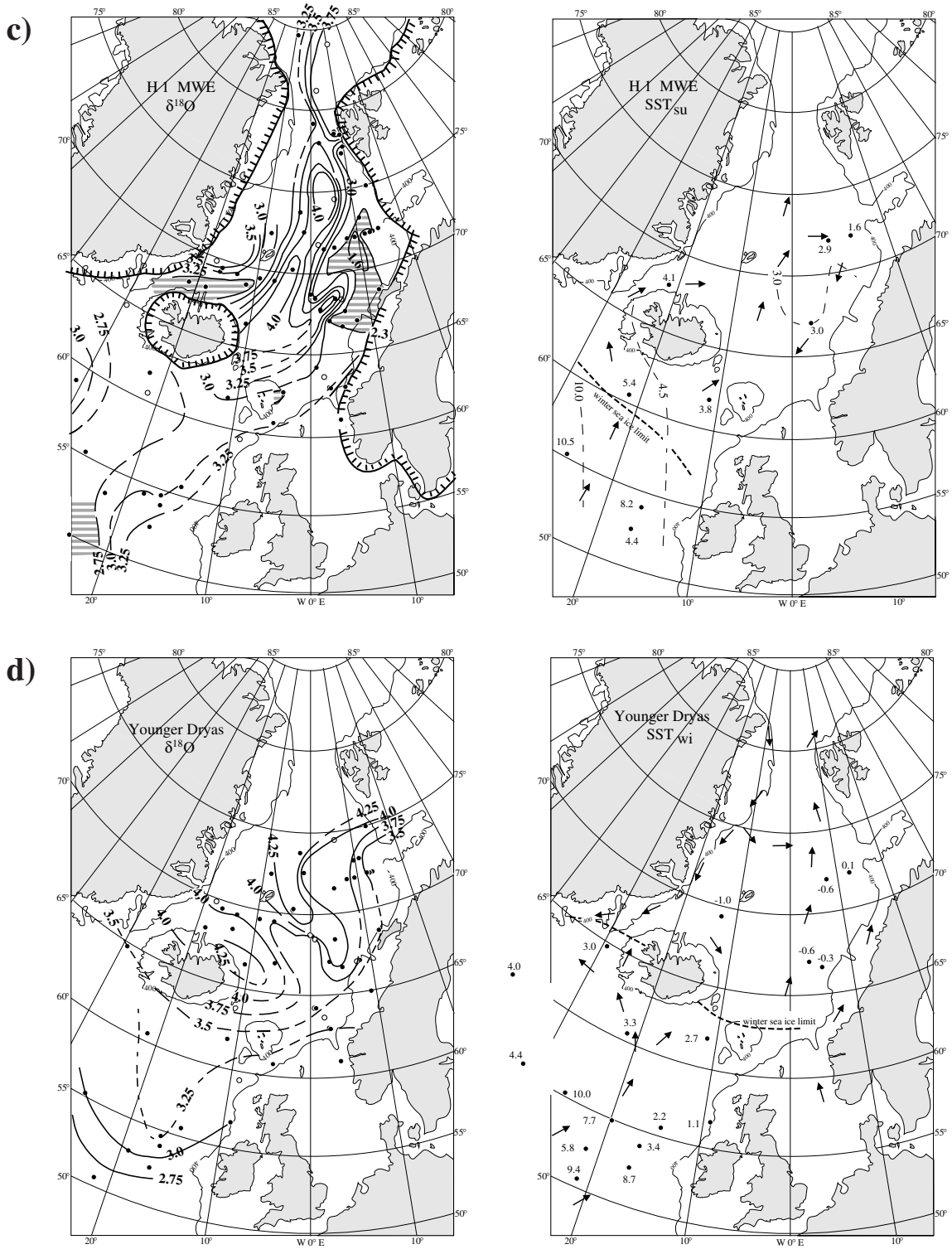

Fig. 12 (continued)

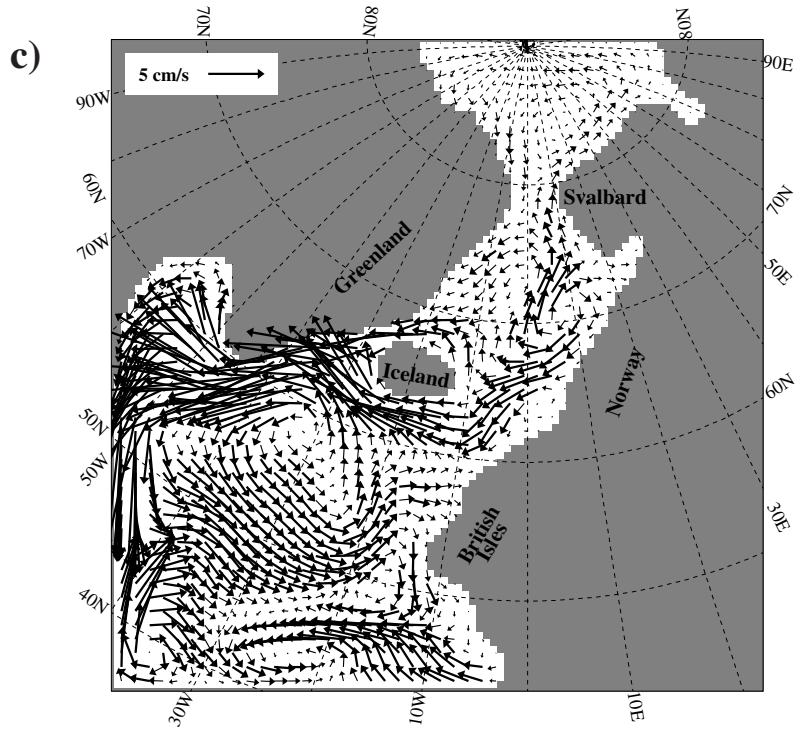

Fig. 12 (continued)

(1) A derivate of southern-source bottom water (SSBW) with minimum ventilation (< 0.2‰ $\delta^{13}C$) is confined to the deep eastern Atlantic continental margin up to approximately 2800–2600 m depth along the Rockall Plateau.

(2) Strongly ventilated (1.5–1.8‰ $\delta^{13}C$) Upper NADW with fairly high densities (4.9–5.2‰ $\delta^{18}O$), a glacial equivalent of the modern Labrador Sea Deep Water (LSD), occurs above 1900 m depth in the Irminger Sea and debouches down to 2200–2400 m in the northeastern Atlantic.

(3) A small-scale but extremely dense (5.25–5.5‰ $\delta^{18}O$) water layer with medium ventilation (up to 0.9‰ $\delta^{13}C$) is ascribed to the Lower NADW, which is sandwiched near 2000–2200 m depth between water masses (1) and (2) along the slopes of the mid-Atlantic Ridge and the southern Rockall Plateau. This dense water mass is traced across the Faeroe Channel back to the glacial Intermediate Water of the Nordic Seas and directly recorded in core PS2644 at 800 m depth north of Iceland. Here benthic $\delta^{18}O$ values of ~ 5.6‰ mark the pertinent extreme density, with benthic $\delta^{13}C$ values of ~ 1.6‰ which reflect the strong ventilation of this water mass (Völker 1999).

In contrast, the glacial planktonic $\delta^{13}C$ values of *N. pachyderma* (sin) are low all over the northern North Atlantic (< 1.1–1.2‰; Keigwin and Boyle 1989; Sarnthein et al. 1995; corrected for a vital effect of 0.85‰; Labeyrie and Duplessy 1985; Simstich 1998) and do not yet reveal any particular source region in surface water, where highly ventilated deep- and intermediate-water masses (2) and (3) may originate.

Finally, (4) a strongly diluted derivate of glacial Mediterranean Outflow Water (MOW) occurs along the upper continental slope of Portugal near 1200 m depth. Its ventilation is similar to that of Upper NADW, its $\delta^{18}O$ values, however, are ~ 1‰ lower, near 4.0–4.2‰. Thus, the temperature and salinity of this glacial MOW derivate exceed that of LSD by > 5 °C and 0.5‰, given a similar density range (Zahn et al. 1997).

Likewise, our high-resolution model experiments identify at least three different current systems at different depth levels in the glacial northern North Atlantic (Figs. 11b, 15; Seidov et al. 1996; Schäfer-Neth 1994). In harmony with the proxy data patterns, the relative flux rates of Upper NADW, Lower NADW and SSBW amount to approximately 14, 0.2 and 3.7 Sv, respectively. As compared to the modern mode, these rates would imply a glacial increase in the formation of LSD (Upper NADW) by ~ 50 % and a 50 % reduction in the formation of Lower NADW. The incursion of SSBW in total may have increased by approximately

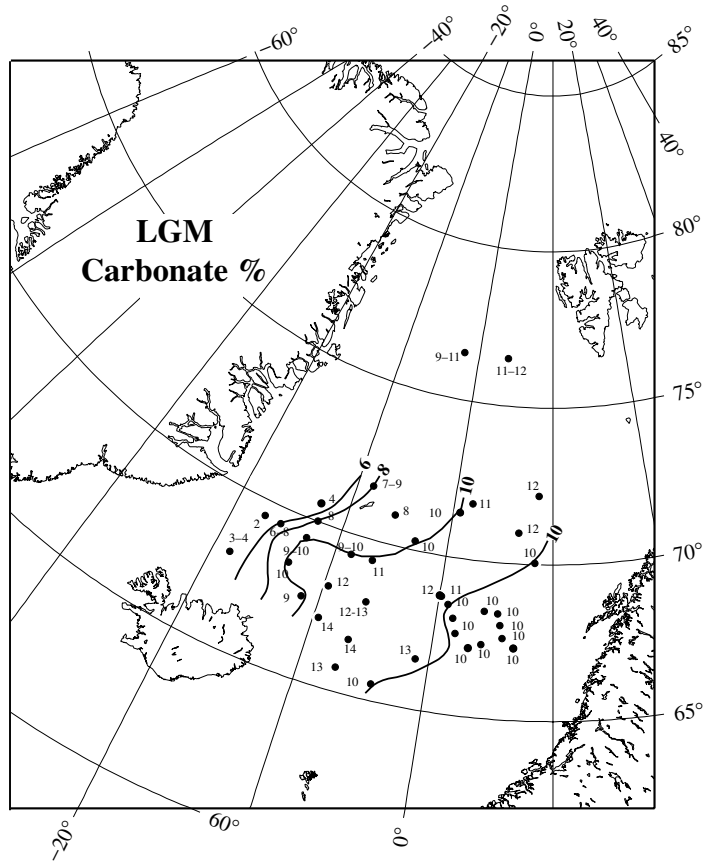

Fig. 13: Distribution of % $CaCO_3$ in southern Nordic Sea sediments during the LGM (Henrich 1998, modified). Values of 12–14 % equate to the values below the modern Arctic convection zone in the eastern Greenland Sea (Fig. 12a)

50 %, but remained generally constant in the eastern Atlantic.

As a result of reduced glacial turnover rates of Lower NADW and the enhanced incursion of SSBW along the eastern Atlantic continental margin, $\delta^{13}C$ isolines in Figure 11a depict a partial upwelling of SSBW directly in front of the zonal Azore fracture zone scarps near 37° N up to approximately 2500–2000 m depth, akin to the SSBW upwelling found south of the Iceland-Scotland Ridge. This topography-induced admixture of upwelled SSBW from below is necessary to balance in- and outflow volumes of deep water and leads to a clear "dilution", i.e., oxygen depletion and nutrient enrichment, of the Lower NADW in the eastern Atlantic between 35° N and the equator (Sarnthein et al. 1994).

The Heinrich-Type Meltwater Mode and Meltwater Budgets

The LGM mode ended abruptly with a major reduction in planktonic and benthic $\delta^{18}O$ values (Fig. 7). This shift went along with a dramatic reduction in benthic $\delta^{13}C$ values (Fig. 11) and marks an inversion to a totally different state of the ocean, the Heinrich 1 meltwater mode, implying the greatest change in thermohaline circulation over the last 60 ky. Aware of the broad discussions about the actual meaning of foraminiferal $\delta^{13}C$ (Duplessy et al. 1984; Boyle 1992: until Spero et al. 1997), we still simply interpret this $\delta^{13}C$ reduction as a record of extreme oxygen depletion and nutrient enrichment in Atlantic subsurface and deep waters. At the same time, the deep-water age increased from several 100 y to nearly 1500 y in the Norwegian Sea (based on the ^{14}C vs. U/Th age anomaly of a deep-water coral in growth position; Dreger et al. in prep.), an age similar to that of modern Pacific deep water (Broecker et al. 1988).

For a better understanding of the processes which actually governed this inversion of the ocean system, the precise age control of deglacial sediment records (Fig. 7) enables us to constrain the salinity, density and carbon budgets (see below) which ultimately may have

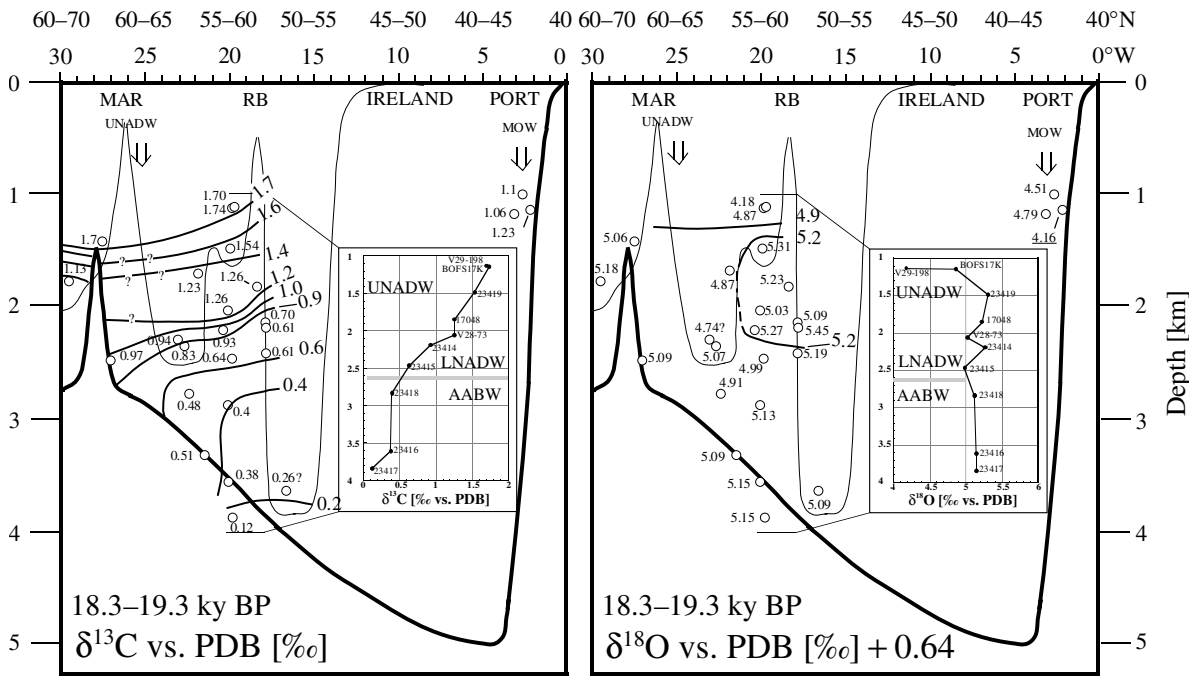

Fig. 14: Vertical transects of benthic $\delta^{18}O/\delta^{13}C$ during the LGM, running from northwest to southeast, from the Mid-Atlantic Ridge (MAR) across the southern slopes of the Rockall Bank (RB) and Ireland down to northern Portugal (PORT). Insets show $\delta^{18}O/\delta^{13}C$ transects across the southern slope of the Rockall Bank from 1–4 km water depth, with position of Upper (UNADW) and Lower NADW (LNADW) and of Antarctic source Bottom Water (AABW) (compiled by Jung 1996, from various data sources)

induced the early deglacial change in thermohaline circulation and to identify the potential significance, synchroneity, leads and lags of iceberg-induced processes acting in different Atlantic regions, processes which have already been discussed at length along with the origin of D-O events.

Based on spatial $\delta^{18}O$ anomalies in surface water (Fig. 12c), meltwater lids were indeed present during H1 in the central North Atlantic, west of 20° W, and to the north of Iceland. The most pronounced meltwater injection, however, is registered in the northeastern Norwegian Sea (Jones and Keigwin 1988; Weinelt 1993; Sarnthein et al. 1995; Fronval et al. 1995). Here, extensive local salinity anomalies reached extremes of 2.5 to > 6.0 per mill vs. the general meltwater-free background, depending on the different regression slopes employed for deducing salinity from $\delta^{18}O$ values (Erlenkeuser unpubl. data; Simstich 1998; Schäfer-Neth 1998; Duplessy et al. 1991; Vogelsang 1990; Craig and Gordon 1965). Principally, these anomaly estimates are still conservative, because they are based on the $\delta^{18}O$ composition of planktonic *Neogloboquadrina pachyderma* (sin). This species calcifies in polar waters at water depths of 20–120 m, which is well below the actual salinity minimum at the sea surface (Simstich 1998). Minor meltwater patches also occurred near the northeastern tips of the Faeroe Islands and Jan Mayen.

Based on rough quantitative estimates and using $\delta^{18}O$ values of –25 ‰ for ice, the glacial surge from the Barents shelf during late H1 produced a 50 to 100-m-thick meltwater layer at a rate of > 1500–4500 cubic km/y, equal to a gross sea-level rise of > 3 m/1000 y. This amount was indeed surpassed by a meltwater rate of 7000 cubic km/y or more, derived from the Laurentian ice sheet, for which MacAyeal (1993b) also contemplated a 3.5-m sea-level rise which, however, may be twice as high after 1000 years. The meltwater lid off northern Iceland equaled to further 1800 cubic km/y. Nevertheless, when assessing the actual impact of iceberg surges, the proximity of the Barents meltwater flux to LGM cells of deep-water convection may have been more important for controlling variations in deep-water formation than were larger meltwater volumes stemming from Labrador.

Different from the Rahmstorf (1995) model, a recent sensitivity study employing the 3-D model developed by Schäfer-Neth (1998) showed that the total turnoff of the LGM THC during H1 (and likewise H6) is forced by (1) a general large-scale decrease in North Atlantic SSS, a sort of preconditioning of the high-latitude

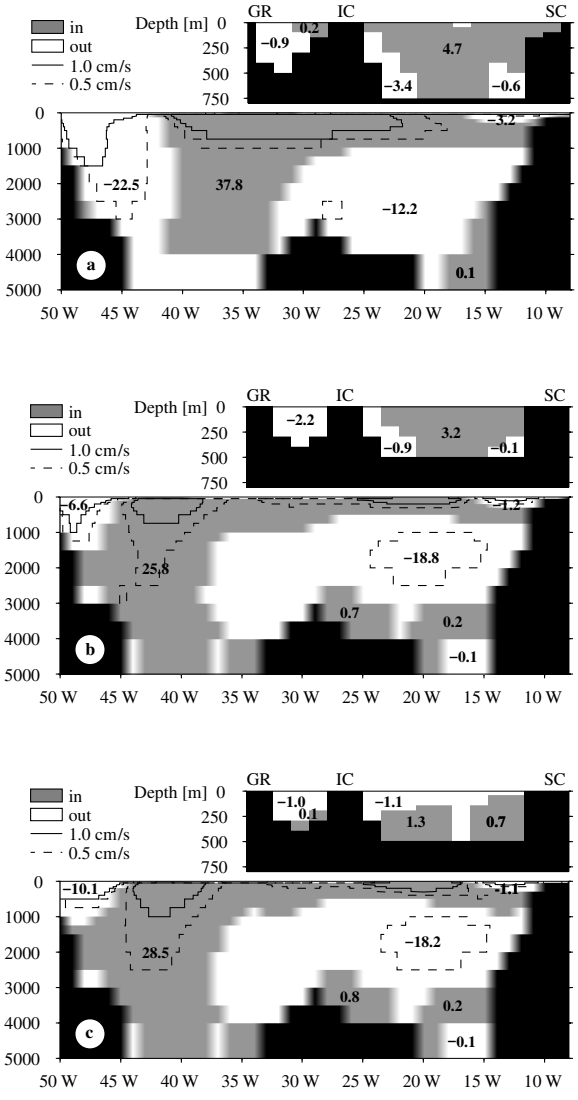

Fig. 15: Velocity zonal sections 0–5000 m depth modeled along 50° N (lower panel) and along 60°–65° N from Greenland (GR) across Iceland (IC) to Scotland (SC) (upper panel). Shaded and blank areas indicate northward or southward flow directions. Bold numbers give total transports in Sv. **a)** modern winter; **b)** LGM summer; **c)** summer during the Heinrich 1 MWE

ocean, as induced by the onset of a general disintegration of northern hemisphere ice sheets, reflected by H1 icebergs from Labrador, but (2) more specifically, by the narrowly confined input of iceberg-derived meltwater from the Barents shelf and Iceland into the eastern Nordic and Irminger Seas, hitting the prime sites of convection. Hence no convection was possible at any one site during this time. All together, these findings support the MacAyeal (1993b) model, claiming internal ice oscillators as the ultimate forcing of short-term climatic change. However, the model must be supplemented by the need of meltwater injection proximal to the sites of deep-water formation. This aspect may also be crucial for assessing the Younger Dryas problem (see below).

Meltwater influence on deep-water formation during Heinrich events is also recorded in major benthic $\delta^{18}O$ brine water signals (Jansen and Veum 1990). West of the Mid-Atlantic Ridge it extended nearly as far as the Azores (~ 40° N; Vidal et al. 1997), in the east, at least, to the flanks of the Rockall Plateau, down to approximately 2800 m water depth (Fig. 8a). Further below, the brine-water flux was weak. Here the total Atlantic was flooded by poorly ventilated deep and intermediate water from the Southern Ocean, except for a weakened outflow from the Mediterranean Sea (Fig. 11a; Sarnthein et al. 1994).

As a result of the turned-off THC, summer SST during H1 were > 1–2 °C lower than during the LGM in the eastern Nordic Seas, but slightly warmer in the eastern North Atlantic (Figs. 5 and 12b, c). Accordingly, heat advection to the far north ceased at that time to the absolute minimum of the last 60 ky. These low temperatures also imply a broad expansion of perennial sea ice, possibly up to the south of Iceland. However, accurate sea-ice boundaries are still controversial (e.g. Koç et al. 1993).

Note that the short-term temperature drop in northern high latitudes just matches, within the limits of dating precision, a 1.5–3.0 °C warming of the tropical western Atlantic (Guilderson et al. 1994; Curry and Oppo 1997; Rühlemann et al. 1998; Hüls et al. 1998; however, opposed to a minor cooling in the western Caribbean; Prell et al. 1976). The same anti-phase warming during H1 is even more striking in two Antarctic ice records (Blunier et al. 1998) and the isotope records from the sub-Antarctic Atlantic (Ninnemann et al. 1999).

On the one hand, temperature increase in the low-latitude and southern Atlantic during H1 appears to be consistent with a coeval deglacial increase in atmospheric CO_2 (Sowers and Bender 1995) and CH_4 (Blunier et al. 1998), which had already begun prior to H1. Accordingly, the possible role of early greenhouse warming in the tropics may be speculated upon. On the other hand, the reversed THC, driven more by haline than by thermal gradients, may have been more important, since it stopped North Atlantic "heat piracy" (Berger and Wefer 1996) from the tropical and southern Atlantic and thus may have contributed significantly and in various ways to western and southern Atlantic warming. Basically this concept receives support from

various coupled ocean-atmosphere models which have simulated successfully, although not with perfectly consistent results, the north-south ocean anti-phasing triggered by meltwater in the North Atlantic (Manabe and Stouffer 1997; Schiller et al. 1997; Marchal et al. 1998).

The Onset of the Modern/Holocene Mode and the Conundrum of the Younger Dryas

Based on benthic $\delta^{13}C$ values the modern/Holocene mode of deep-water circulation (Fig. 11a) started with full intensity throughout the Atlantic approximately 12.8 ^{14}C ky ago (Sarnthein et al. 1994; Charles and Fairbanks 1992: 12.83 ka). This ^{14}C age is also recorded at the base of the Bølling warm phase (1) in terraces on Svalbard (12.83 ka; Mangerud et al. 1992), (2) in core MD952012 from the Barents slope (12.79 ka; Figs. 5 and 7; Dreger 1999), and (3) the Cariaco Basin (Hughen et al. 1998; ~ 12.75 ka). Moreover, the date corresponds to the abrupt beginning of the Bølling interstadial at ~ 14.7 cal. ka in the GISP2 ice core (Alley et al. 1993). At this time, density in the central Nordic Seas reached a level (Fig. 11a; Sarnthein et al. 1995) sufficient for triggering the abrupt and full resumption of thermohaline circulation mode I, which possibly was also brine-water induced (Figs. 8b, 9). This reversal provided the pathway for a sudden and immense heat and moisture flux up to the Arctic within a time span as short as 7–14 y (Alley et al. 1993), also reflected in a SST rise of > 3 °C at 72° N (Fig. 5; Dreger 1999) and again in anti-phase with an abrupt cooling recorded in two Antarctic ice cores (Blunier et al. 1998).

Subsequent to the early Bølling ocean inversion prior to the Younger Dryas (YD), significant meltwater is not encountered either in the Nordic Seas (Sarnthein et al. 1995) or in the northwestern Atlantic (de Vernal 1996; opposed to Broecker 1992; Keigwin and Jones 1995), i.e., meltwater which may have throttled NADW formation and induced the cooling of the YD, 10.9–10.2 ^{14}C ka or 12.9–11.6 cal. ka (Hughen et al. 1998; Alley et al. 1993). Bodén et al. (1997) proposed the drainage of the Baltic Ice Lake as a likely candidate for a major meltwater release during this time. However, its meltwater volume is minor and, in particular, occurs too late, only near the Younger Dryas-Preboreal boundary.

Likewise, both benthic $\delta^{13}C$ (Boyle and Keigwin 1987) and recent benthic Cd/Ca records (Marchitto et al. 1998; incorrectly plotting a "YD" arrow as late as 11.8 cal. ka) of western Atlantic deep and intermediate water show that the Younger Dryas began with a Holocene level of NADW formation at 12.9 cal. ka and *prior* to a minimum in intermediate water strength at 12.4 cal. ka. A dramatic shut-down in NADW production occurred much later, culminating near 11.8–9.8 ka cal. ka, that is, near the end of the YD and mainly during the early Preboreal, which becomes evident when age control is closely inspected (Fairbanks 1989). These results are in line with the age of a well-dated $\delta^{13}C$ minimum in three other high-sedimentation rate cores from 2300–2500 m water depth in the eastern Atlantic (ODP Site 658, 25 cm/ka, Maslin et al. 1996; V23-81, > 12 cm/ka, Jansen and Veum 1990, Sarnthein et al. 1994; 23415, Jung 1996, suppl. by Weinelt, 7 cm/ka). Various other high-resolution cores from pertinent depths in the eastern Atlantic do not reveal any $\delta^{13}C$ minimum along with the YD (Sarnthein et al. 1994).

Accordingly, the Atlantic THC in the *early* Younger Dryas was little different from the modern mode (Fig. 11; Sarnthein et al. 1994; Berger and Jansen 1995). In contrast, a marked cooling of the sea surface in the Nordic Seas is encountered, in particular during YD winter (Fig. 12; Sarnthein et al. 1995), which may imply that the Nordic Seas were largely sea-ice covered during the cold season. Accordingly, the main question still remains unsolved: Which mechanism then induced the significant, primarily seasonal reduction in heat transport to the high-latitude North Atlantic (Berger and Jansen 1995)?

In their Hamburg atmospheric general-circulation model (GCM) experiments Renssen et al. (1996) showed that this sea-ice cover during winter was crucial in forcing the atmospheric circulation pattern of the YD. In particular, the jet stream over the North Atlantic and cyclonic activity over northern Eurasia were strengthened considerably. However, this model does not explain the considerable expansion of sea ice itself.

Here recent findings by Spielhagen et al. (1998) may provide a genuine breakthrough. They report a conspicuous meltwater discharge from the Siberian Lena river over less than 500 years at approximately 11 ^{14}C ky B.P., that is, right at the onset of the YD. At the same time a major brine-water signal occurs in the deep central Arctic (core PS2458; 60–65 cm/ky; Spielhagen et al. 1998). This massive meltwater flux, after having passed the Fram Strait into the Greenland-Iceland-Norwegian Seas, possibly led to conspicuous sea-ice formation and, accordingly, to major cooling in the Nordic Seas during winter. On the other hand, both the entrainment of cold brine deep water from the Arctic and salt transport from the Central Atlantic during summer induced an "internal momentum" of the THC, which was probably strong enough to maintain the Holocene-type circula-

tion system over the first part of the Younger Dryas, in total a regime reminiscent of the recent Great Salinity Anomaly (Dickson et al. 1996; Belkin et al. 1998) when Arctic freshwater influx only induced a regional suppression of deep-water formation.

Atlantic Ocean Modes and Global Carbon Cycle

Takahashi et al. (1997 and 1995) measured the air-sea difference in the partial pressure of CO_2 (pCO_2) in the modern North Atlantic and calculated an air-sea net flux of CO_2, totaling up to 0.2–0.5 Gt C/y north of 42° N. This estimate may be conservative in view of the $\delta^{13}C$ values of Late Holocene alkenones, where the air-sea pCO_2 difference was doubled (Jasper et al. 1995). In line with these figures, Broecker and Peng (1992) concluded that the pre-industrial NADW flux supported a net transport of approximately 0.6 Gt C/y (only 0.3 Gt C/y according to Keeling and Peng 1995) from the Northern to the Southern Hemisphere. By contrast, the cross-equatorial net transport of carbon is only 0.15 Gt C/y in the model proposed by Sarmiento et al. (1995: Fig. 8).

Probable long-term, i.e., glacial-to-interglacial and millennial-scale variability in interhemispheric carbon fluxes and air-sea fluxes in general have been identified. Past variabilities in carbon fluxes were deduced from biological productivity changes in North Atlantic surface water, with special attention to abrupt changes in THC tied to the Heinrich and Dansgaard-Oeschger cycles (Kiefer 1998; Weinelt et al. in prep.). Short-term variations in deep-water ventilation in a vertical $\delta^{13}C$ transect extending over 4 km across the northeastern Atlantic water masses (Fig. 8a; Jung 1996) have also been reconstructed. Finally, actual numbers of the carbon budgets were derived from modeling the carbon cycle during the three fundamental modes defined for Atlantic (and global) circulation (Schulz et al. in press).

Carbon Transfer via Plankton Productivity: The "Biological Pump"

Near the southern margin of the Heinrich iceberg track (Fig. 10; approximately 40°–50° N; Grousset et al. 1993), foraminifera-based paleoproductivity estimates are generally increased by a factor of two over glacial MIS 2 and 3 as compared to stage 1 (Fig. 16; Kiefer 1998). In addition, inferior maxima bracket most Heinrich IRD events, which themselves are linked to a short episode of slightly reduced production (H2, H3, H4, H5). Along the northern margin of the Heinrich iceberg track (Fig. 16, core 23415) a series of short-term but prominent pigment maxima have been interpreted as a paleoproductivity record (Harris et al. 1996). In contrast to the southern margin, the general productivity level in core 23415 barely increases from interglacial to glacial times, as shown by pigment accumulation rates (Weinelt et al. in prep.). However, short prominent productivity spikes each match the top of (supposedly strictly coeval) Heinrich IRD layers 1, 2, 4 and 5, equal to the onset of D-O interstadials 1, 2, 8 and 12. Moreover, they coincide with D-O events 5, 6 and 13 and the Preboreal subsequent to the Younger Dryas.

In the Nordic Seas, few glacial paleoproductivity records have been established (for technical reasons; Weinelt et al. this volume), except for some rough estimates based on the accumulation rates of planktonic foraminifera (Weinelt unpubl. data). They may indicate a general drop in foraminifera production from approximately $125 \cdot 10^3$ specimens cm^{-2} ky^{-1} today to approximately $15 \cdot 10^3$ specimens cm^{-2} ky^{-1} during the last glacial, probably induced by long-lasting seasonal sea-ice cover. Accordingly, glacial paleoproductivity reached a level as low as that in the modern Arctic domain, nearly an order of magnitude less than in the modern Atlantic domain.

In summary, plankton productivity (and carbon transfer to the deep ocean) during MIS 2–3 was nearly doubled in comparison with the Holocene to the south of the Heinrich iceberg track in the subtropics (Kiefer et al. in prep.; Kiefer 1998). North of the Heinrich track, productivity was as low as in the Holocene during glacial times and stage-3 stadials, i.e., along with circulation modes II and III. At this location, however, productivity reached large maxima just near the onset of D-O interstadials. These productivity pulses may result from an extreme upward supply of nutrients from the deep Atlantic right at any transition from THC mode III to THC modes II or I.

Carbon Storage and Transport in Surface and Deep Water: The "Conveyor Pump"

The modern transport of dissolved inorganic carbon (DIC) by the Atlantic THC is reflected in north-south gradients of $\delta^{13}C$ in Atlantic surface and deep waters (Kroopnick 1985; Sarnthein et al. 1994), which in turn are recorded in planktonic and benthic foraminifera tests (Duplessy 1982; Duplessy et al. 1988; Shackleton 1977; Spero et al. 1997; Zahn et al. 1986). In modern sediments close to the sites of NADW formation, high $\delta^{13}C$ values of 1.6–1.7‰ in *N. pachyderma* (corrected

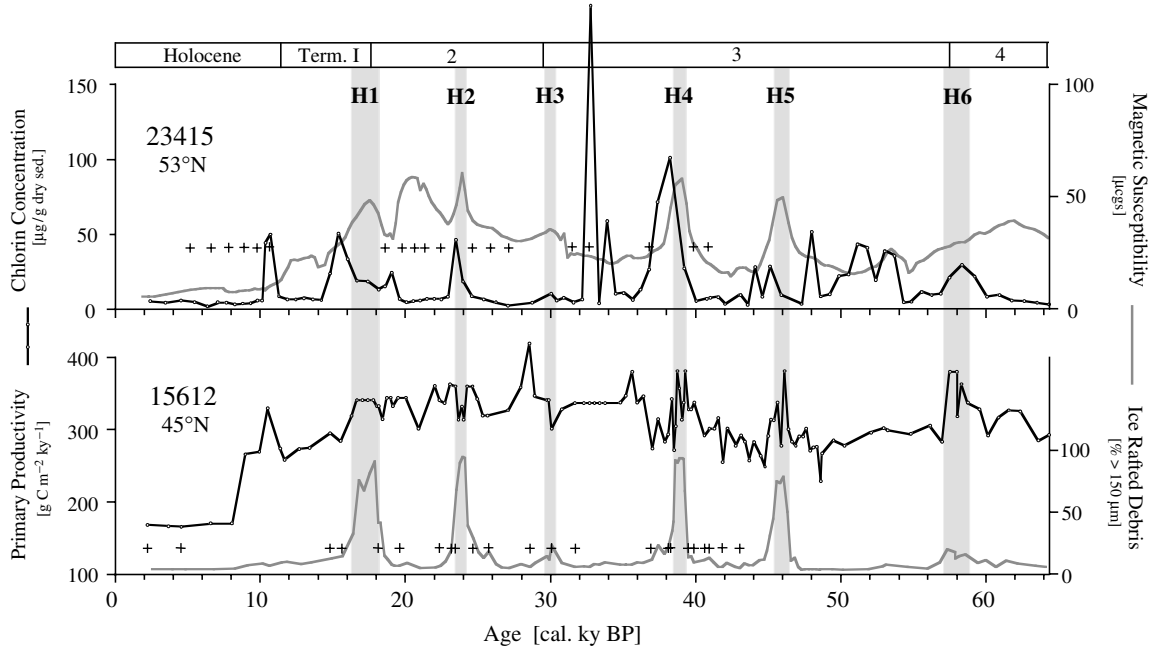

Fig. 16: Paleoproductivity records obtained from chlorin concentrations (= pigments; Weinelt et al. in prep.) near the northern margin and from planktonic foraminifera assemblages (Kiefer 1998) near the southern margin of the Heinrich iceberg track across the North Atlantic (core locations 15612 and 23415 in Table 2 and Fig. 2). Grey bars show Heinrich IRD layers H1–H6, based on IRD grain counts and magnetic susceptibility maxima. Time scales based on a total of 60 AMS ^{14}C ages converted to cal. ages following the scheme of Voelker et al. (1998). Age of marine isotope-stage boundaries 2–4 slightly modified, based on new ^{14}C calendar age conversion scheme

for a vital effect of 0.85‰; Labeyrie and Duplessy 1985; Simstich 1988) depict a DIC depleted surface water mass which is suitable for the uptake of atmospheric CO_2 (Sarnthein et al. 1995). The initial $\delta^{13}C$ signature of NADW, as shown in the epibenthic record of *C. wuellerstorfi*, is approximately 1.3–1.5‰ near and directly below the convection sites in the Greenland Sea (Sarnthein et al. 1994; Weinelt et al. this volume). As the NADW flows southward, the ongoing remineralization of low-$\delta^{13}C$ organic carbon results in a progressive $\delta^{13}C$ depletion of DIC in deep water down to less than 0.4‰ in the Southern Ocean (Fig. 11a). This $\delta^{13}C$ gradient reflects interhemispheric enrichment in DIC and finally implies CO_2 degassing near Antarctica, where NADW is upwelled to the sea surface.

Despite a basically similar circulation pattern during the late LGM (Fig. 11), integrated benthic $\delta^{13}C$ anomalies (−0.2 to −1.0‰) below 2000 m water depth suggest an excess glacial carbon storage of ~ 44 Gt in the eastern Atlantic 60° N – 30° S (Sarnthein et al. 1994) and probably an excess of more than 130 Gt C in the entire Atlantic basin up to the Weddell Sea (when trebling the eastern Atlantic number, assuming a threefold water mass for the total Atlantic). This amount compares well with the glacial-to-interglacial rise in atmospheric carbon content (170 Gt C; Sundquist 1993). No discernible portion of glacial $\delta^{13}C$ anomalies can be ascribed to an eventual increase in preformed nutrients (*sensu* Redfield et al. 1963), since the glacial $\delta^{13}C$ values of deep water close to its source at 60° N were higher by 0.4‰ than they are today (1.75‰ vs. 1.35‰; Fig. 11a).

During the totally different Heinrich meltwater mode III the excess storage of inorganic carbon rose to 70 Gt in the eastern Atlantic (Sarnthein et al. 1994) and presumably, when trebling, to more than 210 Gt C in the entire Atlantic. Possibly, a fraction of the mode II- and mode III-induced $\delta^{13}C$ lowering (0.25 to approximately 0.5‰ in the various water masses) may result from an increase in the carbonate-concentration effect recently postulated by Spero et al. (1997). In this case, estimates of excess carbon storage in the Atlantic should be reduced.

Global Implications of North Atlantic Climate Variability: Modeling Carbon Fluxes During the Glacial and the Heinrich Meltwater Mode

To better assess the global implications of these first-order estimates and the resulting oceanic and air-sea carbon fluxes, they were evaluated independently on the

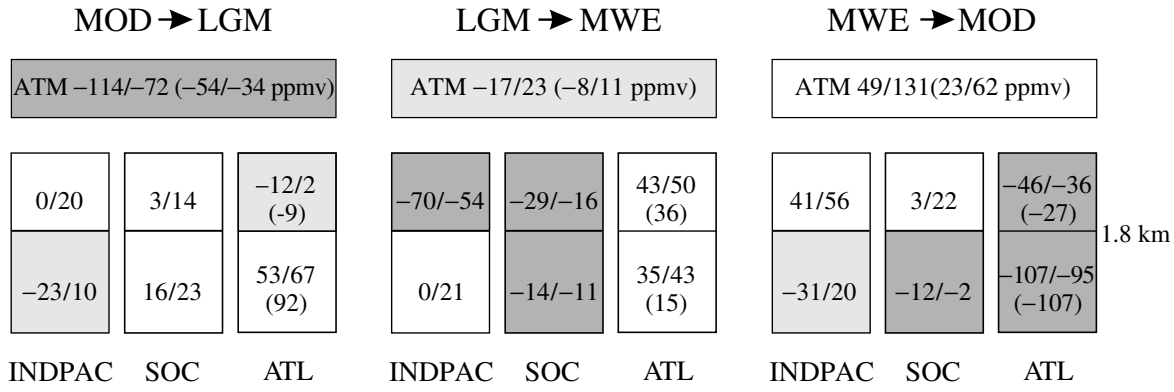

Fig. 17: Modeled variations in DIC storage (maximum / minimum Gt C) over a glacial-to-interglacial cycle. Paleoceanographic estimates (in brackets) were deduced from benthic $\delta^{13}C$ values for 60° N – 30° S (Sarnthein et al. 1994) and extrapolated via doubling to the entire Atlantic. ATM = Atmosphere; ATL = Atlantic (88° N – 32° S); SOC = Southern Ocean (> 32° S); INDPAC = Indo-Pacific Oceans (50° N – 32° S); MOD = modern. Dark shading indicates carbon depletion, light shading inconsistent sign of carbon transfer in several sensitivity experiments (Schulz et al. in press)

basis of the carbon model specified in Figure 3 and Table 3 (Schulz et al. in press) for the three fundamental modes characteristic of the Atlantic THC. Figure 17 shows that modeled shifts in the Atlantic carbon reservoirs generally reach an order of magnitude close to the figures directly deduced from benthic $\delta^{13}C$ anomalies, particularly with regard to the shift from the meltwater mode back to the modern state of the ocean. The model output may thus provide an encouraging basis for assessing past changes in the size of oceanic carbon reservoirs.

Accordingly, the major changes in the carbon budget are the following. From interglacial to LGM times the global air-sea carbon transfer leads to a drop of 72–114 Gt C in the atmosphere (equivalent to 34–54 ppmv CO_2), with carbon sequestered by the deep Atlantic below 1.8 km and the Southern Ocean. This transfer goes along with a small DIC depletion (up to –12 Gt C) in Atlantic surface and intermediate waters. The transfer of 72–114 Gt C does not include the effect of changes in total alkalinity probably needed to explain the observed interglacial-to-glacial shift in atmospheric pCO_2 (Sowers and Bender 1995). With the transition from LGM to Heinrich meltwater times net oceanic carbon uptake is rarely increased or reduced (–17 / +23 Gt C), however, the DIC gradient between the deep Indo-Pacific and Atlantic comes close to zero (Fig. 18) because of a total carbon transfer of approximately 77–93 Gt C from the Indo-Pacific and Southern Ocean to the Atlantic. The most dramatic reorganization in carbon reservoirs in the model results from the renewed onset of deep-water formation in the North Atlantic subsequent to the H1 meltwater event, at the onset of the Bølling. Within a few hundred years nearly 49–131 Gt C are removed from the Atlantic back to the atmosphere (40–85 %) and to the other ocean basins (15–60 %; see Figs. 17, 18) (Schulz et al. in press). This scenario is consistent with pCO_2 data from the Byrd ice core (Sowers and Bender 1995).

This short-term oceanic carbon release of 49–131 Gt C (corresponding to 23–62 ppmv CO_2) comes close to modern industrial carbon release in terms of both time and magnitude (~ 70 ppmv CO_2) and may have contributed to abrupt climate amelioration at the beginning of the Bølling. However, the probable increase in greenhouse warming is coeval with the turning on of the Atlantic THC and "heat pump", which acts in the same direction. Thus, the actual effect of the atmospheric CO_2 rise can rarely be distinguished in paleoclimatic records, either in the Northern or in the Southern Hemisphere. Here it is outbalanced by the onset of North Atlantic "heat piracy" which appears to dominate centennial-to-millennial-scale climate variability in the Southern Ocean (Ninnemann et al. 1999). Future high-resolution ice-core studies may provide the necessary complementary records for a better understanding of unusual climatic shifts tied to the end of Heinrich event 1.

Finally, the onset of the THC and sea-air release of 49–131 Gt C after Heinrich event 1 have also affected the atmospheric ^{14}C balance by reducing the $^{14}C/^{12}C$ ratio by ~ 3 %, reflected in a "^{14}C plateau" of approximately 150 years in the carbon model (Schulz et al. in prep.; similar to the estimate by Stocker and Wright 1996), in contrast to the duration based on deep-water coral dates (Dreger et al. in prep.), which suggest that the plateau may actually have extended over 1000–1300 years. The difference in the duration of reconstructed

and modeled "^{14}C plateaus" may, in part, stem from underestimating the antecedent atmospheric ^{14}C increase linked to the turn-off of thermohaline circulation during Heinrich 1. This, in turn, may stem from an insufficient representation of the Heinrich meltwater lid in the model.

Returning to the initial objective of this section, this carbon model also provides a rough estimate of glacial-to-interglacial variations in interhemispheric carbon flux through the Atlantic. As expected, the model control run results in a fairly small modern net transport of 0.153 Gt C/y to the south (Exp. D in Schulz et al. in press) similar to the number in the model by Sarmiento et al. (1995) with data-based estimates by Broecker and Peng (1982) and Keeling and Peng (1995). In contrast, the model reveals an nearly balanced flux of 0.046 Gt C/y to the north during the LGM and an intensified northward transport of 0.062 Gt C/y during the Heinrich 1 meltwater mode.

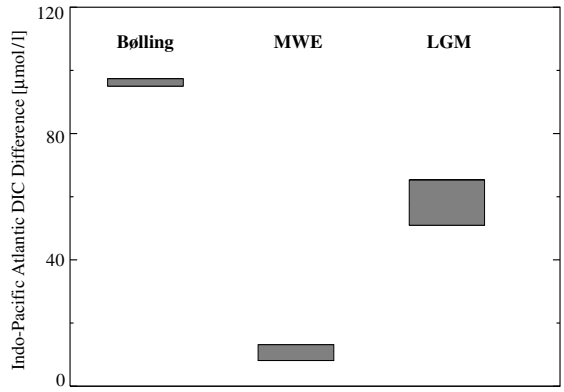

Fig. 18: Average difference in DIC concentration at 2000 m depth between the Atlantic (ATL) and combined Indo-Pacific (INDPAC) for the three basic modes of THC. Width of bars gives range of variability in different sensitivity experiments (Schulz et al. in press)

Synthesis and Highlights

Over the last 60,000 years the North Atlantic realm has played a key role in accentuating, even in triggering global climatic changes on Milankovitch and centennial-to-millennial time scales, even on time scales of less than a decade, as documented in ice cores from Greenland and Antarctica. To better constrain the causal links of these changes paleoceanographic records from approximately 115 sediment cores in the northern North Atlantic, 30 of them AMS ^{14}C dated, and from approximately 100 cores from the eastern Atlantic have been established and compiled over the last decade. This data set has assisted us in the reconstruction and simulation of computational models, of basic modes of Atlantic thermohaline circulation and heat transport and, finally, of interhemispheric and interoceanic carbon fluxes over marine isotope stages 1–3.

In harmony with Sarnthein et al. (1994), Yu et al. (1996) and Stocker (1998) three extreme modes are recognized in the operation of Atlantic THC, more specifically, in the formation or reduction of North Atlantic Deep Water (NADW). Mode I corresponds to the Holocene/modern conditions, with intensive formation of NADW, coupled to strong heat and moisture fluxes to the continents adjacent to the northern North Atlantic. Mode II corresponds to peak glacial climatic conditions, i.e., a stable regime with the fluxes of upper and lower NADW reduced by some 50 % and, accordingly, with a clear reduction in heat flux to northern Europe. Cooling was further enhanced by an anticyclonic eddy west of Ireland, induced by melting icebergs, which resulted in a cold-water flow down to southwestern France. In contrast to previous views, this data suggests that the glacial Nordic Seas remained ice-free during summer. This would have formed, on the one hand, a major source of moisture for the build-up of ice sheets on the adjacent continents and particularly on the Barents shelf, and on the other hand, a minor source of extremely dense deep water as compared to the then dominant sources south of Greenland.

Mode III is associated with the Heinrich meltwater events, also applying to several stadials prior to D-O events. This mode was controlled by large amounts of meltwater from icebergs surging from the ice sheets on the continents near the sites of deep-water convection. The meltwater prevented any deep and intermediate water formation in the North Atlantic and therefore, any heat advection to Europe, probably tied to perennial sea ice in the Nordic Seas. Mode III induced a reversed pattern of the THC, stopped "heat piracy" in the Central and South Atlantic, and hence producing warming in parts of Antarctica and the South Atlantic.

In contrast to previous views (e.g. Broecker 1992), the strongly seasonal THC of the early Younger Dryas cold spell did not resemble mode III, but rather the Holocene mode 1. The YD was possibly initiated by an Arctic meltwater pulse from Siberian rivers (Spielhagen et al. 1997, 1998). These results are based on well-dated cores with sedimentation rates of 7–60 cm/ka. A late YD-to-Preboreal switch to mode III is in line with deep-water records from the western Atlantic (Boyle and Keigwin 1987; Marchitto et al. 1998), when their age control is closely inspected.

Employing this new combined ocean general circulation/biogeochemistry box model (Schulz et al. in press), the three modes of THC defined above resulted in an interglacial-to-glacial drop in atmospheric CO_2 of 34–54 ppmv (72–114 Gt C), primarily sequestered in the deep Atlantic. Mode III did not add much to this figure, but led to a carbon transfer of approximately 78–93 Gt C from the Indo-Pacific and Southern Ocean to the Atlantic. During the abrupt transition from mode III to mode I, such as at the onset of the Bølling, 2–94 Gt C were moved from the Atlantic to the other ocean basins, and 49–131 Gt C (23–62 ppmv) were released to the atmosphere, equivalent to one to two thirds of the amount recently released by fossil fuel burning and land use changes. In the model this spectacular carbon release led to a "^{14}C plateau" of > 150 years.

The origin of the robust Dansgaard-Oeschger (D-O) 1500-y cycles in the GISP2 ice core was constrained in five new ultrahigh- resolution (20–80 y-) paleoceanographic records from the northern North Atlantic, dated by > 320 AMS ^{14}C dates and by fine tuning to the annual layer counted time scale of the GISP2 temperature record (Grootes and Stuiver 1997), with an age uncertainty of ~ 50–100 y relative to the GISP2 age scale, in some cases reaching one-third of a D-O cycle (500 y). The D-O cycles and, in some cases, their multiples represent millennial-scale changes between the three THC modes. In the Irminger and Icelandic Seas the oceanographic characteristics and origin of these cycles, which basically do not differ from those of the 7200-y Heinrich-Bond periodicities between 8 and 60 ka, appear as follows:

In the 1460-y frequency band, the fast cooling of D-O stadials in the Irminger Sea went in phase with initial meltwater injections from East Greenland (and/or the Arctic), here suggesting an internal trigger mechanism in accordance with binge-purge models (MacAyeal 1993a, b; Rahmstorf 1995). Based on the phase lags of IRD, icebergs from East Greenland and Iceland arrived to the north of the Denmark Strait 140 y and in the Irminger Sea only 280–240 y after peak meltwater injection.

In turn, Heinrich ice rafting from the Laurentian ice sheet (H1, H2, H4, H5) lagged ice rafting from Iceland and was therefore probably induced by a slight sea-level rise proceeding from the initial surge from East Greenland and Iceland. Near the end of MIS 2 a major surge from the then glaciated Barents shelf lagged the initial D-O cooling by 1500 y and led to the most prominent and extended reversal in Atlantic THC over the last 60 ky (mode III at H1; probably also at the end of MIS 4, at H6).

Meltwater stratification of the Irminger Sea reached its maximum only 400 y after the IRD maximum and resulted from sea-ice formation in brine-water signals down to 3–4 km water depth, signals which preceded the classic D-O jump to maximum warmth only by < 130 y. Nearly in phase with this warming, brine-water controlled deep-water formation possibly formed as a result of a further entrainment of warm water from the subtropics, the key mechanism for triggering the abrupt onset of the Atlantic THC mode II and, in cases of a favorable insolation regime, the onset of mode I within a decade or so.

No such mechanisms have been conceived yet which are able to explain Holocene IRD and monsoon periodicities near 1500 y (Sirocko et al. 1996; Bond et al. 1997; Wang et al. 1998), thus providing an important objective for future research.

Acknowledgments

We gratefully acknowledge the longlasting and very successful cooperation with Eystein Jansen and his group in Bergen as well as with French and English colleagues within the framework of European projects. We also acknowledge critical discussions and support which came from A. Altenbach (now in Munich), R. Henrich (now in Bremen) and from M. Nadeau and the Leibniz Laboratory working group in Kiel. We thank R. Zahn and an unknown colleague, who acted as experienced and thorough reviewers of this paper, for excellent suggestions, finally J.P. Kennnett for many clarifying discussions while the first author was in Santa Barbara. The study of a great number of fine sediment cores would not have been possible without the great efforts made by the captains and crews of RV Meteor, RV Polar-stern, RV Poseidon and NS Marion Dufresne. We owe sincere thanks to K. Kissling, A. Lüders, W. Rehder, M. Stahlberg and B. van Brevern for dedicated and careful technical assistance both on board and in the lab as well as to H. Cohrt and H. Heckt in the stable isotope lab, finally, to many dozens of students for their help with tedious routine work. We thank the Deutsche Forschungsgemeinschaft, Bonn, for long-term and generous financing of the SFB 313 project, moreover, the German Ministry for Research for funding the National Climate Project, as well as the European Union and the IMAGES project for their support.

References

Alley, R. B., and P. U. Clark, The deglaciation of the northern hemisphere: a global perspective, *Annu. Rev. Earth Planet Sci.*, 27, 149–182, 1999.

Alley, R. B., D. A. Meese, C. A. Shuman, A. J. Gow, K. C. Taylor, P. M. Grootes, J. W. C. White, M. Ram, E. D. Waddington, P. A. Mayewski, and G. A. Zielinski, Abrupt increase in Greenland snow accumulation at the end of the Younger Dryas event, *Nature*, 362, 527–529, 1993.

Alley, R. B., A. - M. Agústsdóttir, and P. J. Fawcett, Ice-core evidence of late-Holocene reduction in North Atlantic ocean heat transport, in Spec. Publ. edn. American Geophysical Union, 28 ms. pp., 1998.

Altenbach, A. V., *Verbreitungsmuster benthischer Foraminiferen im Arktischen Ozean und in glazialen und interglazialen Sedimenten des Europäischen Nordmeeres*, Habilitation Thesis, 111 pp., Univ. of Kiel, Kiel, 1992.

Bainbridge, A. E. (ed), *GEOSECS Atlantic Expedition, Volume 1, Hydrographic data 1972–1973*, U.S. Government Printing Office, Washington, DC, 1981.

Bard, E., Geochemical and geophysical implications of the radiocarbon calibration, *Geochim. Cosmochim. Acta*, 62, 2025–2038, 1998.

Bard, E., M. Arnold, R. G. Fairbanks, and B. Hamelin, ^{230}Th- ^{234}U and ^{14}C ages obtained by mass spectrometry on corals, *Radiocarbon*, 35, 191–199, 1993.

Bard, E., F. Rostek, and C. Sonzogni, Interhemispheric synchrony of the last deglaciation inferred from alkenone palaeothermometry, *Nature*, 385, 707–710, 1997.

Belkin, I. M., S. Levitus, J. Antonov, and S. A. Malmberg, 'Great salinity anomalies' in the northern North Atlantic, *Progr. in Oceanogr.*, 41, 1–68, 1998.

Bender, M., T. Sowers, M. - L. Dickson, J. Orchardo, P. Grootes, P. A. Mayewski, and D. A. Meese, Climate correlations between Greenland and Antarctica during the past 100,000 years, *Nature*, 372, 663–666, 1994.

Berger, A., and M. F. Loutre, Insolation values for the climate of the last 10 Million years, *Quat. Sci. Rev.*, 10, 297–317, 1991.

Berger, A., and M. F. Loutre, Intertropical latitudes and precessional and half-precessional cycles, *Science*, 278, 1476–1478, 1997.

Berger, W. H., and E. Jansen, Younger Dryas episode: ice collapse and super-fjord heat pump, in *Verhandelingen, Sfd. Natuurkunde, Eerste Reeks, deel 44: The Younger Dryas*, edited by S. R. Troelstra, J. E. van Hinte, and G. M. Ganssen, pp. 61–105, Koninklijke Nederlandse Akademie van Wetenschappen, Amsterdam, 1995.

Berger, W. H., and G. Wefer, Expeditions into the past: Paleoceanograpic studies of the South Atlantic, in *The South Atlantic*, edited by G. Wefer, W. H. Berger, G. Siedler, and D. J. Webb, pp. 363–410, Springer, Berlin, 1996.

Berger, W. H., S. Burke, and E. Vincent, Glacial-Holocene transition: Climate fluctuations and sporadic shutdown of NADW production, in *Abrupt climatic change*, edited by W. H. Berger, and L. D. Labeyrie, pp. 279–297, D. Reidel Publ. Company, Dordrecht, 1987.

Blunier, T., J. Chappellaz, J. Schwander, A. Dallenbach, B. Stauffer, T. F. Stocker, D. Raynaud, J. Jouzel, H. B. Clausen, C. U. Hammer, and S. J. Johnsen, Asynchrony of Antarctic and Greenland climate change during the last glacial period, *Nature*, 394, 739–743, 1998.

Boden, P., R. G. Fairbanks, J. D. Wright, and L. H. Burckle, High-resolution stable isotope records from southwest, Sweden, The drainage of the Baltic Ice Lake and Younger Dryas ice margin oscillations, *Paleoceanogr.*, 12, 39–49, 1997.

Bohrmann, G., R. Henrich, and J. Thiede, Miocene to Quaternary paleoceanography in the northern North Atlantic: Variability in carbonate and biogenic opal accumulation, in *Geological History of the Polar Oceans: Arctic versus Antarctic*, edited by U. Bleil, and J. Thiede, pp. 647–675, NATO ASI Series, Kluwer Acad. Publ., Dordrecht, 1990.

Bond, G. C., and R. Lotti, Iceberg discharges into the North Atlantic on millennial time scales during the last glaciation, *Science*, 267, 1005–1010, 1995.

Bond, G., H. Heinrich, W. Broecker, L. Labeyrie, J. McManus, J. Andrews, S. Huon, R. Jantschik, S. Clasen, C. Simet, K. Tedesco, M. Klas, G. Bonani, and S. Ivy, Evidence for massive discharges of icebergs into the North Atlantic ocean during the last glacial period, *Nature*, 360, 245–249, 1992.

Bond, G., W. S. Broecker, S. Johnsen, J. McManus, L. Labeyrie, J. Jouzel, and G. Bonani, Correlations between climate records from North Atlantic sediments and Greenland ice, *Nature*, 365, 143–147, 1993.

Bond, G., W. Showers, M. Cheseby, R. Lotti, P. Almasi, P. Demenocal, P. Priore, H. Cullen, I. Hajdas, and G. Bonani, A pervasive millennial-scale cycle in North Atlantic Holocene and glacial climates, *Science*, 278, 1257–1266, 1997.

Boyle, E. A., Cadmium and ^{13}C paleochemical ocean distributions during the stage 2 glacial maximum, *Annu. Rev. Earth Planet Sci.*, 20, 245–287, 1992.

Boyle, E., Last-Glacial-Maximum North Atlantic deep water: on, off or somewhere in-between?, *Phil. Trans. R. Soc. Lond. B.*, 348, 243–253, 1995.

Boyle, E. A., and L. D. Keigwin, North Atlantic thermohaline circulation during the past 20,000 years linked to high-latitude surface temperature, *Nature*, 330, 35–40, 1987.

Broecker, W. S., The great ocean conveyor, *Oceanogr.*, 4, 79–89, 1991.

Broecker, W. S., The strength of the nordic heat pump, in *NATO ASI Series, Vol. 12: The last deglaciation: Absolute and radiocarbon chronologies*, edited by E. Bard, and W. S. Broecker, pp. 173–181, Springer, Berlin, 1992.

Broecker, W. S., Massive iceberg discharges as triggers for global climate change, *Nature*, 372, 421–424, 1994.

Broecker, W. S., Paleocean circulation during the last deglaciation: A bipolar seesaw?, *Paleoceanogr.*, 13, 119–121, 1998.

Broecker, W. S., and G. H. Denton, The role of ocean atmosphere reorganizations in glacial cycles, *Geochim. Cosmochim. Acta*, 53, 2465–2501, 1989.

Broecker, W. S., and G. M. Henderson, The sequence of events surrounding Termination I. and their implications for the cause of glacial-interglacial CO_2 changes, *Paleoceanogr.*, 13, 352–364, 1998.

Broecker, W. S., and T. - H. Peng, *Tracers in the sea*, Lamont-Doherty Geological Observatory, Palisades, New York, 1982.

Broecker, W. S., and T. - H. Peng, Glacial to interglacial changes in the operation of the glacial carbon cycles, *Radiocarbon*, 28, 309–327, 1986.

Broecker, W. S., and T. - H. Peng, The role of $CaCO_3$ compensation in the glacial to interglacial atmospheric CO_2 change, *Global Biogeochem. Cycles*, 1, 15–29, 1987.

Broecker, W. S., and T. - H. Peng, The cause of the glacial to interglacial atmospheric CO_2 change: a polar alkalinity hypothesis, *Global Biogeochem. Cycles*, 3, 215–239, 1989.

Broecker, W. S., and T. - S. Peng, Interhemispheric transport of carbon dioxide by ocean circulation, *Nature*, 356, 587–589, 1992.

Broecker, W. S., D. M. Peteet, and D. Rind, Does the ocean-atmosphere system have more than one stable mode of operation?, *Nature*, 315, 21–26, 1985.

Broecker, W. S., M. Andree, G. Bonani, W. Wölfli, M. Klas, A. Mix, and H. Oeschger, Comparison between radiocarbon ages obtained from coexisting foraminifera, *Paleoceanogr.*, 3, 647–657, 1988.

Broecker, W. S., J. P. Kennett, B. P. Flower, J. T. Teller, S. Trumbore, G. Bonani, and W. Woelfli, Routing of meltwater from the Laurentide ice sheet during the Younger Dryas cold episode, *Nature*, 341, 318–321, 1989.

Broecker, W. S., G. Bond, M. Klas, G. Bonani, and W. Wolfli, A salt oscillator in the glacial Atlantic? 1. The concept, *Paleoceanogr.*, 5, 469–477, 1990.

Bryan, F., High-latitude salinity effects and interhemispheric thermohaline circulation, *Nature*, 323, 301–304, 1986.

Chapman, M. R., and N. J. Shackleton, Millennial-scale fluctuations in North Atlantic heat flux during the last 150,000 years, *Earth Planet Sci. Lett.*, 159, 57–70, 1998.

Charles, C. D., and R. G. Fairbanks, Evidence from Southern Ocean sediments for the effect of North Atlantic deep-water flux on climate, *Nature*, 355, 416–419, 1992.

Charles, C. D., J. Lynch-Stieglitz, U. S. Ninnemann, and R. G. Fairbanks, Climate connections between the hemisphere revealed by deep sea sediment core ice core correlations, *Earth Planet Sci. Lett.*, 142, 19–27, 1996.

Clement, A. C., and M. A. Cane, Part I. Variability of the tropical Pacific coupled ocean-atmosphere system: precessional response, abrupt change and sub-Milankovitch frequencies. Part II. Global connections, Chapman conference on mechanisms of millenial-sale global climate change. June 14–18, Snowbird, 29 (Abstract)., 1998.

CLIMAP Project Members, *Seasonal reconstructions of the Earth's surface at the last glacial maximum*, Geological Society of America, Map and Chart Series, MC-36, 1981.

Cortijo, E., *La variabilité climatique rapide dans l'Atlantique Nord depuis 128 000 ans: relations entre les calottes de glace et l'océan de surface*, Doctoral Thesis, 108 pp., Universite de Paris-Sud, U.F.R. Scientifique d'Orsay, 1995.

Cortijo, E., L. Labeyrie, L. Vidal, M. Vautravers, M. Chapman, J. C. Duplessy, M. Elliot, M. Arnold, J. L. Turon, and G. Auffret, Changes in sea surface hydrology associated with Heinrich event 4 in the North Atlantic Ocean between 40 and 60 N, *Earth Planet Sci. Lett.*, 146, 29–45, 1997.

Costello, O., and H. A. Bauch, Late Pleistocene-Holocene productivity record of benthic foraminifera from the Iceland Plateau (Core PS 1246-2), in *Contributions to the micropaleontology and paleocean-*

ography of the northern North Atlantic, edited by H. C. Hass, and M. A. Kaminski, pp. 141–148, The Grzybowski Foundation, Kraków, 1997.

Craig, H., and L. I. Gordon, Deuterium and oxygen 18 variations in the ocean and the marine atmosphere, in *Occ. Publ. No. 3: Symposium on marine geochemistry*, 277 pp., Graduate School of oceanography, Univ. Rhode Island, 1965.

Cuffey, K. M., G. D. Clow, R. B. Alley, M. Stuiver, E. D. Waddington, and R. W. Saltus, Large Arctic temperature change at the Wisconsin-Holocene glacial transition, *Science*, 270, 455–458, 1995.

Curry, R. G., *Hydrobase a database of hydrographic stations and tools for climatological analysis. Technical Report*, 44 pp., Woods Hole Oceanographic Institution, Woods Hole, 1996.

Curry, W. B., and D. W. Oppo, Synchronous, high-frequency oscillations in tropical sea surface temperatures and North Atlantic Deep Water production during the last glacial cycle, *Paleoceanogr.*, 12, 1–14, 1997.

Dansgaard, W., J. W. C. White, and S. J. Johnsen, The abrupt termination of the Younger Dryas climate event, *Nature*, 339, 532–534, 1989.

Dansgaard, W., S. J. Johnsen, H. B. Clausen, D. Dahl-Jensen, N. S. Gundestrup, C. U. Hammer, C. S. Hvidberg, J. P. Steffensen, A. E. Sveinbjörnsdottir, J. Jouzel, and G. Bond, Evidence for general instability of past climate from a 250-kyr ice-core record, *Nature*, 364, 218–220, 1993.

de Vernal, A., C. Hillaire-Marcel, and G. Bilodeau, Reduced meltwater outflow from the Laurentide ice margin during the Younger Dryas, *Nature*, 381, 774–777, 1996.

Dickson, R. R., and J. Brown, The Production of North Atlantic Deep Water – Sources, Rates, and Pathways, *J. Geophys. Res.*, C99, 12319–12341, 1994.

Dickson, R., J. Lazier, J. Meincke, P. Rhines, and J. Swift, Long-term coordinated changes in the convective activity of the North Atlantic, *Progr. in Oceanogr.*, 38, 241–295, 1996.

Dokken, T. M., and M. Hald, Rapid climatic shifts during isotope stages 2–4 in the Polar North Atlantic, *Geology*, 24, 599–602, 1996.

Domack, E. W., A. J. T. Jull, J. B. Anderson, T. W. Linick, and C. R. Williams, Application of tandem accelerator mass-spectrometer dating to late Pleistocene-Holocene sediments of the East Antarctic continental shelf, *Quat. Res.*, 31, 277–287, 1989.

Dowdeswell, J. A., M. A. Maslin, J. T. Andrews, and I. N. McCave, Iceberg production, debris rafting, and the extent and thickness of Heinrich layers (H-1, H-2) in north Atlantic sediments, *Geology*, 23, 301–304, 1995.

Dreger, D., *Decadal-to-centennial-scale sediment records of ice advance on the Barents shelf and meltwater discharge into the north-eastern Norwegian Sea over the last 40 kyr*, D.Sc. Thesis, pp. 1–79, Univ. of Kiel, Kiel, 1999.

Duplessy, J. - C., Glacial to interglacial contrasts in the northern Indian Ocean, *Nature*, 295, 494–498, 1982.

Duplessy, J. C., G. Delibrias, J. L. Turon, C. Pujol, and J. Duprat, Deglacial warming of the northeastern Atlantic Ocean; correlation with the paleoclimatic evolution of the European continent, *Palaeogeogr., Palaeoclimatol., Palaeoecol.*, 35, 121–144, 1981.

Duplessy, J. C., N. J. Shackleton, R. K. Matthews, W. L. Prell, W. F. Ruddiman, M. Caralp, and C. H. Hendy, ^{13}C record of benthic foraminifera in the last interglacial ocean; implications for the carbon cycle and the global deep water circulation, *Quat. Res.*, 21, 225–243, 1984.

Duplessy, J. C., N. J. Shackleton, R. G. Fairbanks, L. Labeyrie, D. Oppo, and N. Kallel, Deepwater source variations during the last climatic cycle and their impact on the global deepwater circulation, *Paleoceanogr.*, 3, 343–360, 1988.

Duplessy, J. - C., L. Labeyrie, A. Juillet-Leclerc, J. Duprat, and M. Sarnthein, Surface salinity reconstruction of the North Atlantic ocean during the last glacial maximum, *Oceanol. Acta*, 14, 311–324, 1991.

Duplessy, J. - C., L. Labeyrie, M. Paterne, S. Hovine, T. Fichefet, J. Duprat, and M. Labracherie, High latitude deep water sources during the last glacial maximum and the intensity of the global oceanic circulation, in *The South Atlantic*, edited by G. Wefer, W. H. Berger, G. Siedler, and D. J. Webb, pp. 445–460, Springer, Berlin, 1996.

Eiriksson, J., K. L. Knudsen, and H. Haflidason, Paleoceanography within the boundary area between east Greenland and Irminger currents on the north Icelandic shelf, 6th International Conference on Paleoceanography, Lisbon, 24–28 Aug. Program, 101 (Abstract), 1998.

Elliot, M., L. Labeyrie, G. Bond, E. Cortijo, J. L. Turon, N. Tisnerat, and J. C. Duplessy, Millennial-scale iceberg discharges in the Irminger Basin during the last glacial period: Relationship with the Heinrich events and environmental settings, *Paleoceanogr.*, 13, 433–446, 1998.

Fairbanks, R. G., A 17,000-year glacio-eustatic sea level record: Influence of glacial melting rates on the Younger Dryas event and deep-ocean circulation, *Nature*, 342, 637–642, 1989.

Fichefet, T., S. Hovine, and J. C. Duplessy, A model study of the Atlantic thermohaline circulation during the last glacial maximum, *Nature*, 372, 252–255, 1994.

Fronval, T., and E. Jansen, Eemian and early Weichselian (140–60 ka) paleoceanography and paleoclimate in the Nordic seas with comparisons to Holocene conditions, *Paleoceanogr.*, 12, 443–462, 1997.

Fronval, T., E. Jansen, J. Bloemendal, and S. Johnsen, Oceanic evidence for coherent fluctuations in Fennoscandian and Laurentide ice sheets on millennium timescales, *Nature*, 374, 443–446, 1995.

Ganopolski, A., S. Rahmstorf, V. Petoukhov, and M. Claussen, Simulation of modern and glacial climates with a coupled global model of intermediate complexity, *Nature*, 391, 351–356, 1998.

Ganssen, G., Dokumentation von küstennahem Auftrieb anhand stabiler Isotope in rezenten Foraminiferen vor Nordwest-Afrika, *Meteor. Forsch. Erg.*, C37, 1–46, 1983.

Grootes, P. M., and M. Stuiver, Oxygen 18/16 variability in Greenland snow and ice with 10^{-3}- to 10^{5}-year time resolution, *J. Geophys. Res.*, C102, 26455–26470, 1997.

Grootes, P. M., M. Stuiver, J. W. C. White, S. Johnsen, and J. Jouzel, Comparison of oxygen isotope records from the GISP2 and GRIP Greenland ice cores, *Nature*, 366, 552–554, 1993.

Grousset, F. E., L. Labeyrie, J. A. Sinko, M. Cremer, G. Bond, J. Duprat, E. Cortijo, and S. Huon, Patterns of ice-rafted detritus in the glacial North-Atlantic (40–55 N), *Paleoceanogr.*, 8, 175–192, 1993.

Gwiazda, R. H., S. R. Hemming, and W. S. Broecker, Provenance of icebergs during Heinrich event 3 and the contrast to their sources during other Heinrich episodes, *Paleoceanogr.*, 11, 371–378, 1996.

Guilderson, T. P., R. G. Fairbanks, and J. L. Rubenstone, Tropical temperature variations since 20,000 years ago, Modulating interhemispheric climate change, *Science*, 263, 663–665, 1994.

Gwiazda, R. H., S. R. Hemming, and W. S. Broecker, Tracking the sources of icebergs with lead isotopes: The provenance of ice-rafted debris in Heinrich layer 2, *Paleoceanogr.*, 11, 77–93, 1996b.

Hald, M., T. Dokken, and S. Hagen, Palaeoceanography on the European arctic margin during the last deglaciation, in *Special Publication No. 111: Late Quaternary palaeoceanography of the North Atlantic margins*, edited by J. T. Andrews, W. E. N. Austin, H. Bergsten, and A. E. Jennings, pp. 275–287, Geological Society, London, 1996.

Harris, P. G., M. Zhao, A. Rosell-Mele, R. Tiedemann, M. Sarnthein, and J. R. Maxwell, Chlorin accumulation rate as a proxy for Quaternary marine primary productivity, *Nature*, 383, 63–65, 1996.

Hass, H. C., H. Andruleit, A. Baumann, K. - H. Baumann, A. Kohly, S. Jensen, J. Matthiessen, C. Samtleben, P. Schäfer, A. Schröder-Ritzrau, and J. Thiede, The potential of synoptic plankton analyses for paleoclimatic investigations: Five plankton groups from the Holocene Nordic Seas, in *The northern North Atlantic: a changing environment*, edited by P. Schäfer, W. Ritzrau, M. Schlüter, and J. Thiede, Springer, Berlin, this volume.

Haupt, B. J., D. Seidov, and K. Stattegger, SEDLOB and PATLOB: Two numerical tools for modeling climatically forced sediment and water volume transport in large ocean basins, in *Computerized modeling of sedimentary systems*, edited by J. Harff, W. Lemke, and K. Stattegger, Springer, Berlin, 1998.

Hebbeln, D., T. Dokken, E. S. Andersen, M. Hald, and A. Elverhoi, Moisture supply for northern ice-sheet growth during the Last Glacial Maximum, *Nature*, 370, 357–360, 1994.

Heinrich, H., Origin and consequences of cyclic ice rafting in the Northeast Atlantic ocean during the past 130,000 years, *Quat. Res.*, 29, 142–152, 1988.

Heinze, C., *Zur Erniedrigung des atmosphärischen Kohlendioxidgehalts durch den Weltozean während der letzten Eiszeit*, Examensarbeit 3, pp. 1–180, Max-Planck-Institut für Meteorologie, Hamburg, 1990.

Hellermann, S., and M. Rosenstein, Normal monthly wind stress over the world ocean with error estimates, *J. Phys. Oceanogr.*, 13, 1093–1104, 1983.

Henrich, R., Dynamics of Atlantic water advection to the Norwegian-Greenland Sea – a time-slice record of carbonate distribution in the last 300 ky, *Mar. Geol.*, 145, 95–131, 1998.

Henrich, R., Cycles, rythms, and events in Quaternay Arctic and Antarctic glaciomarine deposits, in *Geological History of the Polar Oceans: Arctic versus Antarctic*, edited by U. Bleil, and J. Thiede, NATO ASI Series, Kluwer Acad. Publ., Dordrecht, 1990.

Hillaire-Marcel, C., A. de Vernal, G. Bilodeau, and G. Wu, Isotope Stratigraphy, Sedimentation Rates, Deep Circulation, and Carbonate Events in the Labrador Sea During the Last 200 ka, *Can. J. Earth Sci.*, 31, 63–89, 1994.

Hopkins, T. S., The GIN Sea – a synthesis of its physical oceanography and literature review 1972–1985, *Earth Sci. Rev.*, 30, 175–319, 1991.

Hüls, M., R. Zahn, and U. Pflaumann, Late Pleistocene SST as inferred from planktonic foraminiferal census

counts in core M35003, Tobago basin. 6th International Conference on Paleoceanography. Lisbon, 24–28 Aug. Program, 128 (Abstract), 1998.

Hughen, K. A., J. T. Overpeck, S. J. Lehman, M. Kashgarian, J. Southon, L. C. Peterson, R. Alley, and D. M. Sigman, Deglacial changes in ocean circulation from an extended radiocarbon calibration, *Nature*, 391, 65–68, 1998.

Hunt, A. G., and P. E. Malin, Possible triggering of Heinrich events by ice-load-induced earthquakes, *Nature*, 393, 155–158, 1998.

Imbrie, J., E. A. Boyle, S. C. Clemens, A. Duffy, W. R. Howard, G. Kukla, J. Kutzbach, D. G. Martinson, A. McIntyre, A. C. Mix, B. Molfino, J. J. Morley, L. C. Peterson, N. G. Pisias, W. L. Prell, M. E. Raymo, N. J. Shackleton, and J. R. Toggweiler, On the structure and origin of major glaciation cycles 1. Linear response to Milankovitch forcing, *Paleoceanogr.*, 7, 701–738, 1992.

Imbrie, J., A. Berger, E. A. Boyle, S. C. Clemens, A. Duffy, W. R. Howard, G. Kukla, J. Kutzbach, D. G. Martinson, A. McIntyre, A. C. Mix, B. Molfino, J. J. Morley, L. C. Peterson, N. G. Pisias, W. L. Prell, M. E. Raymo, N. J. Shackleton, and J. R. Toggweiler, On the structure and origin of major glaciation cycles 2. The 100,000-year cycle, *Paleoceanogr.*, 8, 699–735, 1993.

Isarin, R. F. B., H. Renssen, and E. A. Koster, Surface wind climate during the Younger Dryas in Europe as inferred from aeolian records and model simulations, *Palaeogeogr., Palaeoclimatol., Palaeoecol.*, 134, 127–148, 1997.

Jansen, E., and T. Veum, Evidence for two-step deglaciation and its impact on North Atlantic deep-water circulation, *Nature*, 343, 612–616, 1990.

Jansen, E., M. E. Raymo, and P. Blum, et al. (eds), *Proc. ODP, Init. Repts., 162*, Ocean Drilling Program, College Station, TX, 1996.

Jasper, J. P., E. L. Sikes, and J. M. Hayes, Transfer of CO_2 from equatorial latitudes to high latitudes during the late Quaternary, in *Air-water gas transfer*, edited by B. Jähne, and E. C. Monahan, pp. 879–888, AEON Verlag & Studio, Hanau, 1995.

Johnsen, S. J., D. Dahl-Jensen, W. Dansgaard, and N. S. Gundestrup, Greenland paleotemperatures derived from GRIP bore hole temperature and ice core isotope profiles, *Tellus*, B47, 624–629, 1995.

Johnsen, S. J., H. B. Clausen, W. Dansgaard, N. S. Gundestrup, C. U. Hammer, U. Andersen, K. K. Andersen, C. S. Hvidberg, D. Dahljensen, J. P. Steffensen, H. Shoji, A. E. Sveinbjornsdottir, J. White, J. Jouzel, and D. Fisher, The ^{18}O record along the Greenland Ice Core Project deep ice core and the problem of possible Eemian climatic instability, *J. Geophys. Res.*, C102, 26397–26410, 1997.

Jones, G. A., and L. D. Keigwin, Evidence from Fram Strait (78 N) for early deglaciation, *Nature*, 336, 56–59, 1988.

Jung, S. J. A., Wassermassenaustausch zwischen NE-Atlantik und Nordmeer während der letzten 300.000/80.000 Jahre im Abbild stabiler O- und C-Isotope, *Ber. SFB 313, Univ. Kiel*, 61, 1–104, 1996.

Keeling, R. F., and T. - H. Peng, Transport of heat, CO_2 and O_2 by the Atlantic's thermohaline circulation, *Phil. Trans. R. Soc. Lond. B.*, 348, 133–142, 1995.

Keigwin, L. D., and E. A. Boyle, Late Quaternary paleochemistry of high-latitude surface waters, *Palaeogeogr., Palaeoclimatol., Palaeoecol.*, 73, 85–106, 1989.

Keigwin, L. D., and G. A. Jones, The marine record of deglaciation from the continental margin off Nova Scotia, *Paleoceanogr.*, 10, 973–985, 1995.

Kellogg, T. B., Paleoclimatology and paleo-oceanography of the Norwegian and Greenland seas; glacial-interglacial contrasts, *Boreas*, pp. 115–137, 1980.

Kiefer, T., Produktivität und Temperaturen im subtropischen Nordatlantik: zyklische und abrupte Veränderungen im späten Quartär, *Berichte – Reports, Geol-Paläont. Inst. Univ. Kiel*, 90, 1–127, 1998.

Kiefer, T., M. Weinelt, M. Sarnthein, and U. Pflaumann, High-productivity in the subtropical North Atlantic along with Heinrich meltwater events, in prep.

Koç, N., and E. Jansen, Response of the high-latitude Northern Hemisphere to the orbital climate forcing: Evidence from the Nordic Seas, *Geology*, 22, 523–526, 1994.

Koç, N., E. Jansen, and H. Haflidason, Paleoceanographic reconstructions of surface ocean conditions in the Greenland, Iceland and Norwegian Seas through the last 14 ka based on diatoms, *Quat. Sci. Rev.*, 12, 115–140, 1993.

Kroon, D., W. E. N. Austin, M. R. Chapman, and G. M. Ganssen, Deglacial surface circulation changes in the northeastern Atlantic: Temperature and salinity records off NW Scotland on a century scale, *Paleoceanogr.*, 12, 755–763, 1997.

Kroopnick, P. M., The distribution of ^{13}C of CO_2 in the world oceans, *Deep. Sea. Res.*, 32, 57–84, 1985.

Laberg, J. S., and T. O. Vorren, Late Weichselian submarine debris flow deposits on the Bear Island Trough mouth fan, *Mar. Geol.*, 127, 45–72, 1995.

Laberg, J. S., and T. O. Vorren, The middle and late Pleistocene evolution of the Bear Island Trough

mouth fan, *Global Planet Change*, 12, 309–330, 1996.

Labeyrie, L. D., and J. C. Duplessy, Changes in the oceanic $^{13}C/^{12}C$ ratio during the last 140000 years: high latitude surface water records, *Palaeogeogr., Palaeoclimatol., Palaeoecol.*, 50, 217–240, 1985.

Labeyrie, L. D., J. C. Duplessy, and P. L. Blanc, Variations in mode of formation and temperature of oceanic deep waters over the past 125,000 years, *Nature*, 327, 477–482, 1987.

Labeyrie, L., L. Vidal, E. Cortijo, M. Paterne, M. Arnold, J. C. Duplessy, M. Vautravers, M. Labracherie, J. Duprat, J. L. Turon, F. Grousset, and T. C. E. van Weering, Surface and deep hydrology of the Northern Atlantic Ocean during the past 150,000 years, *Phil. Trans. R. Soc. Lond. B.*, 348, 255–264, 1995.

Lambeck, K., Constraints on the late Weichselian ice sheet over the Barents sea from observations of raised shorelines, *Quat. Sci. Rev.*, 14, 1–16, 1995.

Landvik, J. Y., S. Bondevik, A. Elverhoi, W. Fjeldskaar, J. Mangerud, O. Salvigsen, M. J. Siegert, J. I. Svendsen, and T. O. Vorren, The last glacial maximum of Svalbard and the Barents Sea area: Ice sheet extent and configuration, *Quat. Sci. Rev.*, 17, 43–75, 1998.

Lehman, S., True grit spells double trouble, *Nature*, 382, 25–27, 1996.

Levitus, S., and T. P. Boyer, *World Ocean Atlas 1994, Vol. 4 (Temperature)*, NOAA Natl. Environ. Satell. Data and Inf. Ser., Washington, DC, 1994.

Levitus, S., R. Burgett, and T. P. Boyer, *World Ocean Atlas 1994, Vol. 3 (Salinity)*, NOAA Natl. Environ. Satell. Data and Inf. Ser., Washington, DC, 1994.

Little, M. G., R. R. Schneider, D. Kroon, B. Price, C. P. Summerhayes, and M. Segl, Trade wind forcing of upwelling, seasonality, and Heinrich events as a response to sub-Milankovitch climate variability, *Paleoceanogr.*, 12, 568–576, 1997.

Lorenz, S., B. Grieger, P. Helbig, and K. Herterich, Investigating the sensitivity of the atmospheric general circulation model ECHAM 3 to paleoclimatic boundary conditions, *Geol. Rundsch.*, 85, 513–524, 1996.

Lotter, A. F., B. Amman, J. Beer, I. Hajdas, and M. Sturm, A step towards an absolute time-scale for the late-glacial: annually laminated sediments from Soppensee (Switzerland), in *NATO ASI Series, Vol. 12: The last deglaciation: Absolute and radiocarbon chronologies*, edited by E. Bard, and W. S. Broecker, pp. 45–68, Springer, Berlin, 1992.

Lozier, S. M., W. B. Brechner-Owens, and R. G. Curry, The climatology of the North Atlantic, *Progr. Oceanogr.*, 36, 1–44, 1995.

Lozier, S. M., M. S. McCartney, and W. B. Owens, Anomalous anomalies in averaged hydrographic data, *J. Phys. Oceanogr.*, 24, 2623–2638, 1994.

MacAyeal, D. R., Binge/Purge Oscillations of the Laurentide Ice Sheet as a Cause of the North Atlantic's Heinrich Events, *Paleoceanogr.*, 8, 775–784, 1993a.

MacAyeal, D. R., A Low-Order Model of the Heinrich Event Cycle, *Paleoceanogr.*, 8, 767–773, 1993b.

Mackensen, A., H. - W. Hubberten, T. Bickert, G. Fischer, and D. K. Fütterer, The ^{13}C in benthic foraminiferal tests of *Fontbotia wuellerstorfi* (Schwager) relative to ^{13}C of dissolved inorganic carbon in southern ocean deep water: Implications for glacial ocean circulation models, *Paleoceanogr.*, 8, 587–610, 1993.

Majewski, P. A., L. D. Meeker, M. S. Twickler, S. Whitlow, Q. Yang, W. B. Lyons, and M. Prentice, Major features and forcing of high-latitude northern hemisphere atmospheric circulation using a 110,000-year-long glaciogeochemical signal, *J. Geophys. Res.*, 102, 26, 345–26, 267, 1997.

Manabe, S., and R. J. Stouffer, Two stable equilibria of a coupled ocean-atmosphere model, *J. Climate*, 1, 841–866, 1988.

Manabe, S., and R. J. Stouffer, Coupled ocean-atmosphere model response to freshwater input: Comparison to Younger Dryas event, *Paleoceanogr.*, 12, 321–336, 1997.

Mangerud, J., M. Bolstad, A. Elgersma, D. Helliksen, J. Y. Landvik, I. Lönne, A. K. Lycke, O. Salvigsen, T. Sandahl, and J. I. Svendsen, The last glacial maximum on Spitsbergen, Svalbard, *Quat. Res.*, 38, 1–31, 1992.

Marchal, O., T. F. Stocker, and F. Joos, Impact of oceanic reorganizations on the ocean carbon cycle and atmospheric carbon dioxide content, *Paleoceanogr.*, 13, 225–244, 1998.

Marchitto, T. M., W. B. Curry, and D. W. Oppo, Millennial-scale changes in North Atlantic circulation since the last glaciation, *Nature*, 393, 557–561, 1998.

Marotzke, J., and J. Willebrand, Multiple equlibria of the global thermohaline circulation, *J. Phys. Oceanogr.*, 21, 1372–1385, 1991.

Maslin, M. A., N. J. Shackleton, and U. Pflaumann, Surface water temperature, salinity, and density changes in the northeast Atlantic during the last 45,000 years: Heinrich events, deep water formation, and climatic rebounds, *Paleoceanogr.*, 10, 527–544, 1995.

Maslin, M. A., M. Sarnthein, and J. J. Knaack, Subtropical climate during the Eemian, *Naturwiss.*, 83, 122–126, 1996.

Maslin, M. A., E. Thomas, N. J. Shackleton, M. A. Hall, and D. Seidov, Glacial northeast Atlantic surface water $p(CO_2)$: Productivity and deep-water formation, *Mar. Geol.*, 144, 177–190, 1997.

Mayewski, P. A., L. D. Meeker, M. S. Twickler, S. Whitlow, Q. Z. Yang, W. B. Lyons, and M. Prentice, Major features and forcing of high-latitude northern hemisphere atmospheric circulation using a 110,000-year-long glaciochemical series, *J. Geophys. Res.*, C102, 26345–26366, 1997.

McCabe, A. M., and P. U. Clark, Ice-sheet variability around the north Atlantic Ocean during the last deglaciation, *Nature*, 392, 373–377, 1998.

McCave, I. N., B. Manighetti, and N. A. S. Beveridge, Circulation in the glacial North Atlantic inferred from grain-size measurements, *Nature*, 374, 149–151, 1995.

McIntyre, A., and B. Molfino, Forcing of Atlantic equatorial and subpolar millennial cycles by precession, *Science*, 274, 1867–1870, 1996.

McManus, J. F., R. F. Anderson, W. S. Broecker, M. Q. Fleisher, and S. M. Higgins, Radiometrically determined sedimentary fluxes in the sub-polar North Atlantic during the last 140,000 years, *Earth Planet Sci. Lett.*, 155, 29–43, 1998.

Meese, D. A., R. B. Alley, A. J. Gow, P. Grootes, P. A. Mayewski, M. Ram, K. C. Taylor, E. D. Waddington, and G. Zielinski, *Preliminary depth-age scale of the GISP2 ice core*, CRRL Spec. Rep. 94-1, U.S. Army Cold Reg. Res. and Eng. Lab., 66 pp., Hannover, NH, 1994.

Ninnemann, U. S., C. D. Charles, and D. A. Hodell, Origin of global millennial-scale climate events: Constraints from the Southern Ocean deep-sea sedimentary record, in *Chapman Conference on Mechanisms of Millennial-Scale Global Climate Change*, edited by R. S. Webb, AGU Geoph Monogr (in press), 1999.

O'Brien, S. R., P. A. Mayewski, L. D. Meeker, D. A. Meese, M. S. Twickler, and S. I. Whitlow, Complexity of Holocene climate as reconstructed from a Greenland ice core, *Science*, 270, 1962–1964, 1995.

Pacanowski, R., K. Dixon, and A. Rosati, *The GFDL modular ocean model users guide*, Geophysical Fluid Dynamics Laboratory, Princeton University, Princeton, GFDL Ocean Group Technical Report No. 2, 1993.

Paillard, D., and L. Labeyrie, Role of the thermohaline circulation in the abrupt warming after Heinrich events, *Nature*, 372, 162–164, 1994.

Paillard, D., L. Labeyrie, and P. Yiou, Macintosh program performs time-series analysis, *EOS Transactions* AGU, 77, 379, 1996.

Peltier, W. R., Ice age paleotopography, *Science*, 265, 195–201, 1994.

Prell, W. L., J. V. Gardner, A. W. H. Be, and J. D. Hays, Equatorial Atlantic and Caribbean foraminiferal assemblages, temperatures, and circulation; interglacial and glacial comparisons, in *Memoir. No. 145: Investigation of late Quaternary paleoceanography and paleoclimatology*, edited by R. M. Cline, and J. D. Hays, pp. 247–265, Geological Society of America, Boulder, CO, 1976.

Rahmstorf, S., Bifurcations of the Atlantic thermohaline circulation in response to changes in the hydrological cycle, *Nature*, 378, 145–149, 1995.

Rahmstorf, S., Influence of Mediterranean outflow on climate, *EOS Trans.* AGU, 79, 281–282, 1998.

Rahmstorf, S., J. Marotzke, and J. Willebrand, Stability of the thermohaline circulation, in *The warmwatersphere of the North Atlantic Ocean*, edited by W. Krauss, pp. 129–157, Gebrüder Borntraeger, Berlin, 1996.

Rasmussen, T. L., E. Thomsen, T. C. E. van Weering, and L. Labeyrie, Rapid changes in surface and deep water conditions at the Faeroe margin during the last 58,000 years, *Paleoceanogr.*, 11, 757–771, 1996.

Raymo, M. E., W. F. Ruddiman, J. Backman, B. M. Clement, and D. G. Martinson, Late Pliocene variation in northern Hemisphere ice sheets and North Atlantic deep water circulation, *Paleoceanogr.*, 4, 413–446, 1989.

Redfield, A. C., B. H. Ketchum, and F. A. Richards, The influence of organisms on the composition of seawater, in *The Sea, Vol. 2*, edited by M. N. Hill, pp. 26–77, Interscience Publisher, New York, 1963.

Renssen, H., The global response to Younger Dryas boundary conditions in an AGCM simulation, *Clim. Dyn.*, 13, 587–599, 1997.

Renssen, H., M. Lautenschlager, and C. J. E. Schuurmans, The atmospheric winter circulation during the Younger Dryas stadial in the Atlantic/European sector, *Clim. Dyn.*, 12, 813–824, 1996.

Robinson, S. G., and I. N. McCave, Orbital forcing of bottom-current enhanced sedimentation on Feni Drift, NE Atlantic, during the mid-Pleistocene, *Paleoceanogr.*, 9, 943–972, 1994.

Robinson, S. G., M. A. Maslin, and I. N. McCave, Magnetic susceptibility variations in Upper Pleistocene deep-sea sediments of the NE Atlantic: Implications for ice rafting and paleocirculation at the last glacial maximum, *Paleoceanogr.*, 10, 221–250, 1995.

Ruddiman, W. F., and A. McIntyre, Oceanic mechanisms for amplification of the 23,000-year ice-volume cycle, *Science*, 212, 617–627, 1981.

Ruddiman, W. F., M. E. Raymo, D. G. Martinson, B. M. Clement, and J. Backman, Pleistocene evolution: Northern hemisphere ice sheets and North Atlantic Ocean, *Paleoceanogr.*, 4, 413–446, 1989.

Rühlemann, C., S. Mulitza, P. J. Müller, and G. Wefer, Cooling by 3–4 C of southern Caribbean surface water during the last glacial maximum: evidence from alkenone paleothermometry. 6th International Conference on Paleoceanography. Lisbon, 24–28 Aug. Program, 196 (Abstract), 1998.

Sakai, K., and W. R. Peltier, A simple model of the Atlantic thermohaline circulation: Internal and forced variability with paleoclimatological implications, *J. Geophys. Res.*, C100, 13455–13479, 1995.

Saltzman, B., and M. Y. Verbitsky, Multiple instabilities and modes of glacial rhythmicity in the Plio-Pleistocene: A general theory of late Cenozoic climate change, *Clim. Dyn.*, 9, 1–15, 1993.

Sarmiento, J. L., R. Murnane, and C. Le Quéré, Air-sea CO_2 budget of the North Atlantic, *Phil. Trans. R. Soc. Lond. B.*, 348, 211–219, 1995.

Sarnthein, M., and R. Tiedemann, Younger Dryas-style cooling events at glacial terminations I-VI at ODP Site 658; associated benthic ^{13}C anomalies constrain meltwater hypothesis, *Paleoceanogr.*, 5, 1041–1055, 1990.

Sarnthein, M., K. Winn, S. J. A. Jung, J. C. Duplessy, L. Labeyrie, H. Erlenkeuser, and G. Ganssen, Changes in East Atlantic deepwater circulation over the last 30,000 years – 8 time slice reconstructions, *Paleoceanogr.*, 9, 209–267, 1994.

Sarnthein, M., E. Jansen, M. Weinelt, M. Arnold, J. C. Duplessy, H. Erlenkeuser, A. Flatoy, G. Johannessen, T. Johannessen, S. Jung, N. Koç, L. Labeyrie, M. Maslin, U. Pflaumann, and H. Schulz, Variations in Atlantic surface ocean paleoceanography, 50–80 N: A time-slice record of the last 30,000 years, *Paleoceanogr.*, 10, 1063–1094, 1995.

Schäfer-Neth, C., and K. Stattegger, Circulation of the glacial Atlantic: combining global and regional modelling, in *Computerized modeling of sedimentary systems*, edited by J. Harff, W. Lemke, and K. Stattegger, Springer, Berlin, 1998.

Schäfer-Neth, C., Modellierung der Paläoozeanographie des nördlichen Nordatlantiks zur letzten Maximalvereisung, *Ber. SFB 313, Univ. Kiel*, 51, 1–106, 1994.

Schäfer-Neth, C., Changes in the seawater salinity-oxygen isotope relation between last glacial and present: sediment core data and OGCM modelling, *Paleoclim.*, 2, 101–131, 1998.

Schäfer-Neth, C., and A. Paul, Circulation of the glacial Atlantic: A synthesis of global and regional Modeling, in *The northern North Atlantic: a changing environment*, edited by P. Schäfer, W. Ritzrau, M. Schlüter, and J. Thiede, Springer, Berlin, this volume.

Schäfer-Neth, C., and K. Stattegger, Meltwater pulses in the northern North Atlantic: retrodiction and forecast by numerical modelling, *Geol. Rundsch.*, 86, 492–498, 1997.

Schiller, A., U. Mikolajewicz, and R. Voss, The stability of the North Atlantic thermohaline circulation in a coupled ocean-atmosphere general circulation model, *Clim. Dyn.*, 13, 325–347, 1997.

Schmitz, W. J., On the interbasin-scale thermohaline circulation, *Rev. Geophys.*, 33, 151–173, 1995.

Schmitz, W. J. Jr, and M. S. McCartney, On the North Atlantic circulation, *Rev. Geophys.*, 31, 29–49, 1993.

Schulz, H., Meeresoberflächentemperaturen vor 10.000 Jahren – Auswirkungen des frühholozänen Insolationsmaximums, *Berichte – Reports, Geol.-Paläont. Inst. Univ. Kiel*, 73, 1-156, 1995.

Schulz, M., Numerische Modellexperimente zur Veränderung des Ozean-Atmospäre-Kohlenstoffkreislaufes während der letzten 21000 Jahre: Der Einfluß von Variationen der thermohalinen Ozeanzirkulation, *Ber. SFB 313, Univ. Kiel*, 74, 1–177, 1998.

Schulz, M., D. Seidov, M. Sarnthein, K. Stattegger, Modeling ocean-atmosphere carbon budgets during the Last Glacial Maximum – Heinrich 1 Meltwater Event – Bølling transition, *Geol. Rundsch.*, in press.

Schulz, M., and K. Stattegger, SPECTRUM: Spectral analysis of unevenly spaced paleoclimatic time series, *Computers and Geosci.*, 23, 929–945, 1997.

Seidov, D., An intermediate model for large-scale ocean circulation studies, *Dyn. Atmos. Oceans*, 25, 25–55, 1996.

Seidov, D., and B. J. Haupt, Numerical study of glacial and meltwater global ocean thermohaline conveyor, in *Computerized modeling of sedimentary systems*, edited by J. Harff, W. Lemke, and K. Stattegger, pp. 79–113, Springer, Berlin, 1998.

Seidov, D., and M. Maslin, Seasonally ice free glacial Nordic seas without deep water ventilation, *Terra Nova*, 8, 245–254, 1996.

Seidov, D., M. Sarnthein, K. Stattegger, R. Prien, and M. Weinelt, North Atlantic ocean circulation during the last glacial maximum and subsequent meltwater event: A numerical model, *J. Geophys. Res.*, C101, 16305–16332, 1996.

Shackleton, N. J., Carbon-13 in Uvigerina: Tropical rainforest history and the equatorial Pacific carbonate dissolution cycles, in *The fate of fossil fuel*

CO_2 in the oceans, edited by N. R. Andersen, and A. Malahoff, pp. 401–427, Plenum Press, New York, 1977.

Simstich, J., *Die ozeanische Deckschicht des Europäischen Nordmeers im Abbild stabiler Isotope von Kalkgehäusen unterschiedlicher Planktonforaminiferenarten*, D.Sc. Thesis, pp. 1–83, Univ. of Kiel, Kiel, 1998.

Simstich, J., M. Sarnthein, and H. Erlenkeuser, Surface layer stratification in the nordic seas: stable isotope anomalies of *N. pachyderma* (sin) and *T. quinqueloba*, 6th International Conference on Paleoceanography, Lisbon, 24–28 Aug. Program, 211 (Abstract), 1998.

Sirocko, F., D. Garbe-Schönberg, A. McIntyre, and B. Molfino, Teleconnections between the subtropical monsoons and high-latitude climates during the last deglaciation, *Science*, 272, 526–529, 1996.

Sowers, T., and M. Bender, Climate records covering the last deglaciation, *Science*, 269, 210–214, 1995.

Spero, H. J., J. Bijma, D. W. Lea, and B. E. Bemis, Effect of seawater carbonate concentration on foraminiferal carbon and oxygen isotopes, *Nature*, 390, 497–500, 1997.

Spielhagen, R. F., G. Bonani, A. Eisenhauer, M. Frank, T. Frederichs, H. Kassens, P. W. Kubik, A. Mangini, N. Nørgaard-Pedersen, N. R. Nowaczyk, S. Schäper, R. Stein, J. Thiede, R. Tiedemann, and M. Wahsner, Arctic Ocean evidence for late Quaternary initiation of northern Eurasian ice sheets, *Geology*, 25, 783–786, 1997.

Spielhagen, R. F., N. Nørgaard-Pedersen, H. Erlenkeuser, P. M. Grootes, and J. Heinemeier, A meltwater event in the Arctic Ocean before the Younger Dryas, 6th International Conference on Paleoceanography, Lisbon, 24–28 Aug. Program, 213 (Abstract), 1998.

Steinsund, P. I., M. Hald, and D. A. R. Poole, Modern benthic foraminiferal distribution in the southwestern Barents Sea; paleooceanographic applications, *Norsk Geologisk Tidsskrift*, 71, 169–171, 1991.

Stocker, T. F., Climate change – The seesaw effect, *Science*, 282, 61–62, 1998.

Stocker, T. F., and D. G. Wright, Rapid changes in ocean circulation and atmospheric radiocarbon, *Paleoceanogr.*, 11, 773–795, 1996.

Stocker, T. F., D. G. Wright, and W. S. Broecker, The influence of high-latitude surface forcing on the global thermohaline circulation, *Paleoceanogr.*, 7, 529–541, 1992.

Stommel, H., Thermohaline convection with two stable regimes of flow, *Tellus*, 13, 224–228, 1961.

Stoner, J. S., J. E. T. Channell, and C. Hillaire-Marcel, A 200 ka geomagnetic chronostratigraphy for the Labrador Sea:Indirect correlation of the sediment record to SPECMAP, *Earth Planet Sci. Lett.*, 159, 165–181, 1998.

Sy, A., M. Rhein, J. R. N. Lazier, K. P. Koltermann, J. Meincke, A. Putzka, and M. Bersch, Surprisingly rapid spreading of newly formed intermediate waters across the North Atlantic Ocean, *Nature*, 386, 675–679, 1997.

Struck, U., Stepwise postglacial migration of benthic foraminifera into the abyssal northeastern Norwegian Sea, *Mar. Micropaleontol.*, 26, 207–213, 1995.

Sundquist, E. T., The global carbon dioxide budget, *Science*, 259, 934–941, 1993.

Takahashi, T., T. T. Takahashi, and S. C. Sutherland, An assessment of the North Atlantic as a CO_2 sink, *Phil. Trans. R. Soc. Lond. B.*, 348, 143–152, 1995.

Takahashi, T., R. A. Feely, R. F. Weiss, R. Wanninkhof, D. W. Chipman, S. C. Sutherland, and T. T. Takahashi, Global air-sea flux of CO_2: An estimate based on mesurements of sea-air pCO_2 difference, *Proc. Natl. Acad. Sci. USA*, 94, 8292–8299, 1997.

Tans, P. P., I. Y. Fung, and T. Takahashi, Observational constraints on the global CO_2 budget, *Science*, 247, 1431–1438, 1990.

Taylor, K. C., C. U. Hammer, R. B. Alley, H. B. Clausen, D. Dahl-Jensen, A. J. Gow, N. S. Gundestrup, J. Kipfstuhl, J. C. Moore, and E. D. Waddlington, Electrical conductivity measurements from the GISP2 and GRIP Greenland ice cores, *Nature*, 366, 549–552, 1993.

Thiede, J., A. M. Myhre, J. V. Firth, G. L. Johnson, W. F. Ruddiman (eds), *Proc. ODP, Sci. Results, 151*, Ocean Drilling Program, College Station, TX, 1996.

Thiede, J., A. Winkler, T. Wolf-Welling, O. Eldholm, A. M. Myhre, K. H. Baumann, R. Henrich, and R. Stein, Late Cenozoic history of the Polar North Atlantic: Results from ocean drilling, *Quat. Sci. Rev.*, 17, 185–208, 1998.

Tziperman, E., Inherently unstable climate behaviour due to weak thermohaline ocean circulation, *Nature*, 386, 592–595, 1997.

van Kreveld, S. A., M. Knappertsbusch, J. Ottens, G. M. Ganssen, and J. E. van Hinte, Biogenic carbonate and ice-rafted debris (Heinrich layer) accumulation in deep-sea sediments from a Northeast Atlantic piston core, *Mar. Geol.*, 131, 21–46, 1996.

van Kreveld, M. Sarnthein, H. Erlenkeuser, P. M. Grootes, S. A., S. Jung, M. J. Nadeau, U. Pflaumann and A. Voelker, Potential links between surg-

ing ice sheets, circulation changes, and the Dansgaard-Oeschger cycles in the Irminger sea, 60–18 ka, *Paleoceanogr.*, submitted.

Veum, T., E. Jansen, M. Arnold, I. Beyer, and J. C. Duplessy, Water mass exchange between the North Atlantic and the Norwegian Sea during the past 28,000 years, *Nature*, 356, 783–785, 1992.

Vidal, L., L. Labeyrie, E. Cortijo, M. Arnold, J. C. Duplessy, E. Michel, S. Becque, and T. C. E. van Weering, Evidence for changes in the North Atlantic Deep Water linked to meltwater surges during the Heinrich events, *Earth Planet Sci Lett.*, 146, 13–27, 1997.

Voelker, A., *Zur Deutung der Dansgaard-Oeschger Ereignisse in ultra-hochauflösenden Sedimentprofilen aus dem Europäischen Nordmeer*, D.Sc. Thesis, pp. 1–180, Univ. of Kiel, Kiel, 1999.

Voelker, A. H. L., M. Sarnthein, P. M. Grootes, H. Erlenkeuser, C. Laj, A. Mazaud, M. J. Nadeau, and M. Schleicher, Correlation of marine C-14 ages from the Nordic Seas with the GISP2 isotope record: Implications for C-14 calibration beyond 25 ka BP, *Radiocarbon*, 40, 517, 1998.

Vogelsang, E., Paläo-Ozeanographie des Europäischen Nordmeeres an Hand stabiler Kohlenstoff- und Sauerstoffisotope, *Ber. SFB 313, Univ. Kiel*, 23, 1–136, 1990.

von Bodungen, B., F. Theilen, and F. Werner, POSEIDON-Reise 141-2/142 vom 17.10.87 bis 18.11.87; POSEIDON-Reise 146/1 vom 25.4.87 bis 11.5.87; POSEIDON-Reise 146/3 vom 29.5.88 bis 19.6.88, *Ber. SFB 313, Univ. Kiel*, 11, 1–66, 1988.

Vorren, T. O., and J. S. Laberg, Late glacial air temperature, oceanographic and ice sheet interactions in the southern Barents Sea region, in *Special Publication No. 111: Late Quaternary palaeoceanography of the North Atlantic margins*, edited by J. T. Andrews, W. E. N. Austin, H. Bergsten, and A. E. Jennings, pp. 303–321, Geological Society, London, 1996.

Wang, L., M. Sarnthein, H. Erlenkeuser, J. Grimalt, P. Grootes, S. Heilig, E. Ivanova, M. Kienast, C. Pelejero, and U. Pflaumann, East Asian monsoon climate during the late Pleistocene: High-resolution sediment records from the South China Sea, *Mar. Geol.*, 156, 245–284, 1999.

Weinelt, M., Veränderungen der Oberflächenzirkulation im Europäischen Nordmeer während der letzten 60.000 Jahre – Hinweise aus stabilen Isotopen, *Ber. SFB 313, Univ. Kiel*, 41, 1–106, 1993.

Weinelt, M., M. Sarnthein, U. Pflaumann, H. Schulz, S. Jung, and H. Erlenkeuser, Ice-free nordic seas during the last glacial maximum? Potential sites of deepwater formation, *Palaeoclim.*, 1, 283–309, 1996.

Weinelt, M., W. Kuhnt, M. Sarnthein, A. Altenbach, O. Costello, H. Erlenkeuser, U. Pflaumann, J. Simstich, U. Struck, A. Thies, M. H. Trauth, and E. Vogelsang, Paleoceanographic proxies in the northern North Atlantic, in *The northern North Atlantic: a changing environment*, edited by P. Schäfer, W. Ritzrau, M. Schlüter, and J. Thiede, Springer, Berlin, this volume.

Winton, M., Deep decoupling oscillations of the oceanic thermohaline circulation, in *NATO ASI Series: Ice in the climate system*, edited by W. R. Peltier, pp. 417–432, Springer, Berlin, 1993.

Yu, E. F., R. Francois, and M. P. Bacon, Similar rates of modern and last-glacial ocean thermohaline circulation inferred from radiochemical data, *Nature*, 379, 689–694, 1996.

Zahn, R., K. Winn, and M. Sarnthein, Benthic foraminiferal ^{13}C and accumulation rates of organic carbon: *Uvigerina peregrina* group and *Cibicidoides wuellerstorfi*, *Paleoceanogr.*, 1, 27–42, 1986.

Zahn, R., J. Schönfeld, H. R. Kudrass, M. H. Park, H. Erlenkeuser, and P. Grootes, Thermohaline instability in the North Atlantic during meltwater events: Stable isotope and ice-rafted detritus records from core SO75-26KL, Portuguese margin, *Paleoceanogr.*, 12, 696–710, 1997.